The Abdus Salam
International Centre for Theoretical Physics

United Nations
Educational, Scientific
and Cultural Organization

International Atomic
Energy Agency

SMR 1829 - 5

Winter College on Fibre Optics, Fibre Lasers and Sensors

12 - 23 February 2007

High Power Fibre Lasers and Amplifiers

Andy Clarkson

Optoelectronics Research Centre
University of Southampton
Southampton, SO17 1BJ
United Kingdom

Strada Costiera 11, 34014 Trieste, Italy - Tel. +39 040 2240 111; Fax +39 040 224 163 - sci_info@ictp.it, www.ictp.it

Winter College on Fibre Optics, Fibre Lasers and Sensors
International Centre for Theoretical Physics
12 – 23 February 2007

High Power Fibre Lasers and Amplifiers

Andy Clarkson

Optoelectronics Research Centre
University of Southampton
Southampton, SO17 1BJ
United Kingdom

Contents

3. Pump sources and pump coupling:

4. Thermal effects in fibers:

5. Nonlinear processes:

6. Scaling mode area:

7. Wavelength selection and tuning:

8. High power CW and pulsed fiber sources:

10. Power and brightness scaling via beam combination:

1. Introduction

Background

Scaling the output power from lasers has been an activity that has preoccupied many within the laser community ever since the laser's invention. This has been driven not simply by curiosity, but also to fulfil the needs of huge range of applications, and by the prospect of even more applications:

Application areas include:

- Scientific applications
- Medical applications
- Remote monitoring and sensing
- Free-space communications
- Materials processing
- Defence applications

In addition to high power, many of these applications place other demands on the laser source, for example, in terms of beam quality, efficiency, linewidth, mode of operation, etc, which may be quite difficult to achieve.

For a long time, the high-power laser area has been dominated by gas lasers and conventional 'bulk' solid-state lasers. Fiber lasers and amplifiers are relatively new arrivals to this area!

Brief history of rare-earth doped fibers

1964 *First rare earth doped fiber active fiber device*[1]
Coiled Nd-doped fiber side-pumped by a flashlamp
C. Koester and E. Snitzer, American Optical Co

1974 *First fiber laser pumped by a laser diode*[2]
CW operation of a Nd-doped silica fiber laser pumped by a GaAs laser diode
J. Stone and C. Burrus, Bell Labs

1985 *Fabrication of low-loss RE-doped silica fibers by MCVD and solution doping resulting in the first low-loss Nd-doped fiber laser pumped by a laser diode*[3]
R. J. Mears, L. Reekie, S. B. Poole and D. N. Payne, University of Southampton

1987 *First erbium-doped fiber amplifier*[4]
R. Mears, L. Reekie, I. Jauncey and D. N. Payne, University of Southampton

1988 *First cladding-pumped fiber laser*[5]
Nd-doped fiber laser with offset core
E. Snitzer, H. Po, F. Hakimi, R. Tumminelli, B. C. McCollum, Polaroid

1999 *First >100W cladding-pumped fiber laser*
V. Dominic, S. MacCormack, R. Waarts, S. Sanders, S.Bicknese, R. Dohle, E. Wolak, P. S. Yeh and E. Zucker, SDL

2002 *First fiber laser with > 1 kW output power*[7]
K.-I. Ueda, H. Sekiguchi, H. Kan, University of Electrocommunications, Hoya, and Hamamatsu, Japan

2005 *Ytterbium-doped silica fiber laser with >2kW output*[8]
V. P. Gapontsev, D. V. Gapontsev, N. S. Platonov, O. Shkurihin, V. Fomin, A. Mashkin, M. Abramov and S. Ferin, IPG Photonics

The dramatic rise in output power from cladding-pumped Yb-doped silica fiber lasers

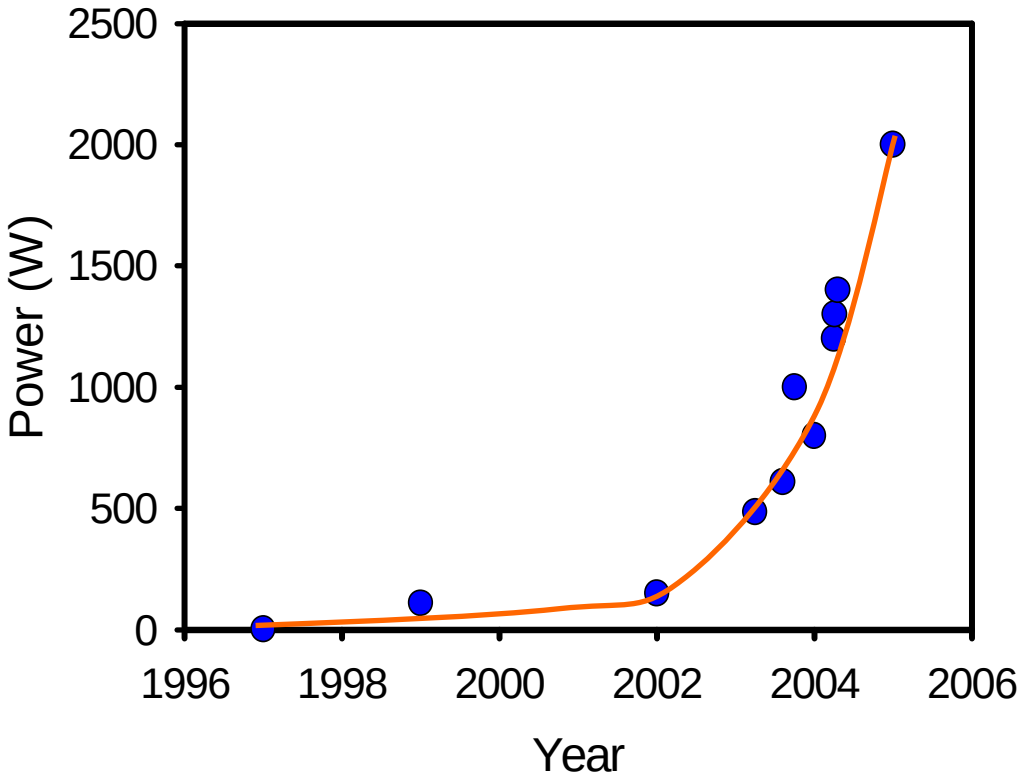

Energy levels is rare-earth ions

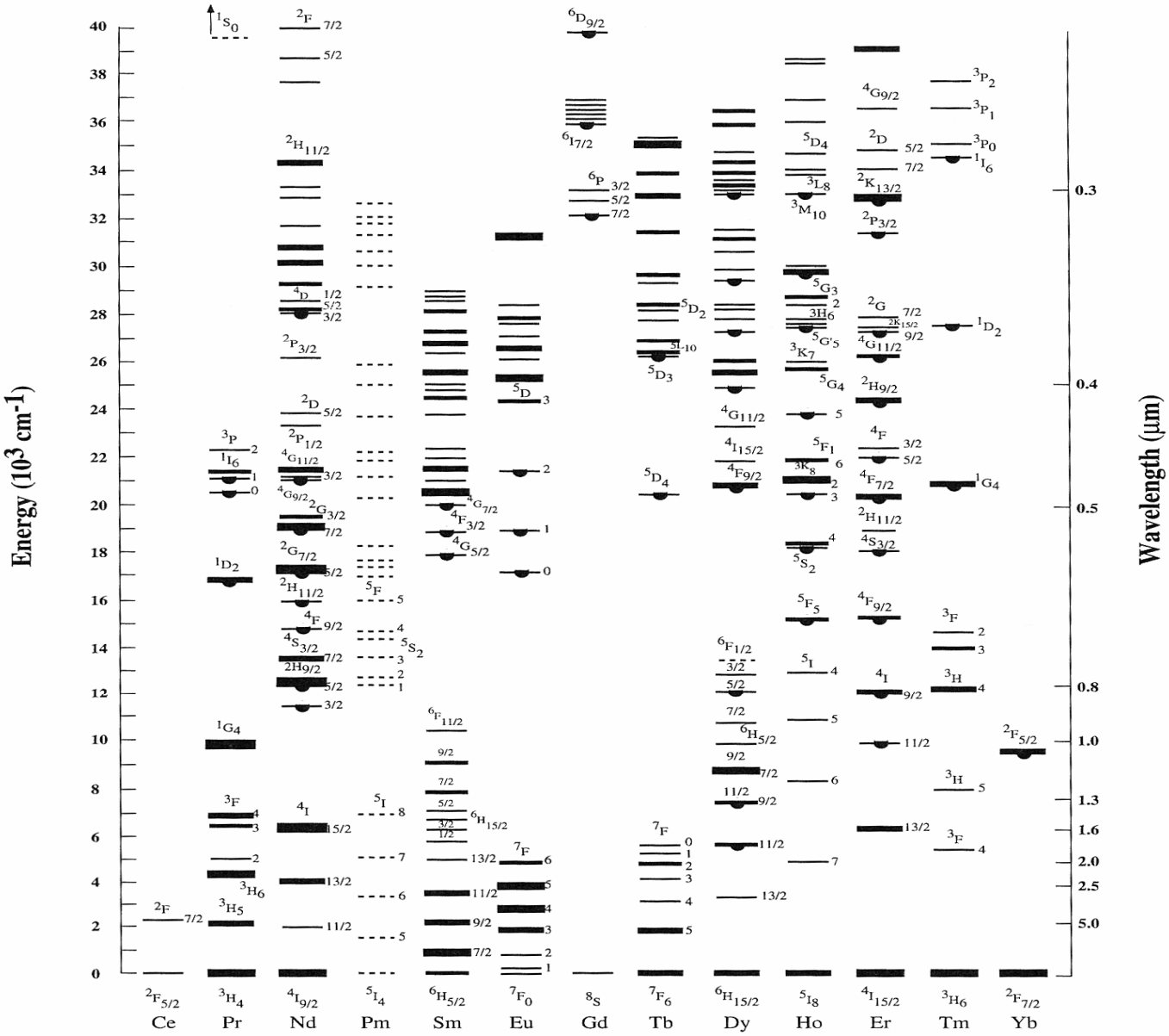

From ref. 9

Operating wavelengths for rare-earth doped fiber lasers in silica and non-silica glasses

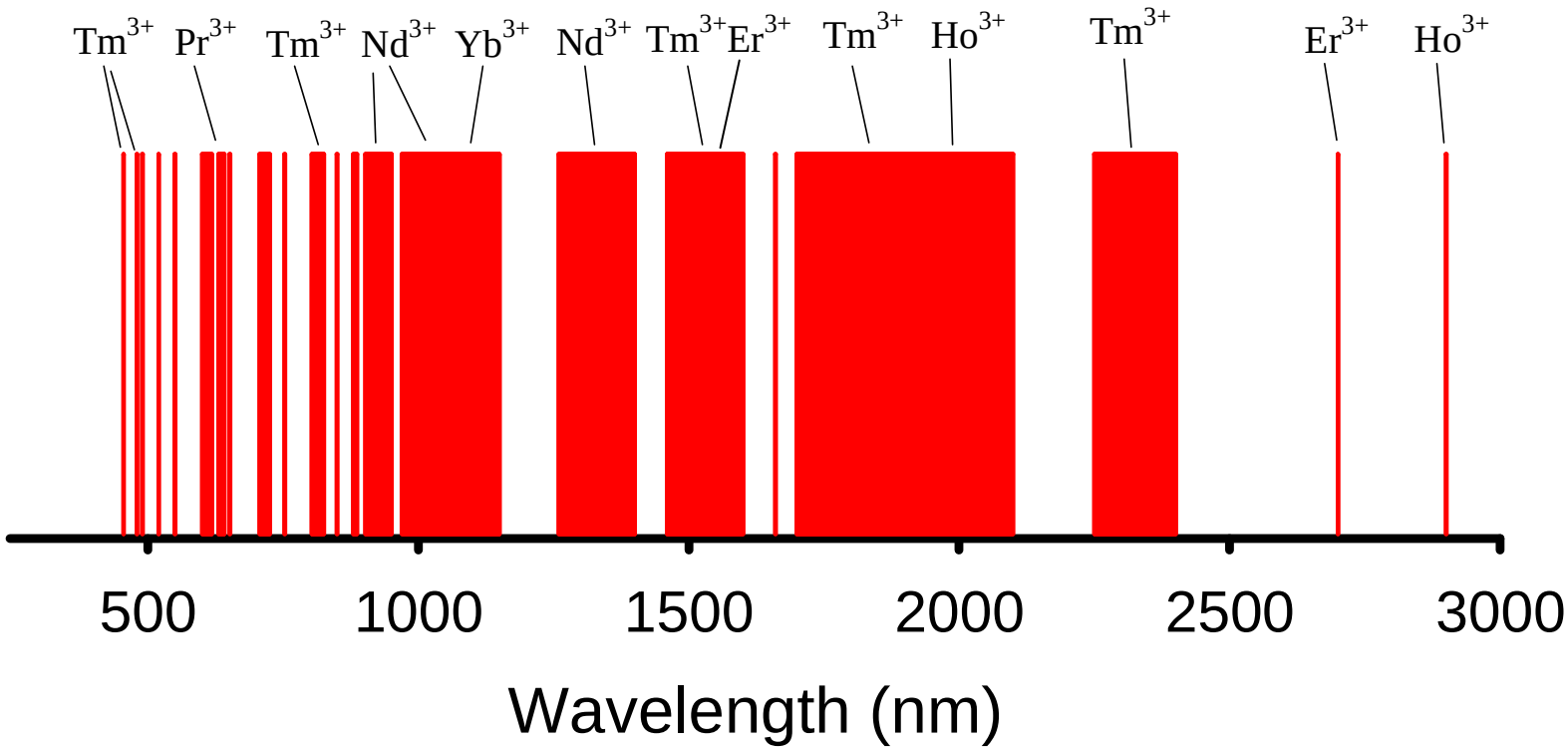

Principles of RE-doped fiber lasers

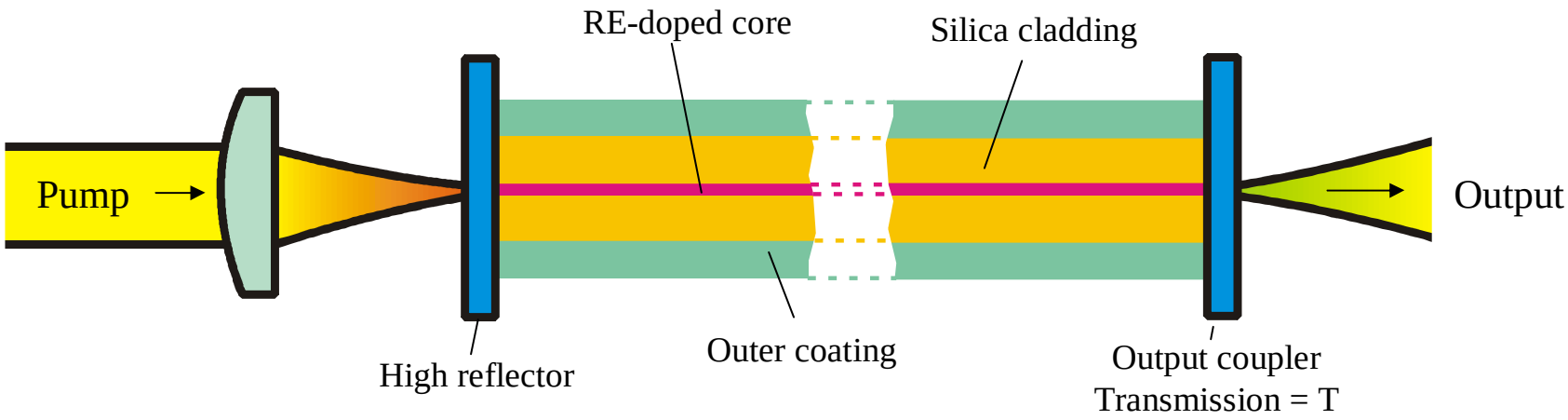

Core: Radius = r_a
Refractive index = n_a

Cladding: Radius = r_b
Refractive index = n_b

$$V = \frac{2\pi r_a}{\lambda}\sqrt{n_a^2 - n_b^2} = \frac{2\pi r_a NA}{\lambda}$$

For single-mode propagation in the core, V<2.405
→ r_a = 4μm for NA = 0.1 and λ = 1.06μm

Gaussian transverse intensity profile approximation for fundamental mode[10]

→ Mode radius = $w_L \approx r_a/(\log_e V)^{0.5}$ = 4.3μm

Typical value for r_b is 62.5μm

Core composition

The core is fabricated from SiO_2 with various dopants including:

- Rare earth ions (e.g. Nd^{3+}, Yb^{3+}, Er^{3+}, Tm^{3+}) in the form of RE_2O_3 with typical concentrations in the range of ~100ppm to >10,000ppm
- Dopants such as Al and P are generally added to modify the environment to increase the RE solubility in SiO_2
- Dopants (e.g. Al, Ge) are added to increase the refractive index of the core relative to surrounding pure silica cladding

The addition of these extra dopants varies the host composition and hence can have an effect on the spectroscopy

For various Yb-doped silica glass compositions[11]:

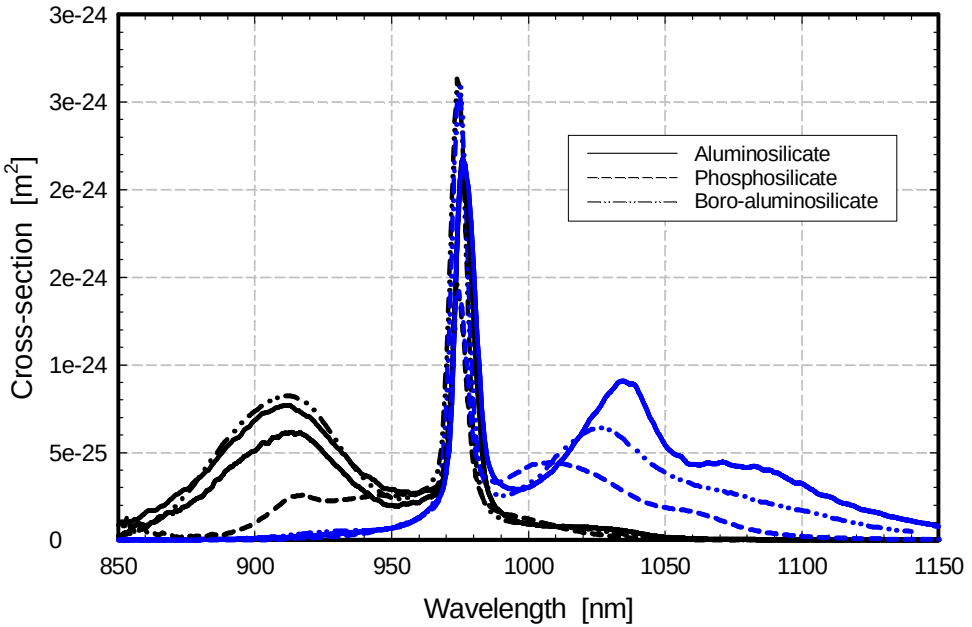

Simple model for four-level lasers

Overview of the advantages and disadvantages of RE-doped fiber lasers versus conventional 'bulk' solid-state lasers using simplified theory for laser performance

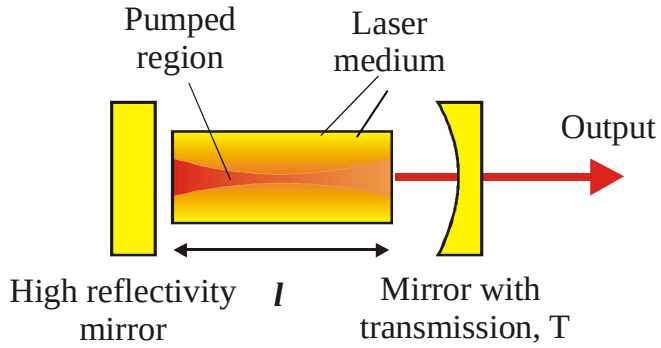

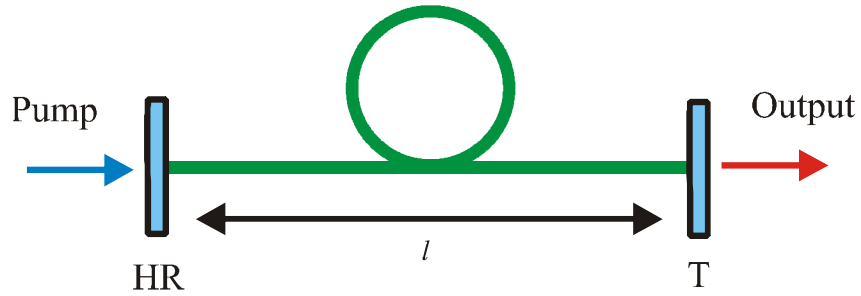

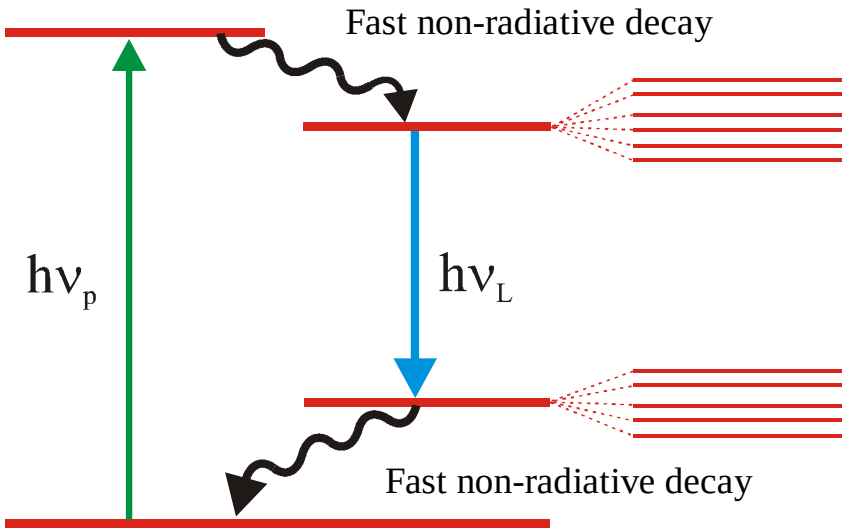

Stark splitting of energy levels due crystal field. Resulting levels are further split / broadened by other mechanisms[11].

RE-doped crystals generally have relatively discrete sub-levels and relatively narrow homogeneously-broadened emission and absorption spectra.

RE-doped glasses generally have very broad (overlapping) sub-levels with very broad continuous emission and absorption spectra. Broadening involves both homogeneous and inhomogeneous mechanisms, but homogeneous broadening usually dominates.

Rate equations:

Population densities for the lower and upper laser levels are: $N_1 = 0$ (from four-level approximation)
$N_2 = N$ = Inversion density

Under steady-state conditions:

$$\frac{dN(r,z)}{dt} = R_p(r,z) - \frac{N(r,z)}{\tau_f} - c_n \sigma_e N(r,z) s(r,z) = 0$$

$$\frac{dS}{dt} = \int_{cavity} c_n \sigma_e N(r,z) s(r,z) dV - \frac{S}{\tau_c} = 0$$

where c_n is the speed of light in the laser medium, τ_f is the fluorescence lifetime of the upper level, τ_c is the cavity photon lifetime, $R_p(r,z)$ is the pump rate density, s(r,z) is the photon density, S is the total number of photons in the laser mode inside the resonator and σ_e is the emission cross-section for the transition. σ_e is usually much smaller for a glass host than for a crystal host.

Material	Nd:YAG	Nd:YVO_4	Nd:YLF	Nd:silica glass	Nd:phosphate glass
λ_L(μm)	1.064	1.064	1.047 (π) 1.053 (σ)	1.060	1.060
σ_e ($10^{-23}m^2$)	3.4	25 (π)	1.9 (π) 1.2 (σ)	~0.14	~0.4
τ_f (μs)	230	90	520	500	350

Simplifying assumptions:

- Gaussian transverse profiles for fundamental laser mode, pump and inversion distribution
- Neglect diffraction spreading of pump and laser mode for bulk laser
- Negligible ground-state depletion
- Low resonator loss: T = transmission of output coupler, L = round-trip loss (excluding output coupler) $\rightarrow$ $(L + T) << 1$

Can solve rate equations to obtain expressions for threshold and slope efficiency as follows[12,13]:

- **Threshold pump power**

$$P_{pth} \approx \frac{\pi h \nu_p (L+T)(w_p^2 + w_L^2)}{4\sigma_e \tau_f \eta_p \eta_{abs}}$$

Low emission cross-section for fiber is more than offset by the small core/beam size compared to bulk laser configurations
$\rightarrow$ Much lower threshold for fiber laser
$\rightarrow$ Threshold powers can be < 1mW

- **Slope efficiency**

$$\eta_s \approx \left(\frac{T}{L+T}\right)\left(\frac{\nu_L}{\nu_p}\right)\eta_p \eta_{abs} \eta_{PL}$$

In practice, slope efficiencies for fiber lasers tend to be higher than for bulk lasers - Why?

where w_p is the pump beam size or fiber core radius, w_L is the laser mode radius, η_p is the pumping quantum efficiency, η_{PL} is the pump – laser mode overlap factor and $\eta_{abs} = [1-\exp(-\alpha_p l)]$ is the of pump light absorbed (α_p is the absorption coefficient for the pump).

Overlap factor:

$$\eta_{PL} \approx \frac{w_L^2(2w_P^2 + w_L^2)}{(w_P^2 + w_L^2)^2} < 1$$ at low powers ($I/I_{sat} << 1$)

and

$$\eta_{PL} \approx 1$$ at high powers ($I/I_{sat} >> 1$)

where I_{sat} is the saturation intensity given by: $I_{sat} = \frac{h\nu_L}{\sigma_e \tau_f}$

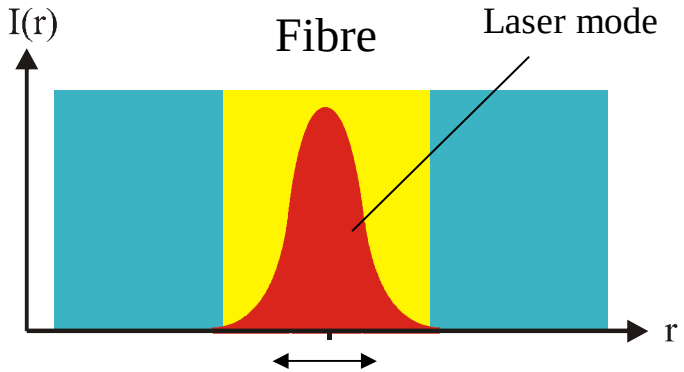

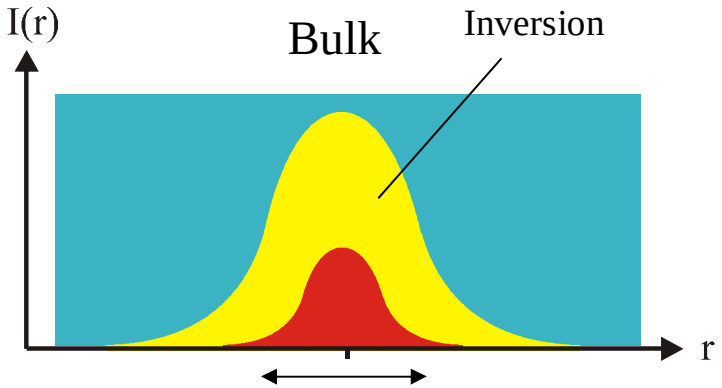

$$R_p(r,z) = \frac{N(r,z)}{\tau_f} + c_n \sigma_e N(r,z) s(r,z)$$

Spontaneous emission — Stimulated emission

$$\frac{\text{Rate of stimulated emission}}{\text{Rate of spontaneous emission}} = c_n s(r,z) \sigma_e \tau_f = \frac{I}{I_{sat}}$$

Stimulated emission will dominate when $I/I_{sat} >> 1$ over the entire inverted region. This is much easier to achieve in a fiber because of the small core size (in spite of the large value for I_{sat}). Hence fiber lasers tend to have higher slope efficiencies than comparable bulk solid-state lasers. At high power levels, bulk lasers also suffer from detrimental thermal effects (notably thermal lensing), which also reduce the efficiency.

References

1. C. J. Koester and E. Snitzer, “Amplification in a fiber laser,” Appl. Opt., vol.3, p.1182-1186 (1964).
2. J. Stone and C. A. Burrus, “Neodymium-doped fiber lasers: room temperature CW operation with an injection laser pump,”Appl. Opt., vol.13, p.1256-1258 (1974).
3. R. J. Mears, L. Reekie, S. B. Poole and D. N. Payne, “Neodymium-doped silica single-mode fibre lasers,” Electron Lett., vol.21, p.737-738 (1985).
4. R. J. Mears, L. Reekie, I. M. Jauncey and D.N.Payne, “Low-noise erbium-doped fibre amplifier operating at 1.54µm,” Electron. Lett., vol.23, p.1026-1028 (1987).
5. E. Snitzer, H. Po, F. Hakimi, R. Tumminelli and B. C. McCollum, “Double-clad, offset-core Nd fiber laser,” Proc. Conf. Optical Fiber Sensors, Postdeadline paper PD5, (1988).
6. V. Dominic, S. MacCormack, R. Waarts, S. Sanders, S.Bicknese, R. Dohle, E. Wolak, P. S. Yeh and E. Zucker, “110W fiber laser,” Electron. Lett., **35**, (1999), p1158-1159.
7. K. Ueda, H. Sekiguchi, and H. Kan, Conference on Lasers and Electro-Optics (Optical Society of America, Washington, D.C.2003), Postdeadline paper CPDC4.
8. V. P. Gapontsev, D. V. Gapontsev, N. S. Platonov, O. Shkurihin, V. Fomin, A. Mashkin, M. Abramov and S. Ferin, “2kW CW ytterbium fiber laser with record diffraction-limited brightness,” CLEO-Europe 2005, paper CJ1-1-THU.
9. P. C. Becker, N. A. Olsson, and J. R. Simpson, “Erbium-doped fiber amplifiers: fundamentals and technology” (Academic Press 1999).
10. A. W. Snyder and J. D. Love, “Optical Waveguide Theory,” (Kluwer Academic Publishers 2000).
11. W. J. Miniscalco, “Optical and electronic properties of rare earth ions in glasses,” in *Rare-Earth-Doped Fiber Lasers and Amplifiers*, edited by M. J. F. Digonnet, 2nd edition, (Marcel Dekker, Inc. New York, 2001).
12. K. Kubodera and K. Otsuka, J. Appl. Phys., vol.50, p.653 (1979).
13. W. A. Clarkson and D. C. Hanna, “Effect of transverse-mode profile on slope efficiency and relaxation oscillations in a longitudinally-pumped laser,” J. Mod. Opt., Vol.36, p.483-498.

2. Cladding pumped fibers

The ‘cladding-pumping’ concept

(a) Core pumping

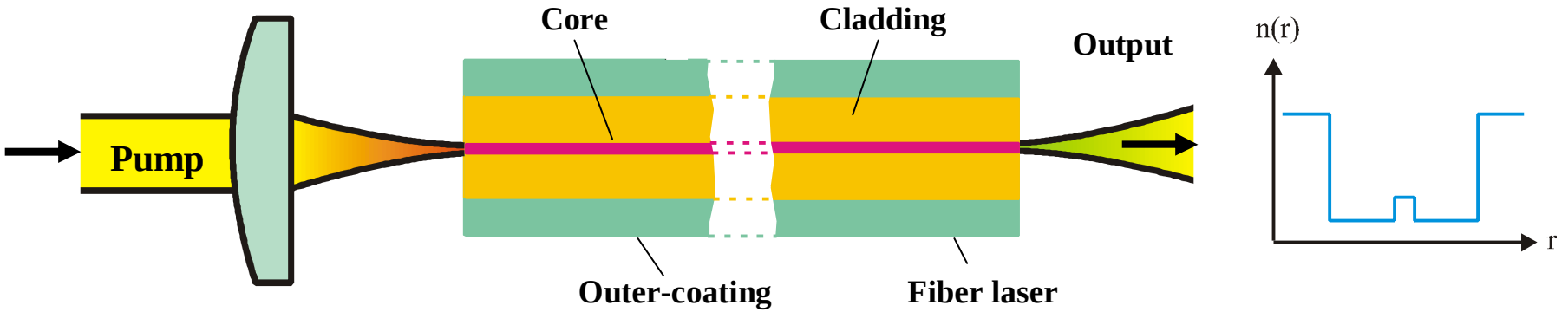

(Pump beam size × Far-field beam divergence) < (Core size × arcsin (Core NA))
→ If the core is single-mode then the pump source must be nearly single-mode

(b) Cladding pumping[1]

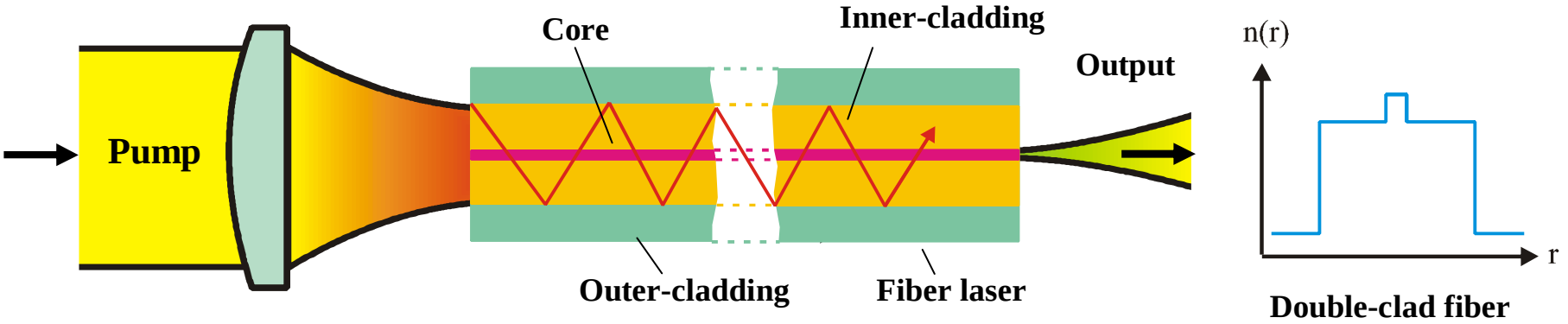

(Pump beam size × Far-field beam divergence) < (Inner-cladding size × arcsin (Inner-cladding NA))
→ Can pump with high power + poor beam quality (i.e. low brightness) diode pump sources

Inner-cladding geometry:

Circular inner-cladding + centred core
- Easy to fabricate + splice
- Rays with trajectories that do not pass through core → Poor pump absorption
- Bending fiber helps but is not very effective with large fibers + high NA's

Circular inner-cladding + off-set core
- Core must be off-set by a large amount for efficient pump absorption
- More difficult to fabricate
- Difficult to splice

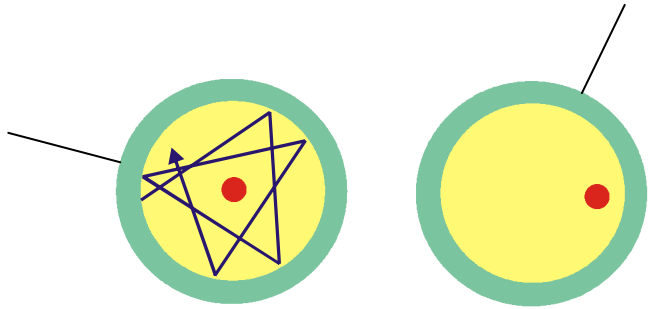

Polygon-shaped inner-cladding + centred core
- More difficult to fabricate
- Very effective way to increase pump absorption efficiency
- Axially-symmetric
- Quite easy to splice

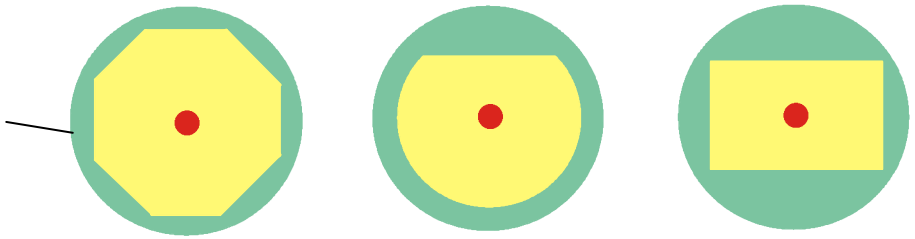

D-shaped inner-cladding + centred core
- Quite easy to fabricate
- Very effective way to increase pump absorption efficiency
- Difficult to splice

Rectangular inner-cladding + centred core
- More difficult to fabricate
- Very effective way to increase pump absorption efficiency
- Helps with asymmetric pump beams
- Difficult to splice

Silica versus other glasses

Silica is generally the material of choice for high-power fiber lasers and amplifiers for the following reasons:

- Very high melting temperature and mechanical strength
- Relatively simple and well-established techniques for fiber fabrication
- Very low loss
- Good handling properties (e.g. splicing and cleaving)
- Compatibility with existing silica-based active and passive low power (e.g. telecom) components
- RE-doping → Useful range of operating wavelengths

Other glasses (e.g. fluoride glass) offer an extended range of operating wavelengths (e.g. in visible and mid-infrared regimes), but fibers have a relatively poor power handling capability and are not compatible with silica-based devices.

Main laser transitions for high-power silica fiber devices

Nd^{3+} doping

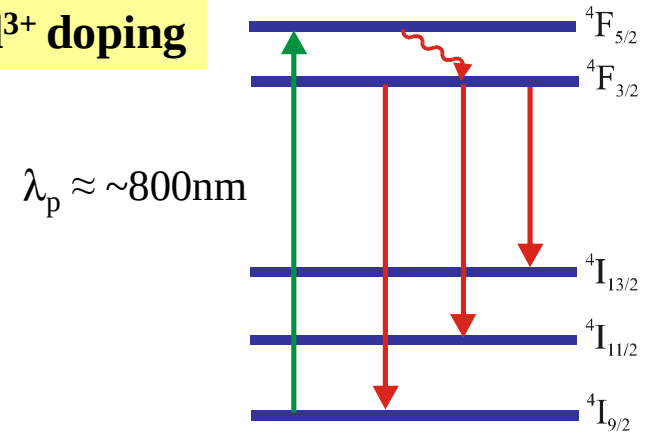

$\lambda_p \approx$ ~800nm

$\lambda_L \approx$ ~1.36μm

$\lambda_L \approx$ 1050 – 1090nm

$\lambda_L \approx$ 905 – 940nm

Nd^{3+}

Yb^{3+} doping

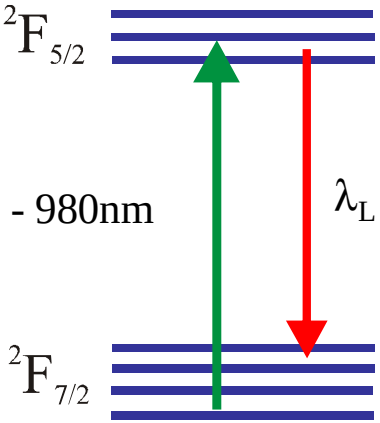

$\lambda_p \approx$ ~900 - 980nm

$\lambda_L \approx$ ~ 980nm, 1030 – 1120nm

Yb^{3+}

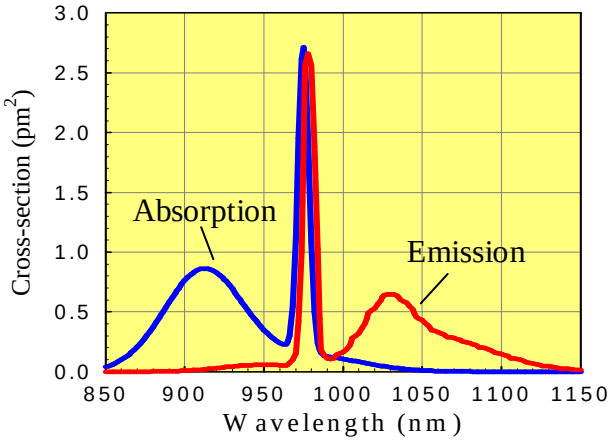

Er^{3+} doping

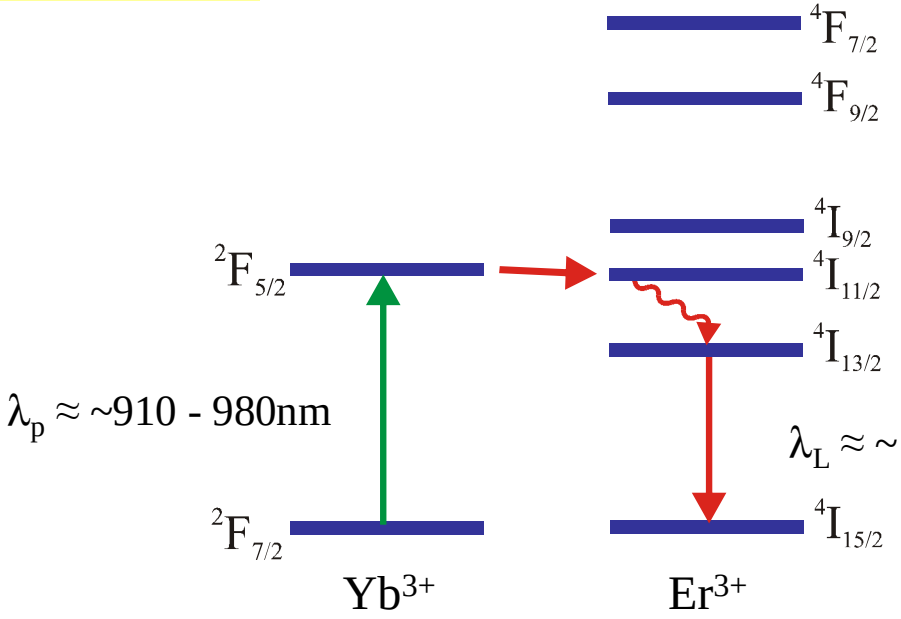

In cladding-pumped fiber configurations Yb^{3+} is used as a sensitizer[2]. Pump light is absorbed by Yb^{3+}, and Er^{3+} is excited by energy transfer from Yb^{3+}

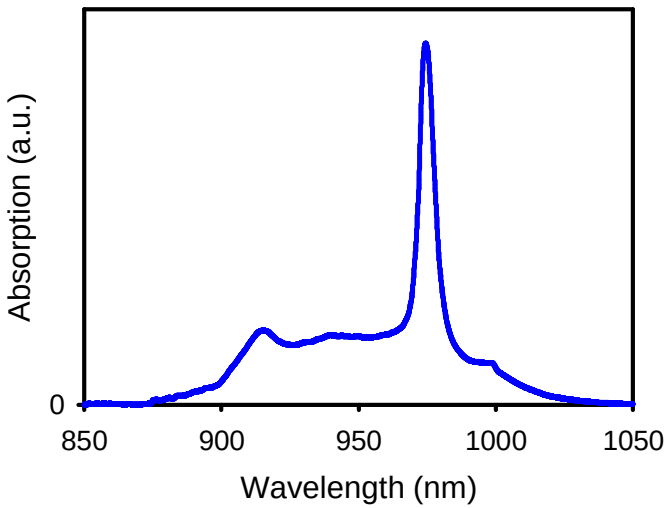

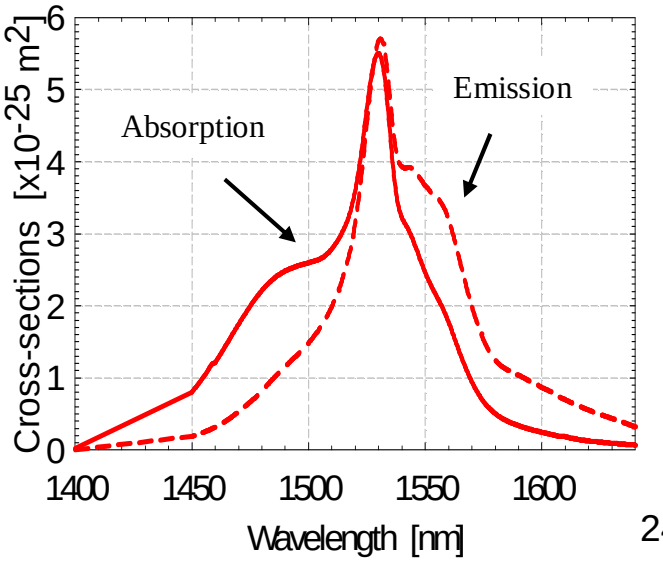

Tm^{3+} doping

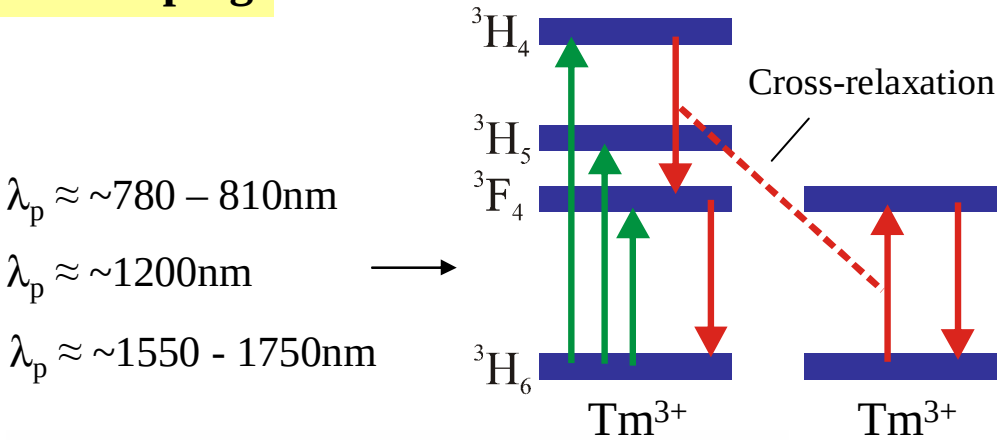

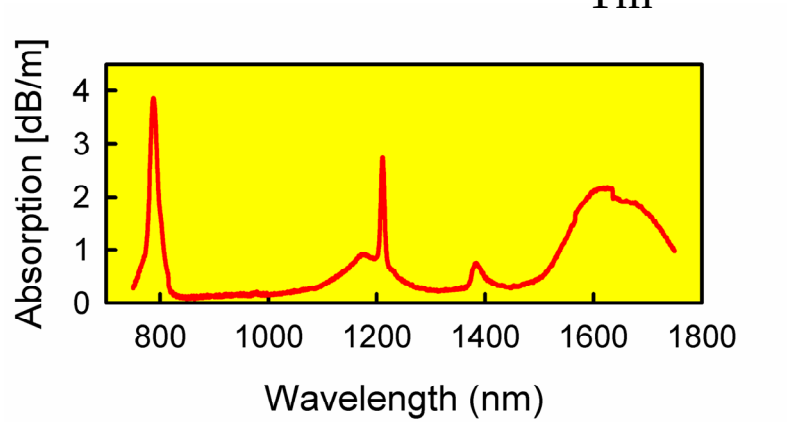

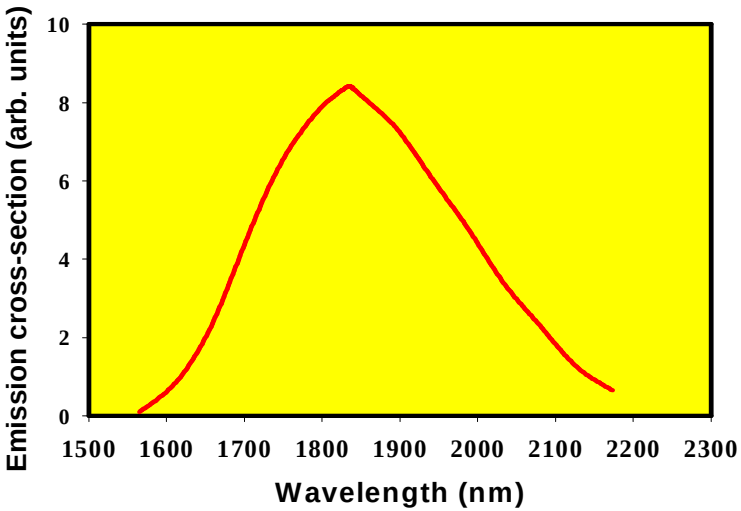

Pumping at ~ 780 – 800nm can be very efficient with careful optimisation of the core composition[3,4]:

- High Tm^{3+} concentration → Efficient 'two-for-one' cross-relaxation
  → Higher absorption coefficient for pump
  → Short device length + reduced loss due to OH^- impurity
- High Al^{3+} concentration → Reduces clustering

Tm^{3+} doping

Can also use Yb^{3+} as a sensitizer[5]. Pump light is absorbed by Yb^{3+}, and Tm^{3+} is excited by energy transfer from Yb^{3+}

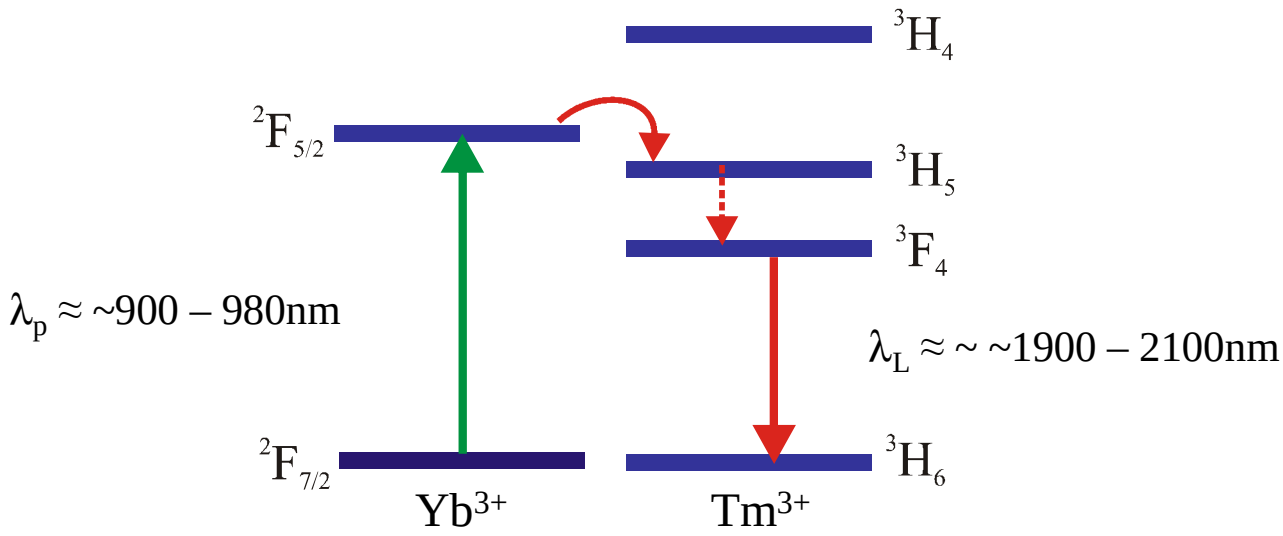

Theory for amplifier and laser performance

Yb-doped silica fibers:

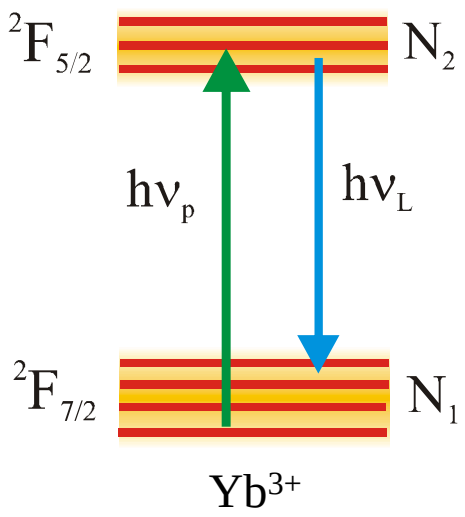

N_1 and N_2 are the population densities for the lower and upper manifolds and N is the total RE ion concentration. λ_p and λ_L are pump and lasing/signal wavelengths respectively.

N_1 and N_2 are determined by the rate equations for upper and lower levels under steady-state conditions[6]:

$$\frac{dN_2}{dt} = (R_{12} + W_{12})N_1 - (R_{21} + W_{21} + A_{21})N_2 = 0 \qquad (1)$$

$$\frac{dN_1}{dt} = -(R_{12} + W_{12})N_1 + (R_{21} + W_{21} + A_{21})N_2 = 0 \qquad (2)$$

where the transition rates are: $R_{12} = \sigma_a(\lambda_p)I_p / h\nu_p$, $R_{21} = \sigma_e(\lambda_p)I_p / h\nu_p$ and $A_{21} = 1/\tau_f$

$$W_{12} = \sigma_a(\lambda_L)I_L / h\nu_L \quad \text{and} \quad W_{21} = \sigma_e(\lambda_L)I_L / h\nu_L$$

σ_a and σ_e are the absorption and emission cross-sections for lower and upper levels respectively and τ_f is the lifetime of the upper level

$$N_1 + N_2 = N \longrightarrow \qquad N_2 = \frac{N(R_{12} + W_{12})}{R_{12} + R_{21} + W_{12} + W_{21} + A_{21}} \qquad (3)$$

The pump loss and growth of the laser/signal light along the fiber are given by:

$$\frac{dP_p}{dz} = \eta_p\left(\sigma_e(\lambda_p)N_2 - \sigma_a(\lambda_P)N_1\right)P_p \qquad (4)$$

$$\frac{dP_L^+}{dz} = \eta_L\left(\sigma_e(\lambda_L)N_2 - \sigma_a(\lambda_L)N_1\right)P_L^+ \qquad (5)$$

$$\frac{dP_L^-}{dz} = -\eta_L\left(\sigma_e(\lambda_L)N_2 - \sigma_a(\lambda_L)N_1\right)P_L^- \qquad (6)$$

where η_p and η_L are overlap factors for the pump and signal/laser light with the doped core. For a double-clad fiber $\eta_p \approx A_{co}/A_{cl}$, where A_{co} is the doped area of the core and A_{cl} is the inner-cladding area and $\eta_L \approx 1$. Equations (4), (5), and (6) can be solved numerically to yield amplifier gain[6] and laser output power.

If we make some simplifying assumptions, then we can obtain approximate expressions for amplifier small signal gain and laser threshold as follows[7]:

In the absence of laser or signal power, and assuming that ASE is negligible, then:

$$\frac{dP_p(z)}{dz} = -\frac{A_{co}h\nu_p N_2(z)}{\eta_q \tau_f} \qquad (7)$$

From (4) and (7):

$$\log_e\left(\frac{P_p(z)}{P_p(0)}\right)+\frac{P_p(z)-P_p(0)}{P_{psat}}=-\eta_p\sigma_a(\lambda_p)N\,z \qquad (8)$$

where

$$P_{psat}=\frac{h\nu_p}{[\sigma_a(\lambda_p)+\sigma_e(\lambda_p)]\tau_f\eta_q}\left(\frac{A_{co}}{\eta_p}\right)$$ is the pump saturation power

In general, equation (8) must be solved numerically to calculate the pump power absorbed in a length of fiber. If $P_p(0) << P_s$ (i.e. there is negligible ground-state depletion) then equation (8) can be simplified to

$$P_p(z)=P_p(0)\exp\left(-\eta_p\sigma_a(\lambda_p)N\,z\right)$$

The single-pass gain G for the fiber is given by:

$$G=\exp\left(\int_0^l g(z)dz-\alpha_L l\right) \qquad \text{where} \qquad g(z)=N_2(z)\sigma_e(\lambda_L)-N_1(z)\sigma_a(\lambda_L)$$

where α_L is the attenuation coefficient for laser/signal light

Using (7), we obtain the following simplified expression for small signal gain:

$$G = \exp\left(\frac{\left(\sigma_e(\lambda_L)+\sigma_a(\lambda_L)\right)\tau_f \eta_q P_{pabs}}{A_{co} h\upsilon_p} - \sigma_a(\lambda_L) N l - \alpha_L l\right)$$

Re-absorption loss Core propagation loss

where P_{pabs} is the absorbed pump power

G can also be expressed in dB as

$$10\log_{10} G = 4.34\left(\frac{\left(\sigma_e(\lambda_L)+\sigma_a(\lambda_L)\right)\tau_f \eta_q P_{pabs}}{A_{co} h\upsilon_p} - \sigma_a(\lambda_L) N l - \alpha_L l\right)$$

Example: Cladding-pumped Yb-doped fiber amplifier

Parameters: $r_a = 10\mu m$, $\eta_q = 1$, $\tau_f = 1ms$, $\lambda_L = 1100nm$
$\sigma_e(\lambda_L) \approx 2 \times 10^{-23} m^2$

Assume: Negligible propagation loss and $\sigma_a(\lambda_L) N l \approx 0$
(i.e. four-level approximation)

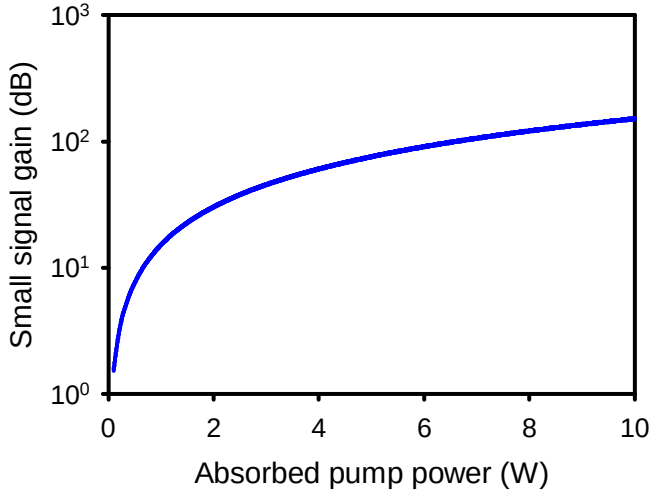

In practice, the small signal gain will be limited by the onset of parasitic lasing or amplified spontaneous emission to < ~30dB

Small-signal gain regime: $G^+ = G^-$

Saturated gain regime: $G^+ < G^-$ → Use counter-propagating pump and signal beams in power amplifier

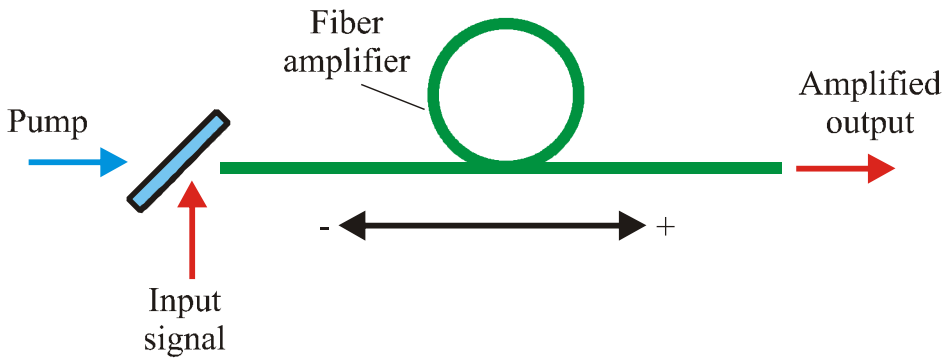

Co-propagating pump and signal beams

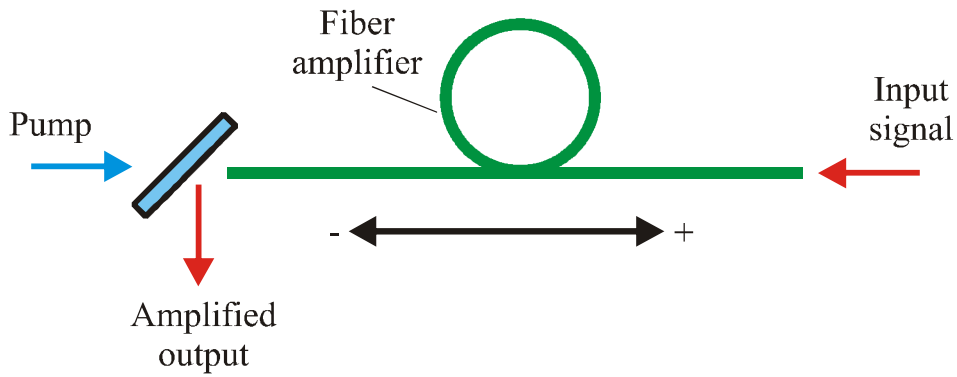

Counter-propagating pump and signal beams

Signal saturation power: $P_{Lsat} \approx \dfrac{h\nu_L A_{co}}{[\sigma_a(\lambda_L)+\sigma_e(\lambda_L)]\tau_f} \approx 0.28\text{W}$ for previous example

Need input signal to exceed saturation power for amplifier to achieve efficient power extraction

→ Limits gain for practical power amplifiers to ~ 10dB – 30dB

Power scaling with a master-oscillator power-amplifier (MOPA)

Need a chain of amplifiers to scale the output power from a low power master-oscillator

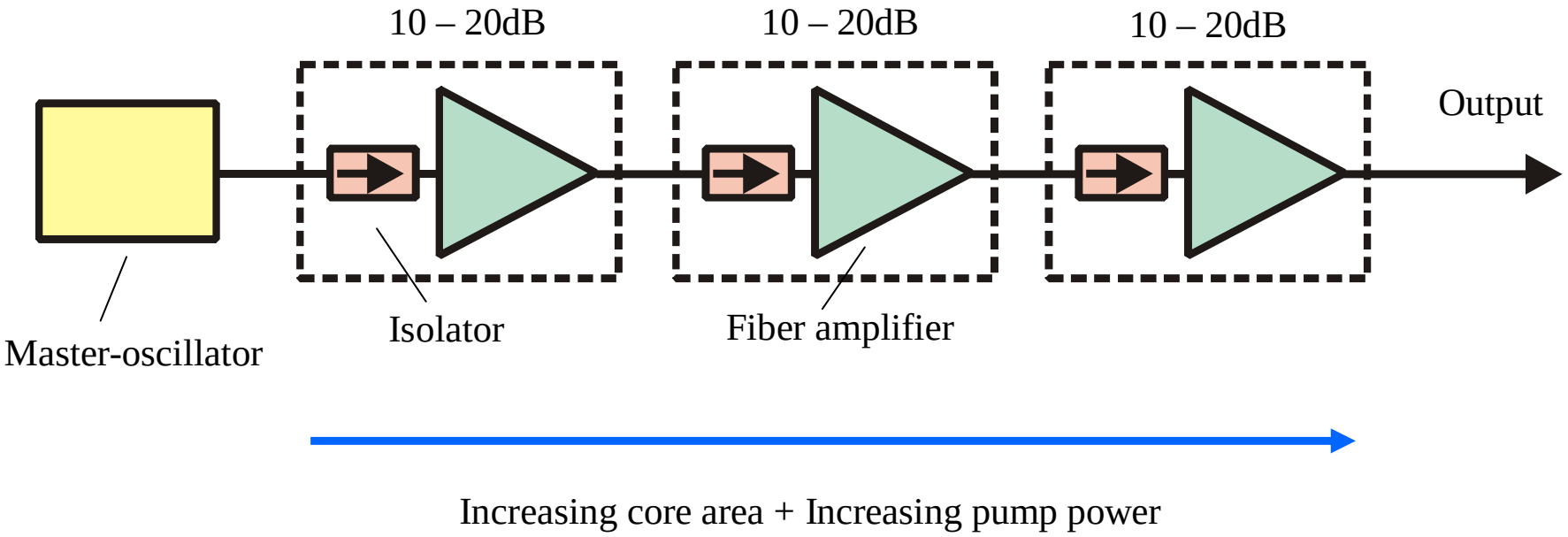

Threshold pump power:

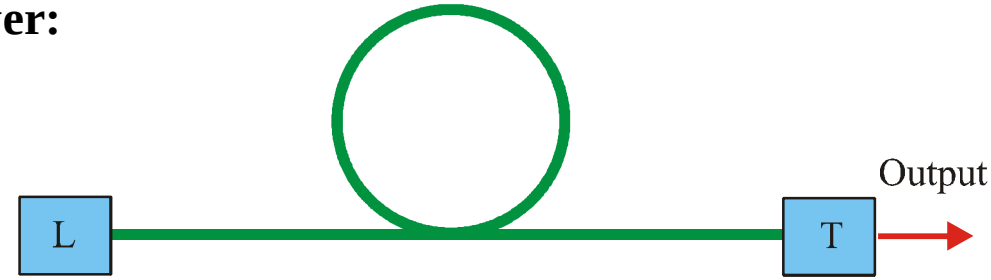

T = transmission of output coupler
L = Cavity loss due to imperfect feedback at opposite end of cavity

Round-trip gain at threshold:

$$G = \left[\exp\left(\frac{\left(\sigma_e(\lambda_L) + \sigma_a(\lambda_L)\right)\tau_f \eta_q P_{pabs}}{A_{co} h\upsilon_p} - \sigma_a(\lambda_L) N l - \alpha_L l \right) \right]^2 (1-T)(1-L) = 1$$

$$\longrightarrow \quad P_{pabs,th} = \frac{A_{co} h\upsilon_p}{2\tau_f \eta_q \left(\sigma_e(\lambda_L) + \sigma_a(\lambda_L)\right)} \left[-\log_e(1-T) - \log_e(1-L) + 2\sigma_a(\lambda_L) N l + 2\alpha_L l \right]$$

Previous example: Cladding-pumped Yb-doped fiber laser

Parameters: $r_a = 10\mu m$, $\eta_q = 1$, $\tau_f = 1ms$, $\lambda_L = 1100nm$
$\sigma_e(\lambda_L) \approx 2 \times 10^{-23} m^2$, L = 0, T = 96%

$\longrightarrow$ $P_{pabs,th} \approx 0.46W$

Assume: Negligible propagation loss and $\sigma_a(\lambda_L) N l \approx 0$
(i.e. four-level approximation)

Slope efficiency:

At power levels well above threshold (i.e. $P_L >> P_{Lsat}$) and assuming that the core propagation loss is negligible, then the slope efficiency is given by the following approximate expression:

$$\eta_s = \frac{dP_{Lout}}{dP_p} \approx \frac{T\sqrt{1-L}}{T\sqrt{1-L}+L\sqrt{1-T}} \cdot \left(\frac{\lambda_p}{\lambda_L}\right) \cdot \eta_q \eta_{abs}$$

When T + L <<1, this simplifies to

$$\eta_s = \frac{dP_{Lout}}{dP_p} \approx \frac{T}{T+L} \cdot \left(\frac{\lambda_p}{\lambda_L}\right) \cdot \eta_q \eta_{abs}$$

In a typical cladding-pumped fiber laser, the transmission of the output coupler is very high and the fiber length is selected so that the absorption efficiency (η_{abs}) is ~1, so $\eta_s \rightarrow \eta_q \lambda_p/\lambda_L$ providing there is sufficient feedback at the opposite (non-output) end of the cavity.

Effect of feedback efficiency on laser performance

P_1 = Output power

P_2 = total power loss in feedback optical arrangement

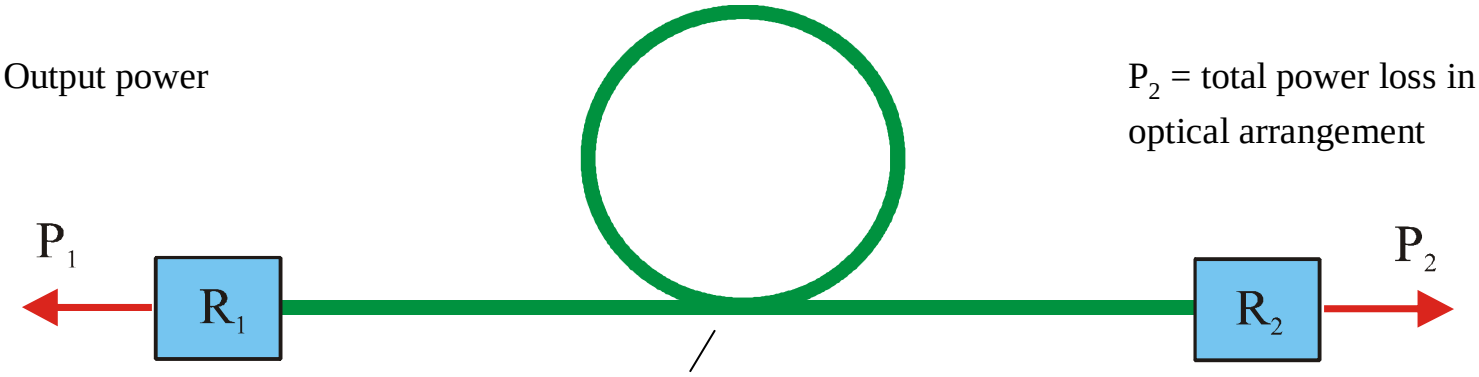

Rigrod analysis[8]:

Power in fiber

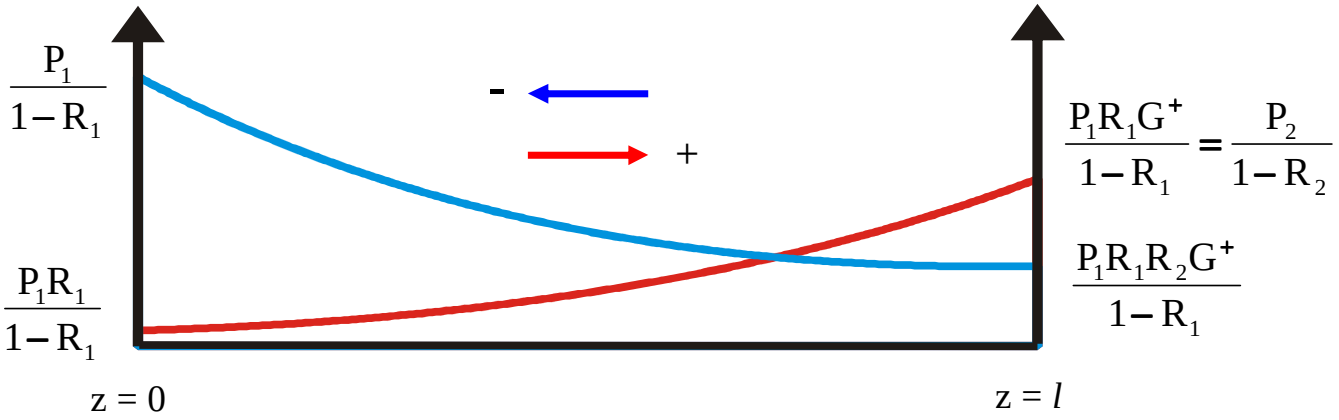

$$\frac{P_1^+}{1-R_1} = \frac{P_1 R_1 R_2 G^+ G^-}{1-R_1} \quad \rightarrow \quad R_1 R_2 G^+ G^- = 1$$

$G^+ = G^-$ = Effective single-pass gain (taking into account core propagation loss)

Simple result:

$$\frac{P_1}{P_2} = \frac{1-R_1}{1-R_2}\sqrt{\frac{R_2}{R_1}}$$

For a high lasing efficiency we require $P_1 >> P_2$

Example: Cladding-pumped fiber laser with feedback for lasing provided by a perpendicularly-cleaved fiber end facet and an external feedback cavity.

Question: What feedback efficiency for the external cavity is required for efficient operation?

- Relatively modest feedback efficiency for external cavity is needed
- Constraints on feedback cavity design can further relaxed by reducing R_1 (e.g. by anti-reflection coating the fiber end facet)

Very high gain → Enormous flexibility in cavity design without compromising efficiency

Warning: Using a very low reflectivity output coupler makes the fiber laser very susceptible to optical feedback from external components

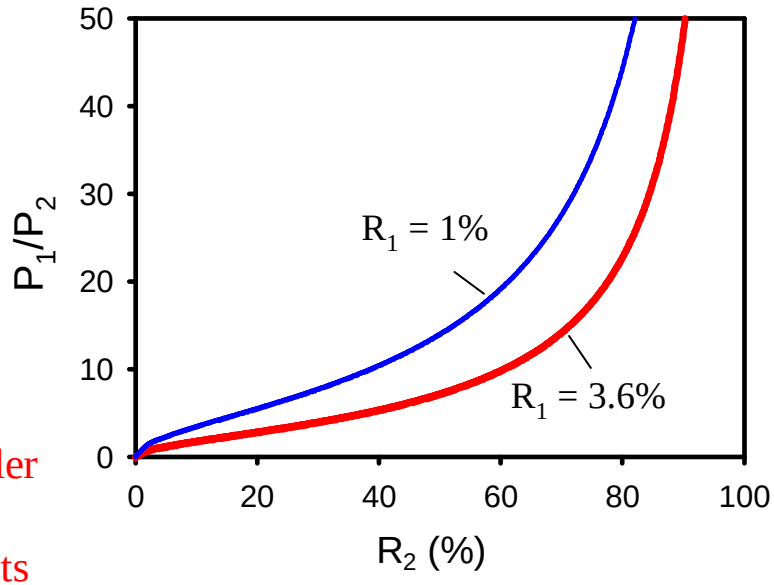

External feedback cavity design

Generalised feedback arrangement:

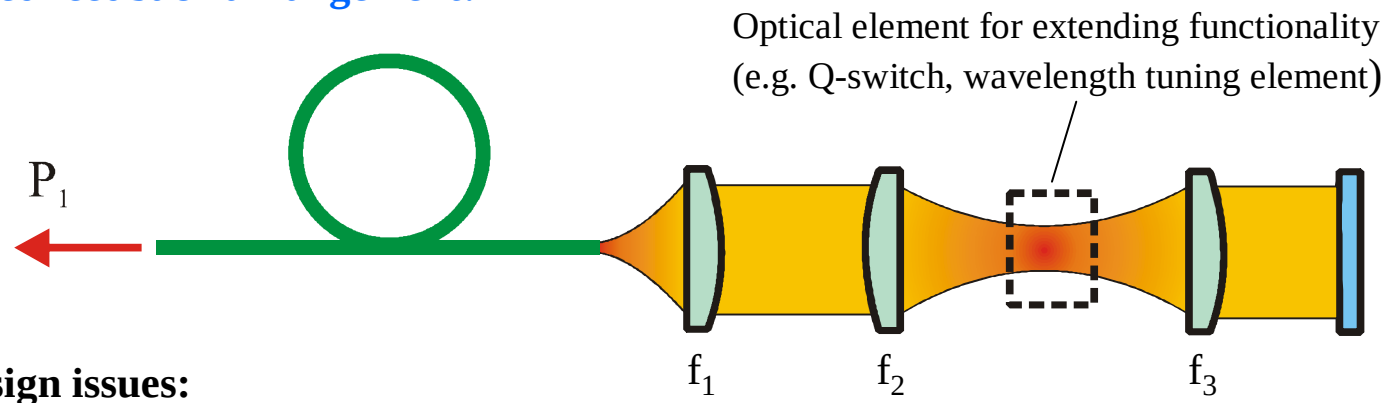

Main design issues:

- Broadband feedback from end-facet adjacent to external cavity should be suppressed so that it does not compete with external cavity's function
- Low loss + AR coated intracavity components required
- Degradation in beam quality (M^2) due to lens aberration[9] can dramatically reduce the feedback efficiency

$$M_f^2 = \sqrt{(M_i^2)^2 + (M_q^2)^2} \quad \text{where} \quad M_q^2 = \frac{8\pi C_4 w_i^4}{f^3 \lambda_L \sqrt{2}} \approx \frac{8\pi C_4 f \theta^4}{\lambda_L \sqrt{2}}$$

where w_i is the beam radius on the lens, θ is the far-field beam divergence and C_4 is the quartic phase aberration coefficient (= 0.29 for a plano-convex lens for infinite conjugate ratio)

→ Need to keep beam divergence <0.05 rad with singlet lenses to avoid degradation in beam quality or use aspheric or multi-element lenses

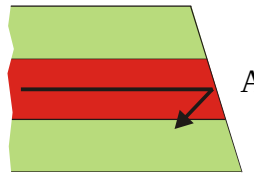

or

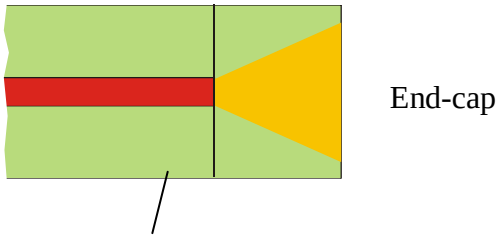

Most of the reflected light is guided in the inner-cladding where the propagation loss is generally much higher and the effective gain is much lower → Dramatic reduction in feedback from end-facet

Simple feedback cavity:

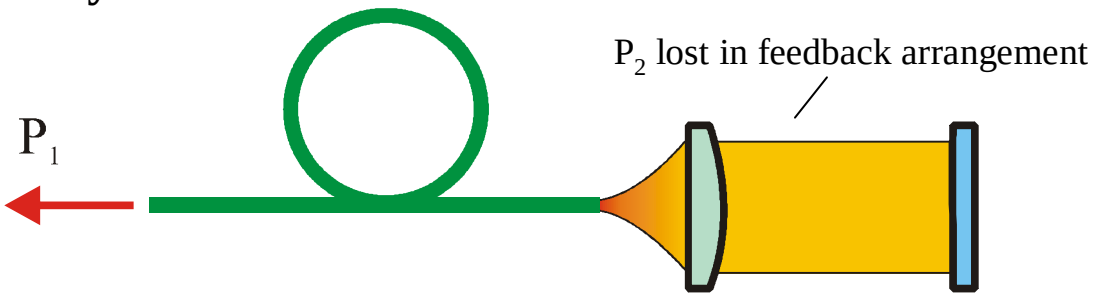

- Power in feedback cavity << Output power (P_1)
- Power handling capability of feedback cavity components may not be an issue

→ Simple + effective method for scaling to very high (>1kW) power levels[10,11]

Alternative resonator feedback schemes:

(a) Butted mirror

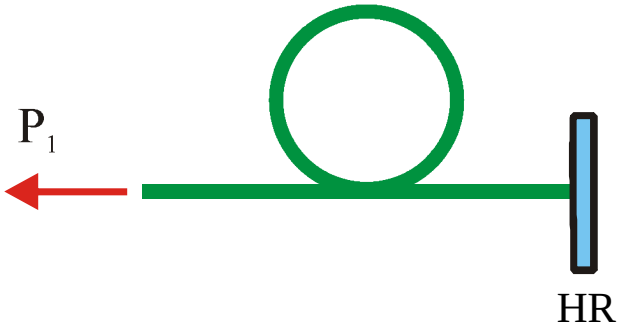

- Simple, but limited scope for power scaling due to mirror damage

(b) Fiber Bragg grating

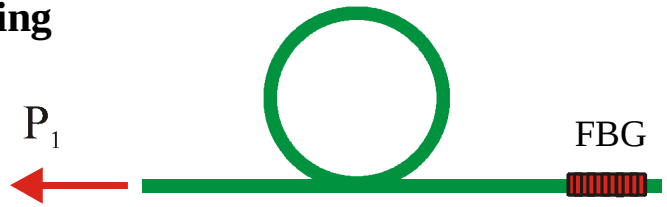

- All fiber
- Very high feedback efficiency
- Power handling??

References

1. E. Snitzer, H. Po, F. Hakimi, R. Tumminelli and B. C. McCollum, “Double-clad, offset-core Nd fiber laser,” Proc. Conf. Optical Fiber Sensors, Postdeadline paper PD5, (1988).
2. J. D. Minelly, W. L. Barnes, R. I. Laming, P. R. Morkel, J. E. Townsend, S. G. Grubb and D. N. Payne, “Diode-array pumping of Er/Yb co-doped fiber lasers and amplifiers,” IEEE Photon Tech. Lett., vol.5, p.301-303 (1993).
3. S. D. Jackson, “Cross relaxation and energy transfer upconversion processes relevant to the functioning of 2μm Tm-doped silica fibre lasers,” Opt. Comm., vol.230, p.197-203 (2004).
4. G. Frith, D. G. Lancaster and S. D. Jackson, “85W Tm^{3+}-doped silica fibre laser,” Electron. Lett., vol.41, p.687-688 (2005).
5. Y. Jeong, P. Dupriez, J. K. Sahu, J. Nilsson, D. Y. Shen, W. A. Clarkson and S. D. Jackson, “ Power scaling of 2μm ytterbium-sensitised thulium-doped silica fibre laser diode-pumped at 975nm,” Electron Lett., vol.41, p.173-174 (2005).
6. R. Paschotta, J. Nilsson, A. C. Tropper and D. C. Hanna, “Ytterbium-doped fiber amplifiers,” IEEE J. Quantum Electron., vol.33, p.1049-1056 (1997).
7. H. Pask, R. J. Carman, D. C. Hanna, A. C. Tropper, C. J. Mackechnie, P. R. Barber and J. M. Dawes, “Ytterbium-doped silica fibers: Versatile sources for the 1-1.2 μm region,” IEEE J. Selected Topics in Quantum Electronics, vol.1, p.2-12 (1995).
8. W. W. Rigrod, “Saturation effects in high-gain lasers,” J. Appl. Phys. vol.36, p.2487-2490 (1965).
9. A. E. Siegman, “Analysis of laser beam quality degradation caused by quartic phase aberrations,” Appl. Opt., vol.32, p.5893-5901 (1993).
10. Y. Jeong, J. K. Sahu, D. N. Payne and J. Nilsson, “Ytterbium-doped large-core fiber laser with 1.36kW continuous-wave output power,” Opt. Express, vol.12, p. 6088-6092 (2004).
11. A. Tunnermann, T. Schreiber, F. Roser, A. liem, S. Hofer, H. Zellmer, S. Nolte and J. Limpert, ”The renaissance and bright future of fiber lasers,” J. Phys. B: At. Mol. Opt. Phys., vol.38, p.681-693 (2005).

3. Pump sources and pump coupling

Introduction

- Efficient coupling of pump light from one or more high power diode laser pumps into double-clad fibers is essential for efficient power and brightness scaling of cladding-pumped fiber sources.

- This requires careful selection of the pump diode(s), and very careful design and precise alignment of the pump light collection, delivery and coupling optical arrangement.

- The choice of pump source and incoupling scheme is a major element of the overall fiber system design and can have a huge impact on the overall system performance and on flexibility in mode of operation.

- Pump brightness is usually the key factor. The higher the pump brightness, the more flexibility there is in the choice of fiber design and mode of operation, and the easier it is to scale to high output powers.

- Advances in high-power diode pump sources and pump coupling techniques over the last decade have been dramatic, and this has probably been the single biggest factor in taking fiber-based sources to the power levels reported to date

Brightness and the M^2 parameter

$$\textbf{Brightness (or radiance)} \equiv \frac{\textbf{Power}}{\textbf{Area} \times \textbf{Solid angle}} \qquad (\text{Units}: \mathrm{Wm^{-2}sr^{-1}})$$

Fundamental transverse mode (diffraction-limited): $B \propto \frac{\text{Power}}{\lambda^2}$

Non-diffraction-limited beam ($M_{x,y}^2 > 1$): $B \propto \frac{\text{Power}}{M_x^2 M_y^2 \lambda^2}$

where $M_{x,y}^2$ is the beam propagation factor[1]

- B determines the maximum focussed intensity
- B is invariant as beam propagates through a (perfect) lens system

B determines the maximum pump power that can be coupled into a double-clad fiber

Calculating pump beam sizes and beam divergences

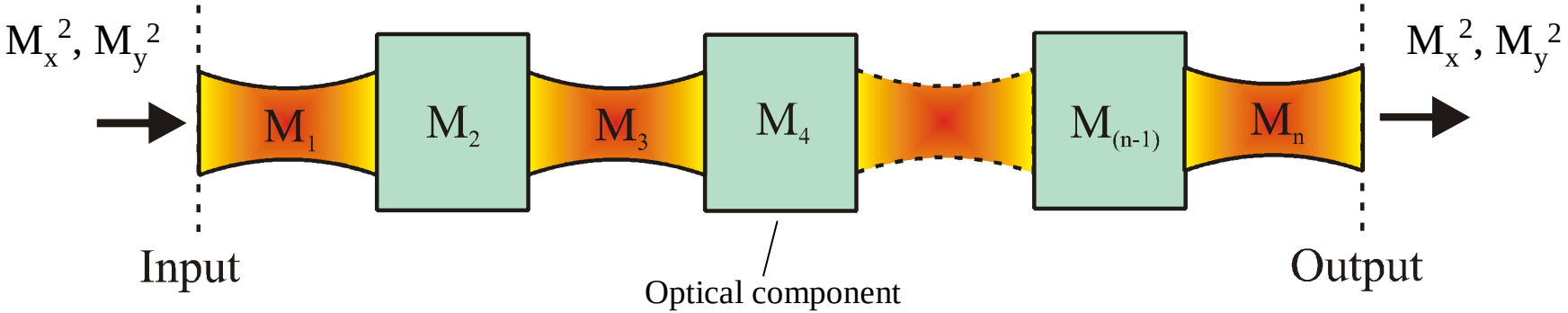

Ray Transfer Matrix for optical system: $M_s = \begin{vmatrix} A_s & B_s \\ C_s & D_s \end{vmatrix} = M_n M_{(n-1)} \ldots\ldots\ldots M_3 M_2 M_1$

Using ABCD law[2]: $q_{out\,x,y} = \dfrac{A_s q_{in\,x,y} + B_s}{C_s q_{in\,x,y} + D_s}$

where q is the complex beam parameter given by : $\dfrac{1}{q} = \dfrac{1}{R} - \dfrac{jM^2\lambda}{\pi w^2}$

w = beam radius and R = radius of curvature of wavefronts

→ Simple procedure for calculating output beam parameters from an optical system given knowledge of the input beam parameters and M_s.

Important assumption: M_x^2 and M_y^2 are preserved

Focusing pump light into double-clad fibers

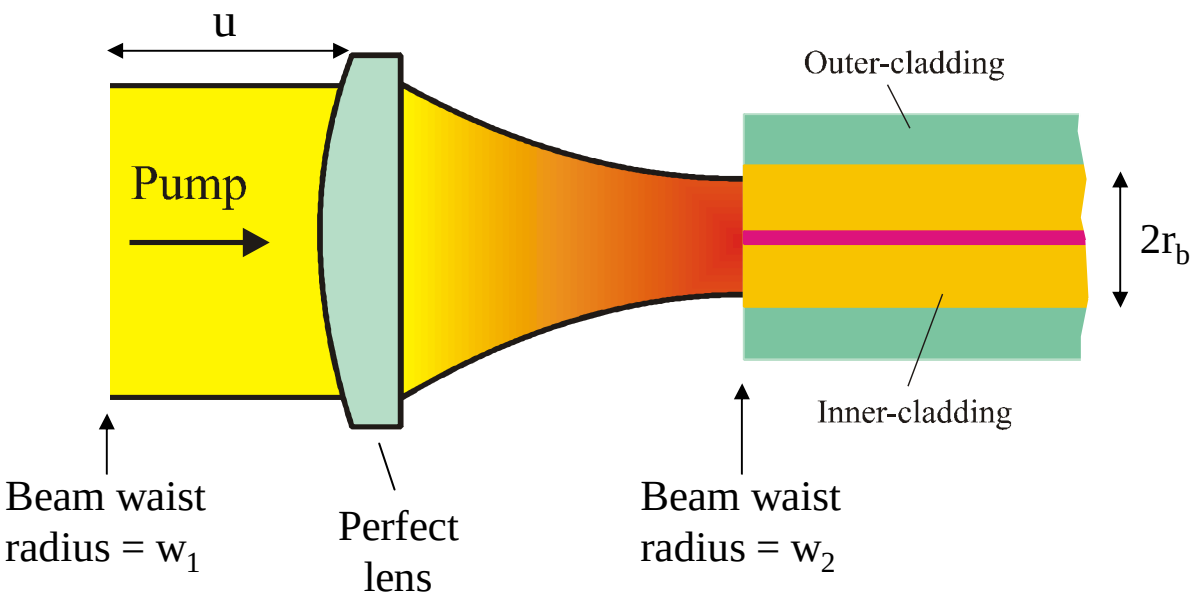

$$\frac{w_2}{w_1} = \frac{f}{\sqrt{z_{o1}^2 + (u-f)^2}}$$

$$z_{o1} = \frac{\pi w_1^2}{M^2 \lambda}$$

For efficient launching of pump light into the inner-cladding:

$$r_b \geq \frac{\lambda M_p^2}{\pi \theta_{na} \gamma_{uf}}$$

where θ_{na} = arcsin(NA) and γ_{uf} is a factor which takes into account the need to underfill the inner-cladding and inner-cladding's NA to avoid pump-induced damage to the outer-coating. The value for γ_{uf} depends on the situation and, in particular, the pump power.

Rough guide: For efficient pump coupling, the beam propagation factor for pump source must satisfy:

$$M_p^2 \leq \frac{\pi \theta_{na} r_b \gamma_{uf}}{\lambda_p}$$

Typical situation:

Double-clad fiber with

- NA = 0.4
- λ_p = 980nm
- γ_{uf} = 0.8

$2r_b$ (μm)	θ_{na} (rad)	M_p^2
125	0.41	66
200	0.41	105
400	0.41	210
600	0.41	315

Diode Laser Pump Sources

Wavelength options:

GaN	→	380-nm – 480nm	→	Pr^{3+}
GaInP, AlGaInP	→	640nm – 680nm	→	Cr:LiCAF, Cr:LiSAF
AlGaAs, GaAs	→	780nm – 860nm	→	Nd^{3+}, Tm^{3+}
InGaAs	→	900nm – 980nm	→	Yb^{3+}, Er^{3+}
InGaAsP/InP	→	1.47μm – 1.6μm	→	Er^{3+}
InGaAsP	→	1.8μm – 1.96μm	→	Ho^{3+}

Diode laser types:

(a) Single-stripe (single-mode) diode lasers

Emitter size ~1μm × few μm

Beam divergence (FWHM): $\theta_y \approx 25°$- $30°$ (perpendicular to junction) and $\theta_x \approx 7°$ (parallel to junction)

$M_y^2 = M_x^2 = 1$

Max. cw output power ~0.5 – 0.8W (limited by catastrophic failure)

(b) Broad area diode lasers

Emitter size ~1µm × ~100µm

Beam divergence (FWHM): $\theta_y \approx 25°\text{-}\ 30^o$ and $\theta_x \approx 8^o$

$M_y^2 = 1$ and $M_x^2 \sim 15\text{-}20$

Max. cw output power ~ 7 - 8W

(c) Diode-bars

Emitting region ~1µm × 10mm

Beam divergence (FWHM): $\theta_y \approx 25°\text{-}\ 30^o$

and $\theta_x \approx 6°\text{-}\ 9^o$

$M_y^2 = 1$ and $M_x^2 \sim 1300\text{-}1800$

Max. cw output power ~ 40-120W

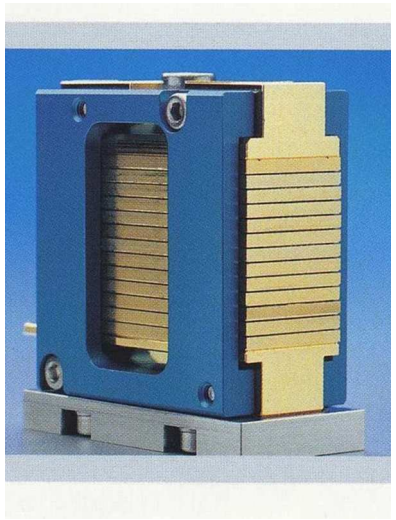

(d) Diode-stacks

Emitter region ~ N × bar spacing × 10mm

Beam divergence (FWHM): $\theta_y \approx 25°\text{-}\ 30^o$ and $\theta_x \approx 9^o$

$M_y^2 \approx [(N\text{-}1) \times$ bar spacing/emitter height$] + 1$

and $M_x^2 \sim 1300\text{-}1800$

Max. cw output power ~ 40-120W × N

Main requirements for efficient pump coupling:

1. Selection of appropriate diode pump laser(s)

2. Pump light collection and aperture filling

3. Re-formatting of the beam using a ‘Beam - Shaper’ to roughly equalise the M^2 parameters in orthogonal planes preferably without decreasing the brightness

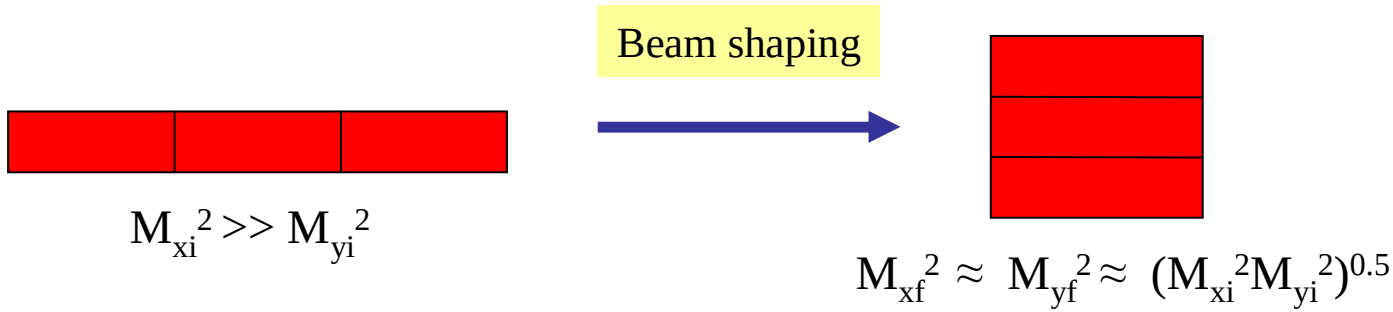

4. Scheme for launching into fiber

5. Management of stray pump light

How much pump light can be launched into a double-clad fiber?

The maximum launched pump power depends on:

- Brightness of a constituent emitter of the pump sources
- Pump collection, delivery and coupling scheme
- Fiber's inner-cladding size and NA

Theoretical upper limit (i.e. for a 'perfect' pump launching scheme) is given by:

$$P_{p\,max} \approx \frac{P_s}{M_x^2 M_y^2}\left(\frac{\pi r_b \theta_{na} \gamma_{uf}}{\lambda_p}\right)^2$$

where P_s is the power of a single (constituent) emitter and M_x^2 and M_y^2 are its beam propagation factors in orthogonal planes

Example: P_s = 8W, M_x^2=20, M_y^2=1

→ Very high launched pump powers, but not possible to achieve in practice due to lens imperfections and tight alignment tolerances

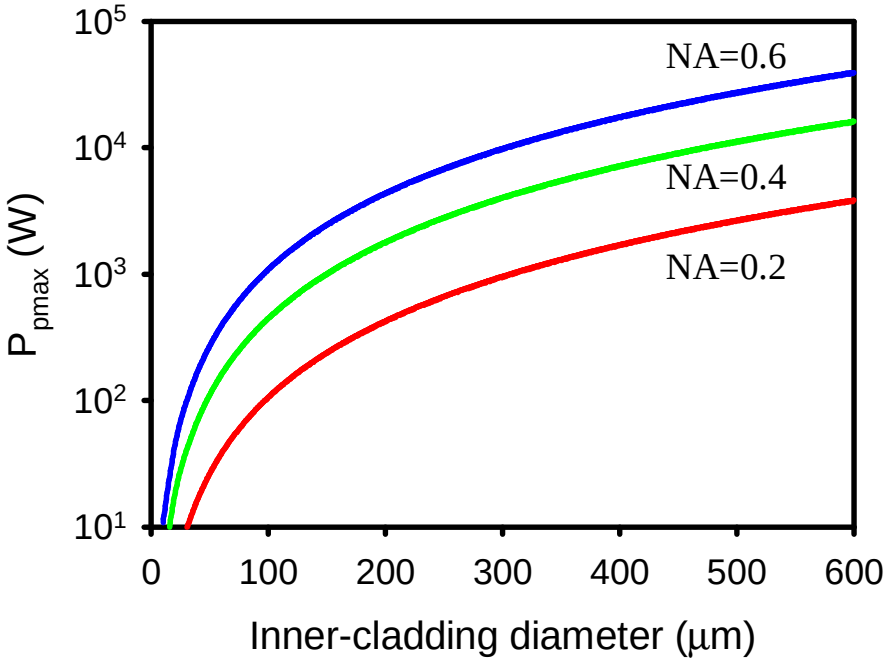

Pump launching schemes:

1. **End-pumping:**
   - Higher brightness pumping
   - Short device length → Higher threshold for unwanted nonlinear loss processes
     → Lower propagation loss
   - Flexibility in fiber design + better fiber laser/amplifier performance
   - Free-space beams → optical components needed
   - Alignment issues
   - High pump deposition density at fiber end

2. **Side-pumping:**
   - Multi-point pump injection and distributed pump injection configurations
   - Distributed heat loading
   - Easy access to fiber ends for splicing to other components
   - All fiber architecture → Robust + fewer optical components + no alignment issues
   - Lower brightness pumping
   - Longer device length → Higher propagation loss
     → Lower threshold for nonlinear loss processes

Examples of pump launching schemes

V-groove scheme:

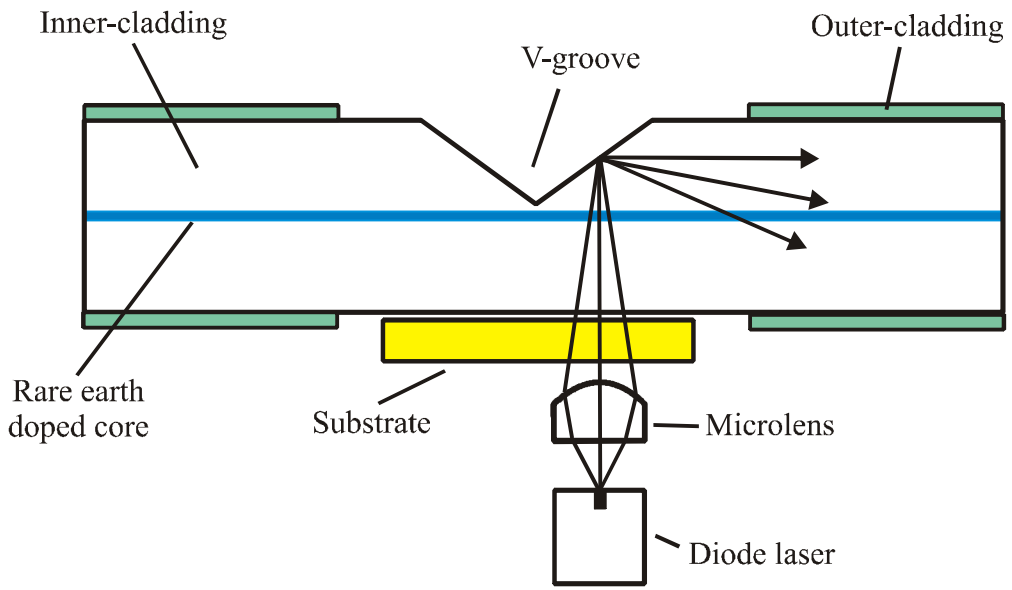

- Simple side pumping scheme that requires few optical components[3,4]
- Beam divergence, $\theta \leq$ arcsin(NA) $\rightarrow$ Limits use to broad-area diode pumps
- Relatively large degradation in pump brightness on launching
- Power scaling via the use of multiple pump injection points

Multimode fiber coupler[5]:

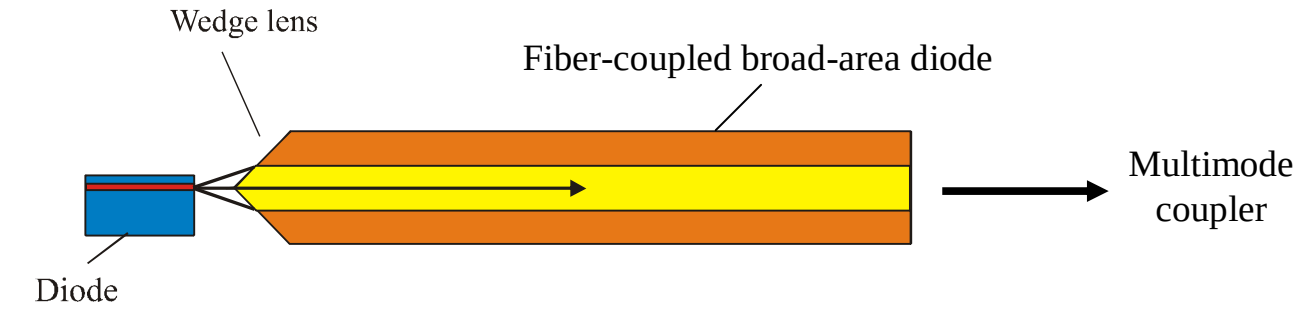

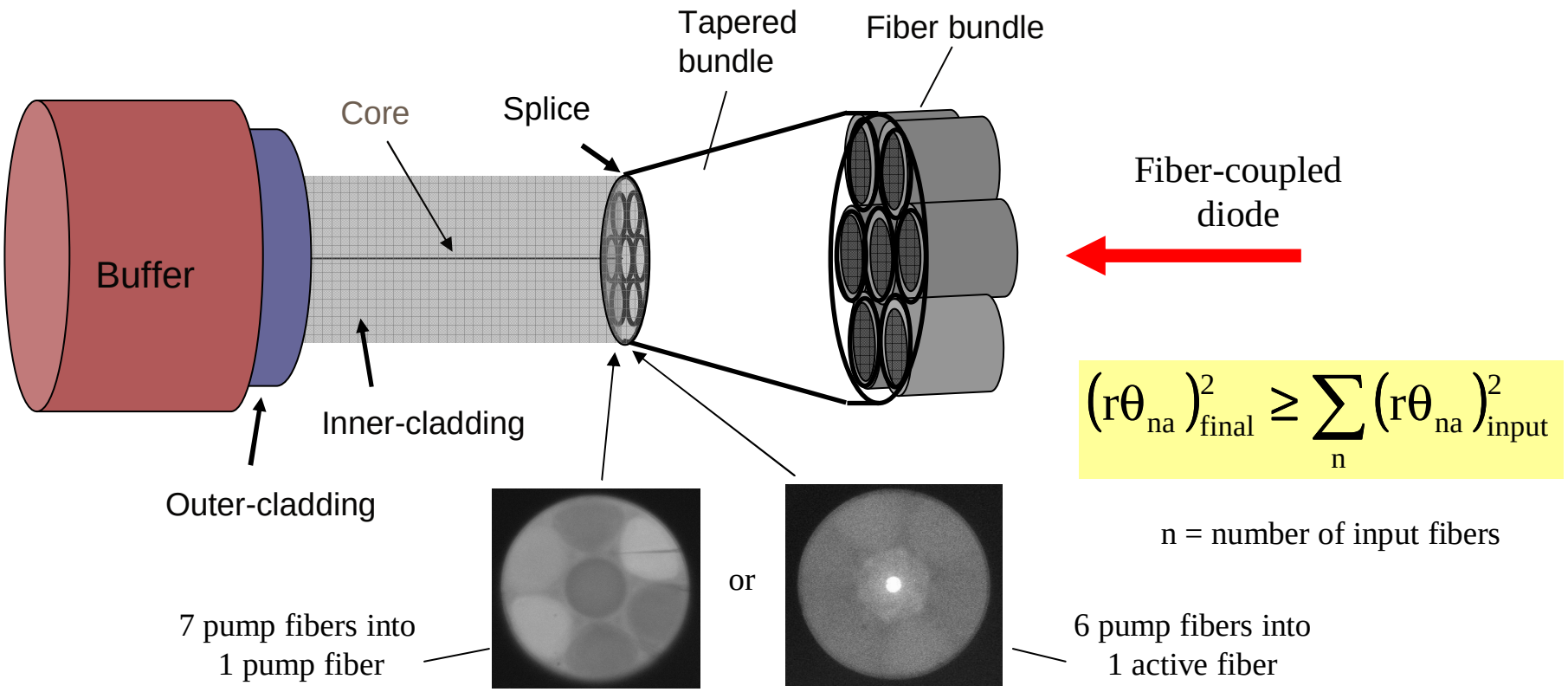

$$(r\theta_{na})^2_{final} \geq \sum_n (r\theta_{na})^2_{input}$$

n = number of input fibers

→ Can be used for end-pumping and/or multi-injection-point side pumping

Distributed pump coupling scheme[7]:

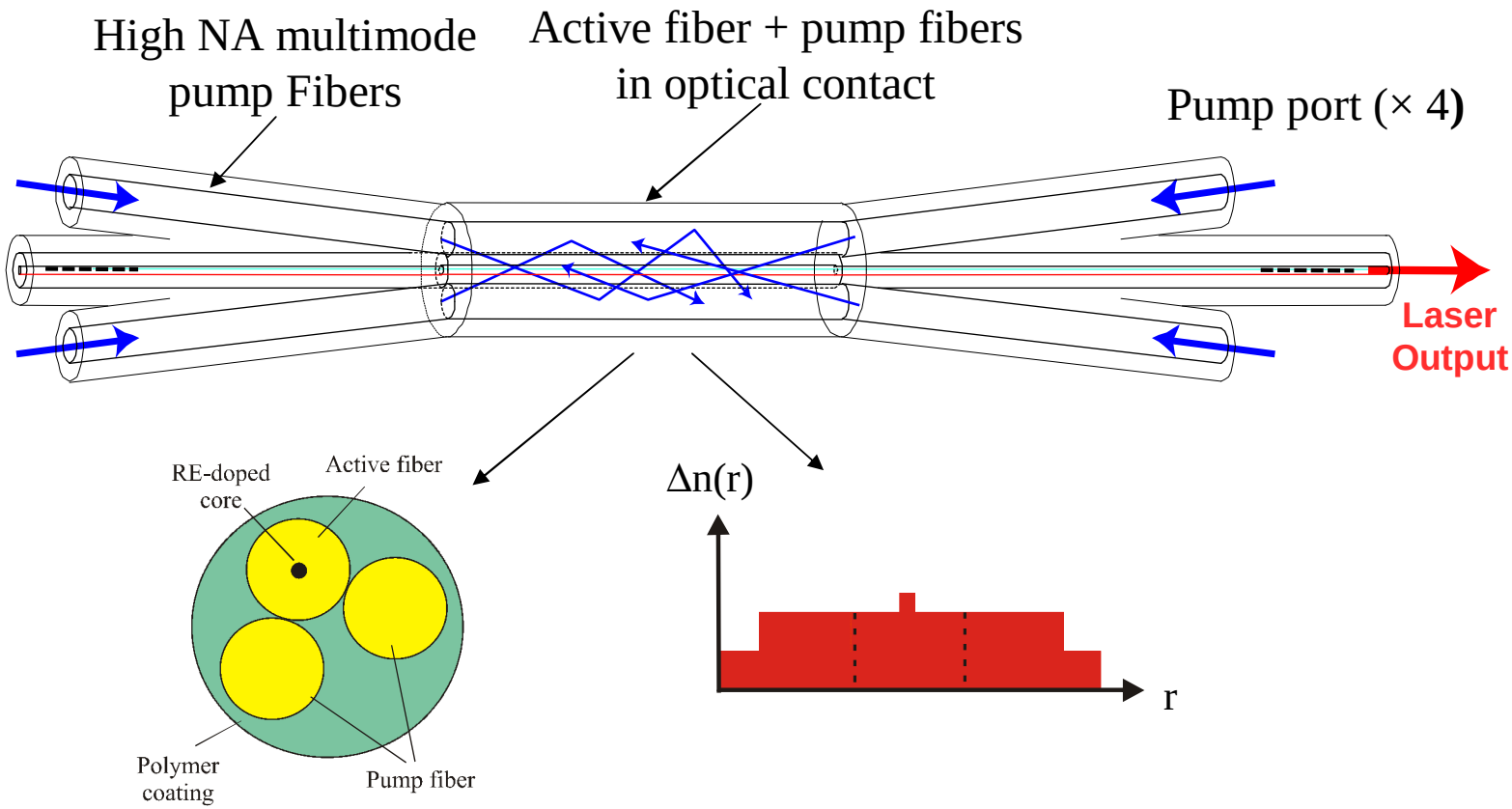

- Pump and active fibers are in optical contact → Breaks symmetry → Efficient pump absorption
- More uniform pump deposition than for end-pumping or multi-point injection
- Access to fiber ends for splicing to other fibers

Side-pumped coiled fiber[8]:

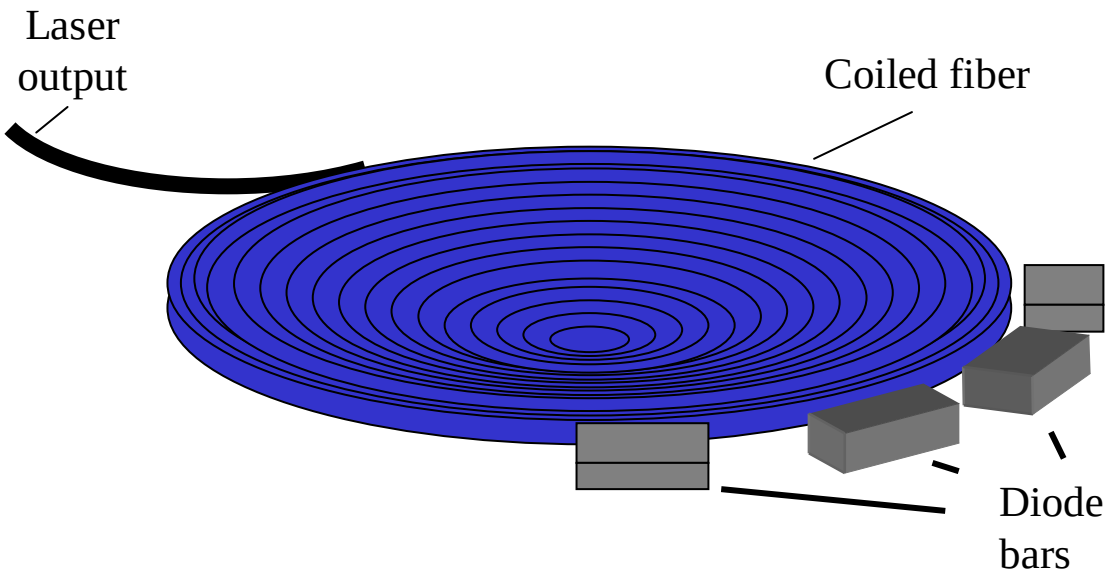

- Coiled fiber with rectangular inner-cladding embedded in a disk that acts as a waveguide for pump light
- Can be pumped by diode bars (or stacks)
- Disk geometry → Simple thermal management
- More suitable for four-level transitions

Pumping schemes for diode arrays

- Side pumping or end pumping schemes may be used
- In both cases, the output from the diode array must be re-formatted to allow efficient coupling into the active fiber or pump delivery fiber
- Fiber end termination must be designed to eliminate the risk of damage due to stray (uncoupled) pump light

Example of fiber end termination:

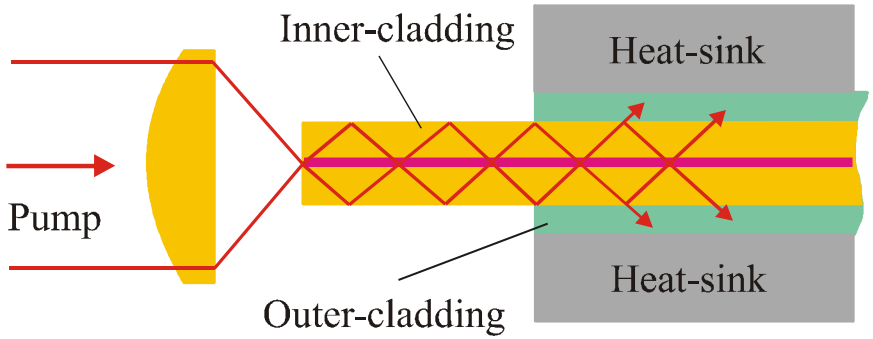

Main features:

- Section of uncoated fiber protruding from heat-sink so that uncoupled pump light spreads out by diffraction and is not incident on the outer-coating
- Heat-sink over first section of coated fiber minimises the risk of damage due to high divergence pump light leaking into the outer-coating

Fiber-bundle-coupled diode-bars: (see refs. 9 and 10)

(a)

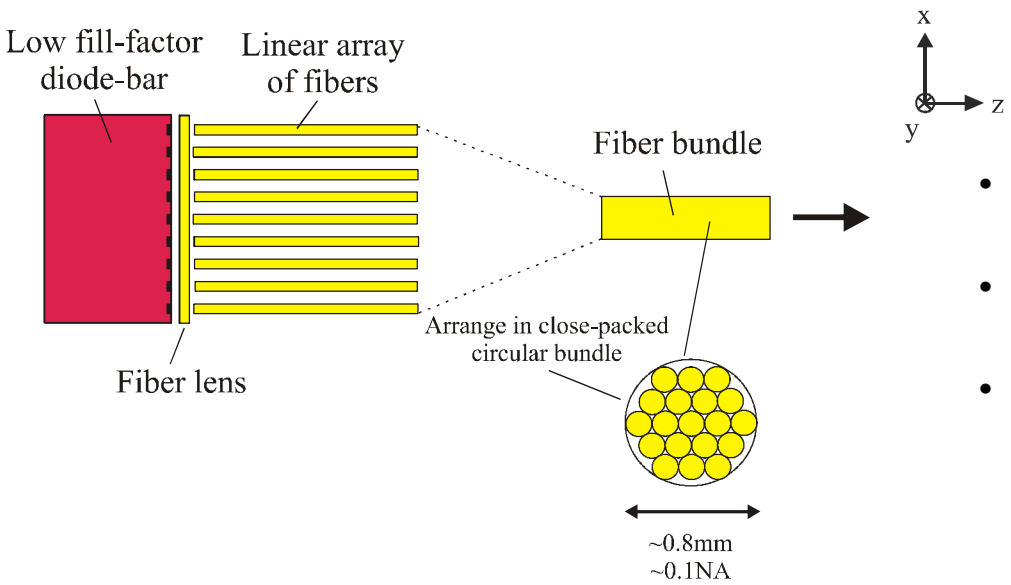

- Simple and robust way to equalise M^2 parameters for diode-bars
- Fibers are under-filled
  → Low brightness
- Output from bundle can be coupled into a single delivery fiber using lenses or a multimode coupler (tapered fiber bundle)

(b)

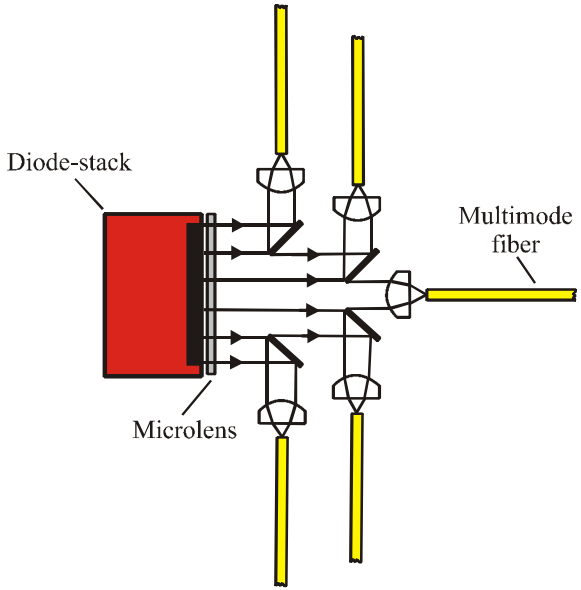

- Combination of free-space optics and fiber bundle approach
- Can be used to equalise M^2 parameters for diode-bars or stacks
- Higher brightness than method (a), but more complicated and expensive
- Output from bundle can be coupled into a single delivery fiber as for method (a)

Aperture filling

Diode bars and stacks have a large area of ‘dead space’ between the actual emitting regions. For applications requiring high brightness beams it is usually necessary to use cylindrical microlenses and cylindrical lens arrays to collimate (reduce the beam divergence) from individual bars and individual emitters to increase the brightness. This is often referred to ‘Aperture filling’ and is crucial for most fiber laser/amplifier pumping applications.

Fast-axis collimation:

$w_{xf,yf}$ = beam width after collimation in the x and y directions
$w_{xi,yi}$ = beam width at emitter in the x and y directions
$\theta_{xf,yf}$ = far-field beam divergence after collimation in the x and y directions
$\theta_{xf,yf}$ = far-field beam divergence without collimation in the x and y directions

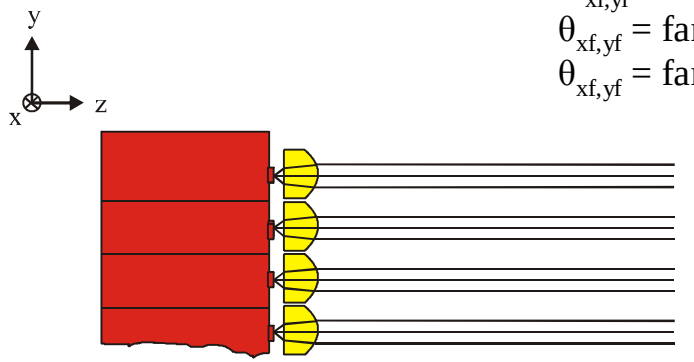

$$\frac{M_{yf}^2}{M_{yi}^2} = \frac{\theta_{yf}}{\theta_{yi}} \approx \frac{w_{yi}}{w_{yf}}$$

Slow-axis collimation:

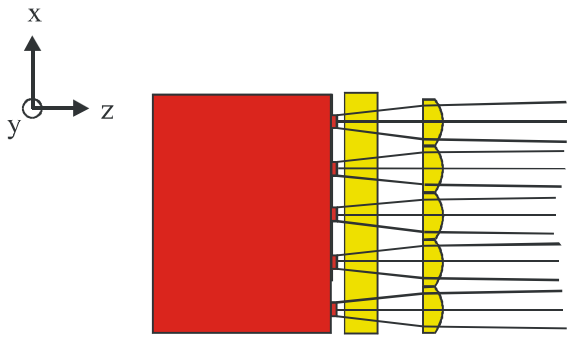

$$\frac{M_{xf}^2}{M_{xi}^2} = \frac{\theta_{xf}}{\theta_{xi}} \approx \frac{w_{xi}}{w_{xf}}$$

Free-space beam shaping techniques

(a) Two-mirror beam shaper[11]

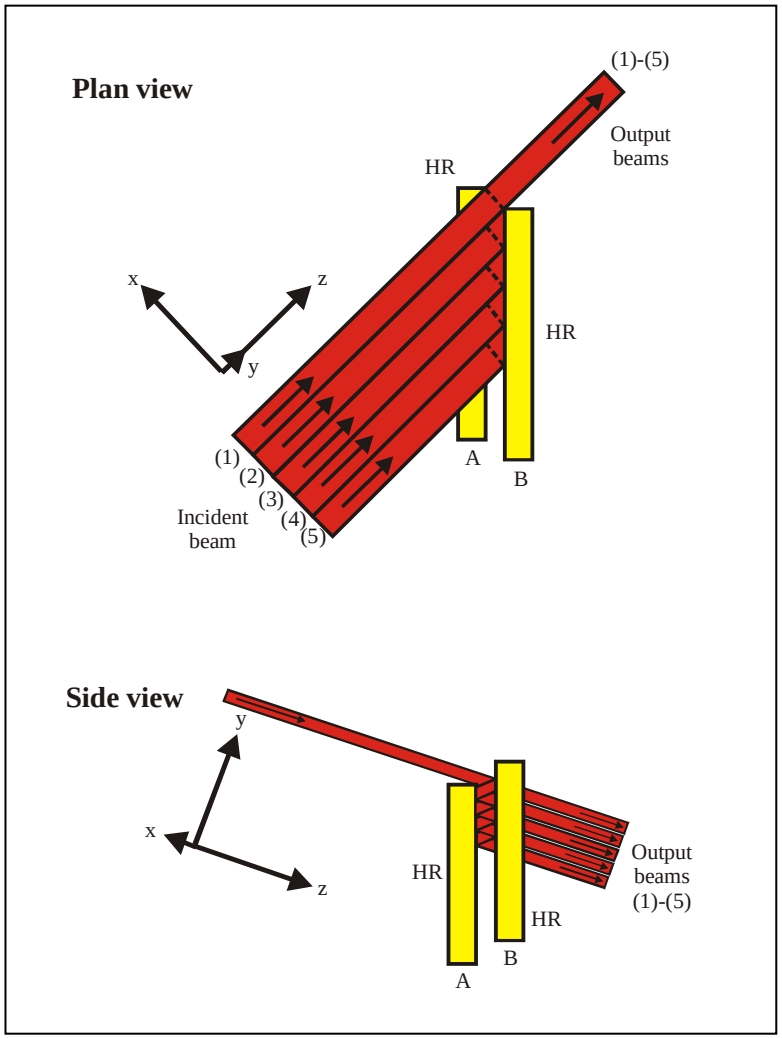

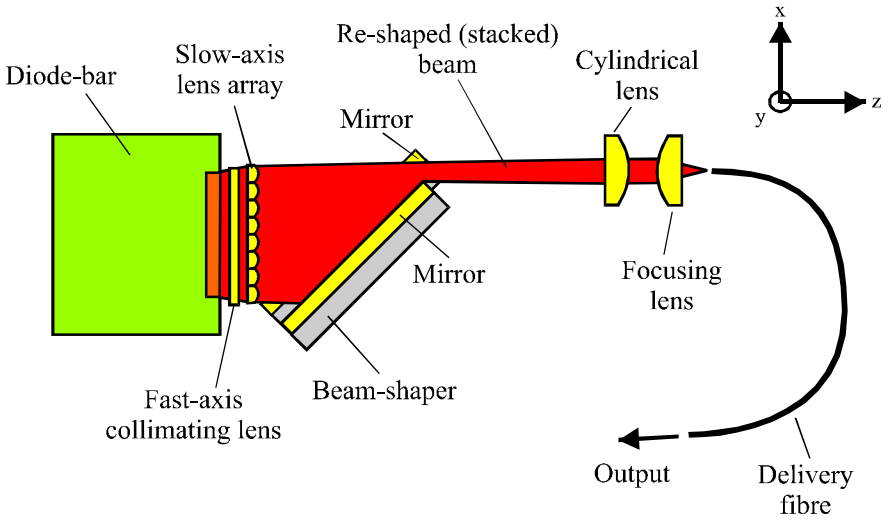

- Two mirrors used to slice beam in poor beam quality direction and stack resulting N beams in the orthogonal direction

$$\rightarrow \qquad M_{xf}^2 \approx M_{yf}^2 \approx \sqrt{1.3 M_{xi}^2 M_{yi}^2}$$

by choosing $\quad N \approx \sqrt{M_{xi}^2 / 1.3 M_{yi}^2}$

- Simple + low loss
- Can be used for bars or stacks
- Output can be focussed into the active fiber or delivery fiber

(b) Stacked-plate beam-shaper[12]

Side view

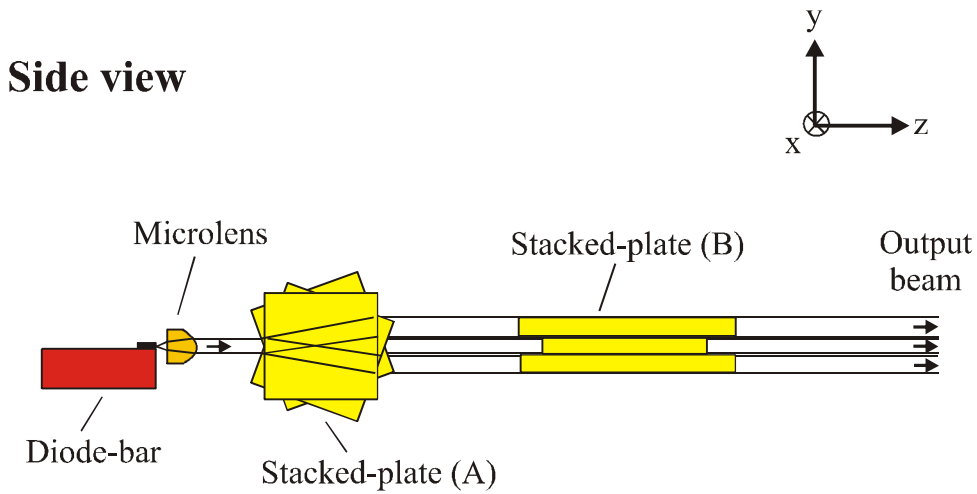

Plan view

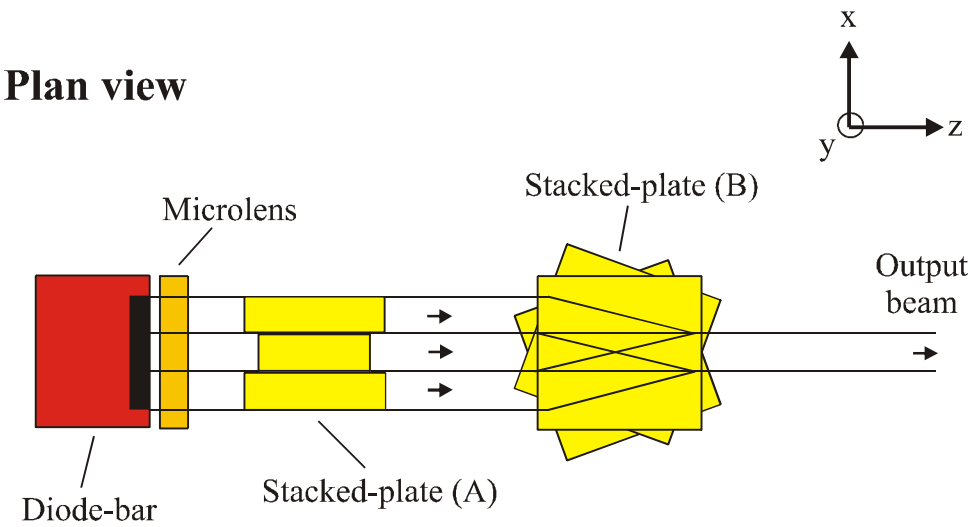

- Beam is sliced and beam components are then re-directed and stacked (by refraction) using two orthogonal stacked multi-glass-plates
- M_x^2 is reduced by factor N, and M_y^2 is increased by factor N, where N is the number of plates in each stack
- Can be used for bars or stacks

Summary

- There are many diode pump source architectures and many different coupling schemes that may be employed to launch pump light into double-clad fibers
- Emitter brightness is ultimately the limiting factor on how much pump power can be launched into a given fiber
- Still a great deal of scope for improvement in pump launching schemes
- Alignment tolerances are difficult to satisfy → Compromise between cost/simplicity and performance

References

1. International standard: ISO 11146 (1999).
2. H. Kogelnik and T. Li, “Laser beams and resonators,” Appl. Opt., vol.5, p.1550-1567 (1966).
3. R. J. Ripin and L. Goldberg, “High efficiency side-coupling of light into optical fibres using imbedded v-grooves,” Electron. Lett., vol.31, (1995), p2204-2205.
4. L. Goldberg, J. P. Koplow and D. A. V. Kliner, “Highly efficient 4W Yb-doped fiber amplifier pumped by a broad-stripe laser diode,” Opt. Lett., vol.24, (1999), p673-675.
5. http://www.itfoptical.com
6. http://www.sifamfo.com
7. www.spioptics.com
8. H. Sekiguchi, G. G. Vienne, A. Tanaka, Y. Senda, K. Ito, Y. Matsuoka, H. Toratani, S. Takahashi, H. Miyajima, H. Kan, and K. Ueda, “New Concept: fiber embedded disk and tube lasers”, International Forum on Advanced high-power lasers and Applications (AHPLA'99) Osaka, Japan, Nov. 1-5. 1999.
9. T. Baer and D. F. Head, “Apparatus for coupling a multiple emitter laser diode to a multimode optical fibre,” US patent No.5579422.
10. D. C. Shannon and R. Wallace, “Multiple diode laser stack for pumping a solid-state laser,” US patent No. 5,299,222 (1994).
11. W. A. Clarkson and D. C. Hanna,”Two-mirror beam-shaping technique for high-power diode bars,” Opt. Lett., vol.21, (1996), p375-377.
12. C. Ullmann and V. Krause, “Diode optics and diode laser,” US patent No. 5986794, (1999).

4. Thermal effects in fibers

Heat generation

Various sources:

- **Quantum defect heating:**

  $\Delta E = h\nu_p - h\nu_L \rightarrow$ HEAT

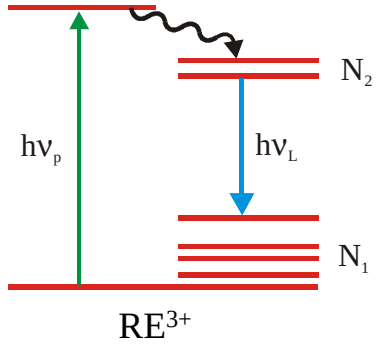

- Excited-state absorption (ESA)

  At pump and/or signal wavelength

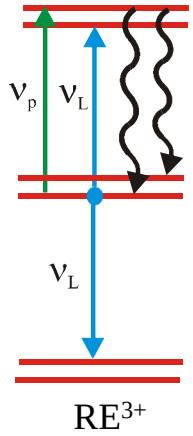

- Energy-transfer-upconversion (ETU)

  Depends on RE^{3+} concentration and excitation density
  High conc. + high excitation density can lead to a significant decrease in efficiency + extra heating due to ETU.

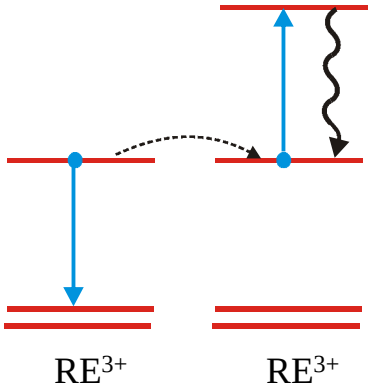

Various sources (cont'd):

- Impurities
- Non-radiative sites
- Absorption of fluorescence and/or stray pump light in outer-cladding and/or mount

Quantum defect heating is often considered to be the main source of heat, but this is not always correct. If it is then:

Fraction of absorbed pump converted to heat: $\gamma_h = 1 - \nu_L / \nu_p$

Rare earth ion	Pump wavelength (nm)	Lasing wavelength (nm)	γ_h
Nd^{3+}	~800	~ 920 - 940 ~ 1050 - 1080 ~1360	~ 0.13 – 0.15 ~0.24 – 0.26 ~0.41
Yb^{3+}	~915 - 980	~ 980 – 1140	~0.05 – 0.20
Er^{3+},Yb^{3+}	~915 - 980	~ 1530 – 1620	~0.36 – 0.44
Tm^{3+}	~790, ~1550	~ 1720 – 2100	~0.10 – 0.62

Thermal effects

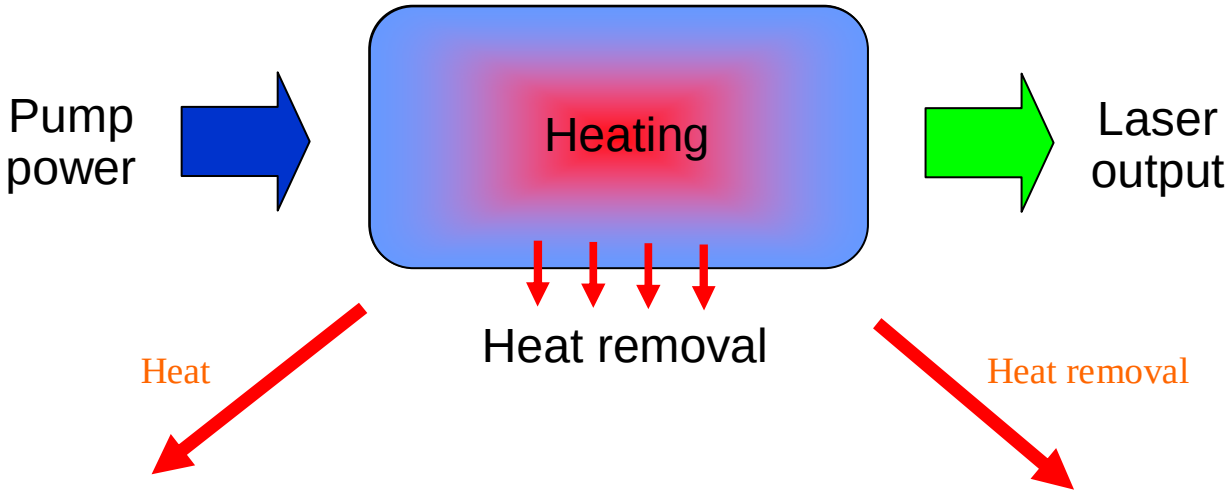

Temperature increase →

- Damage due to melting and/or burning
- Change in spectroscopy
- Change in thermo-optical and thermo-mechanical properties

Temperature gradient →

- Thermal lensing/guiding or anti-guiding
  → beam distortion + loss
- Thermally-induced stress
  → Birefringence + lensing
  → Fracture

Thermal effects become more pronounced at high pump powers
→ Degradation in beam quality + reduced efficiency + eventually damage

Impact of thermal loading on power scalability depends on laser medium geometry

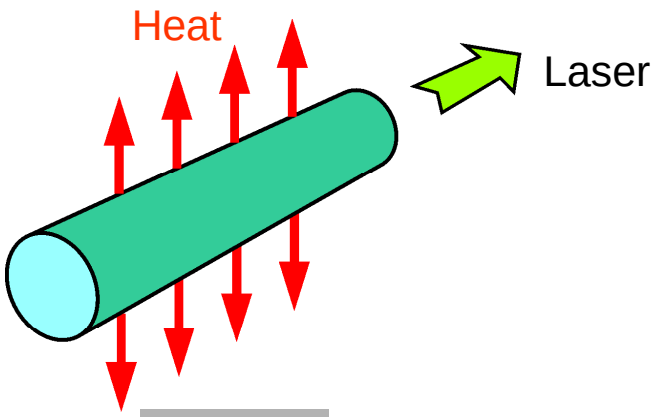

ROD

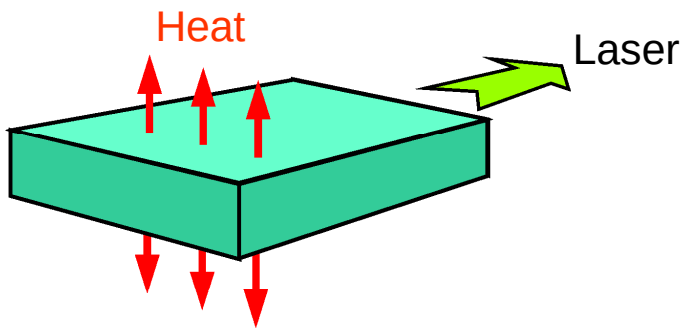

SLAB

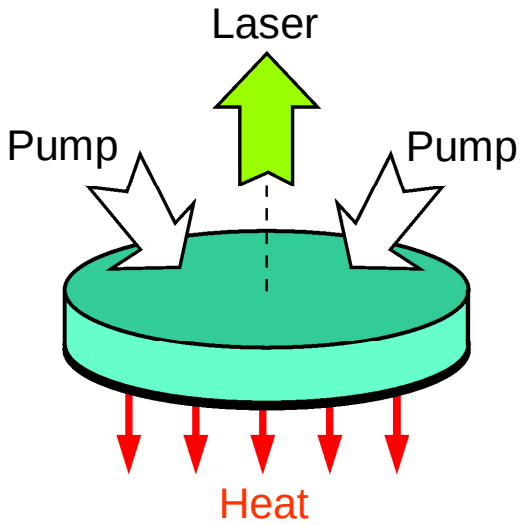

THIN DISC

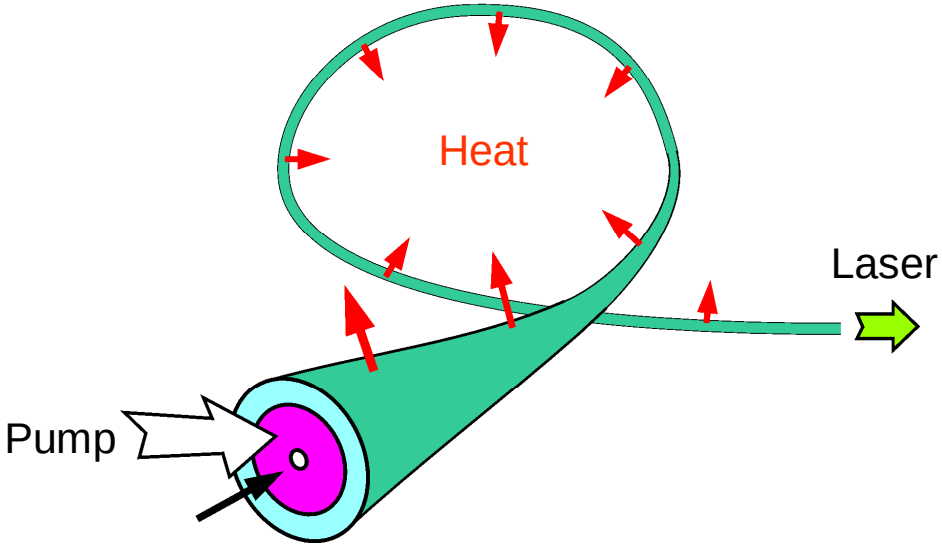

CLADDING PUMPED FIBRE

Attractions of fibers:

- Generated heat can be spread over a long device length (typically a few metres to a few tens-of-metres)
- Large surface area/core volume facilitates heat removal
- Waveguiding properties of core (i.e. refractive index profile) usually dominate over thermally-induced changes in refractive index.

Thermal management is easier than for other laser medium geometries, but fibers are not completely immune to the effects of thermal loading[1,2,3,4,5].

As power levels from cladding-pumped fiber lasers and amplifiers rise, thermal loading is starting to become a serious issue (especially in rare earth-doped fibers with a relatively large value for γ_h).

Also, thermal effects in external components (e.g. Faraday isolators) may impact on the overall performance of the system

Typical fiber heat-sinking configurations:

- For fiber end-section in an end-pumped configuration

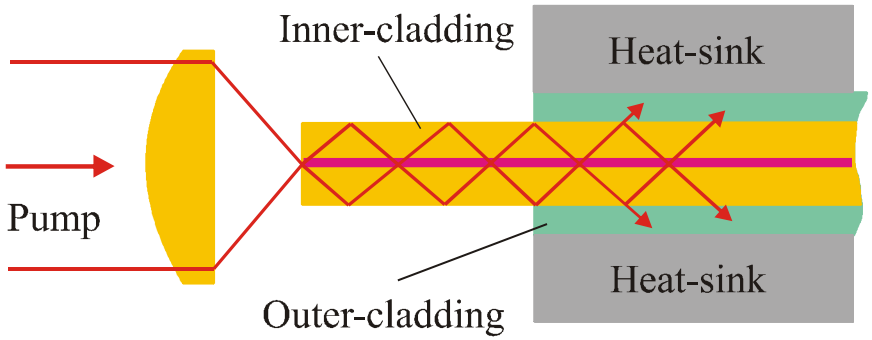

- For a side-pumped fiber configuration

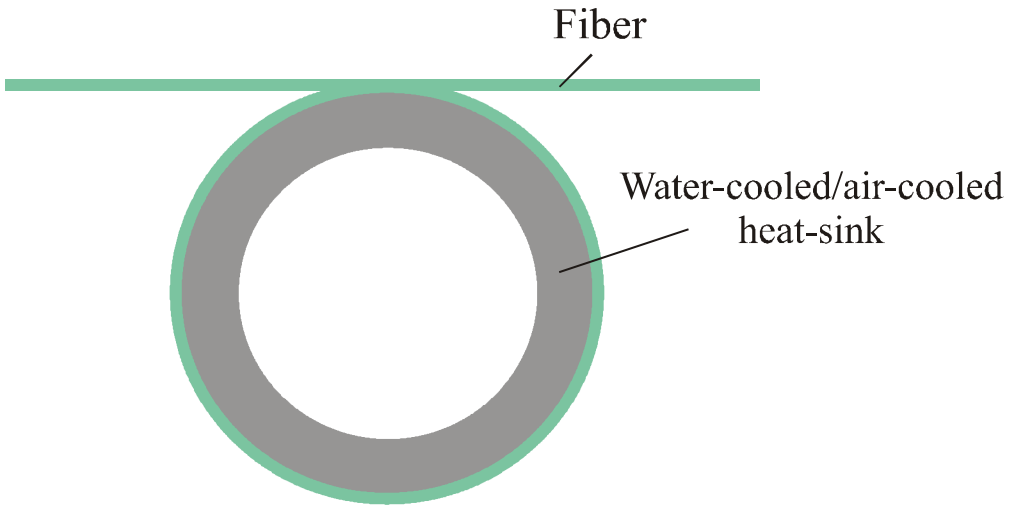

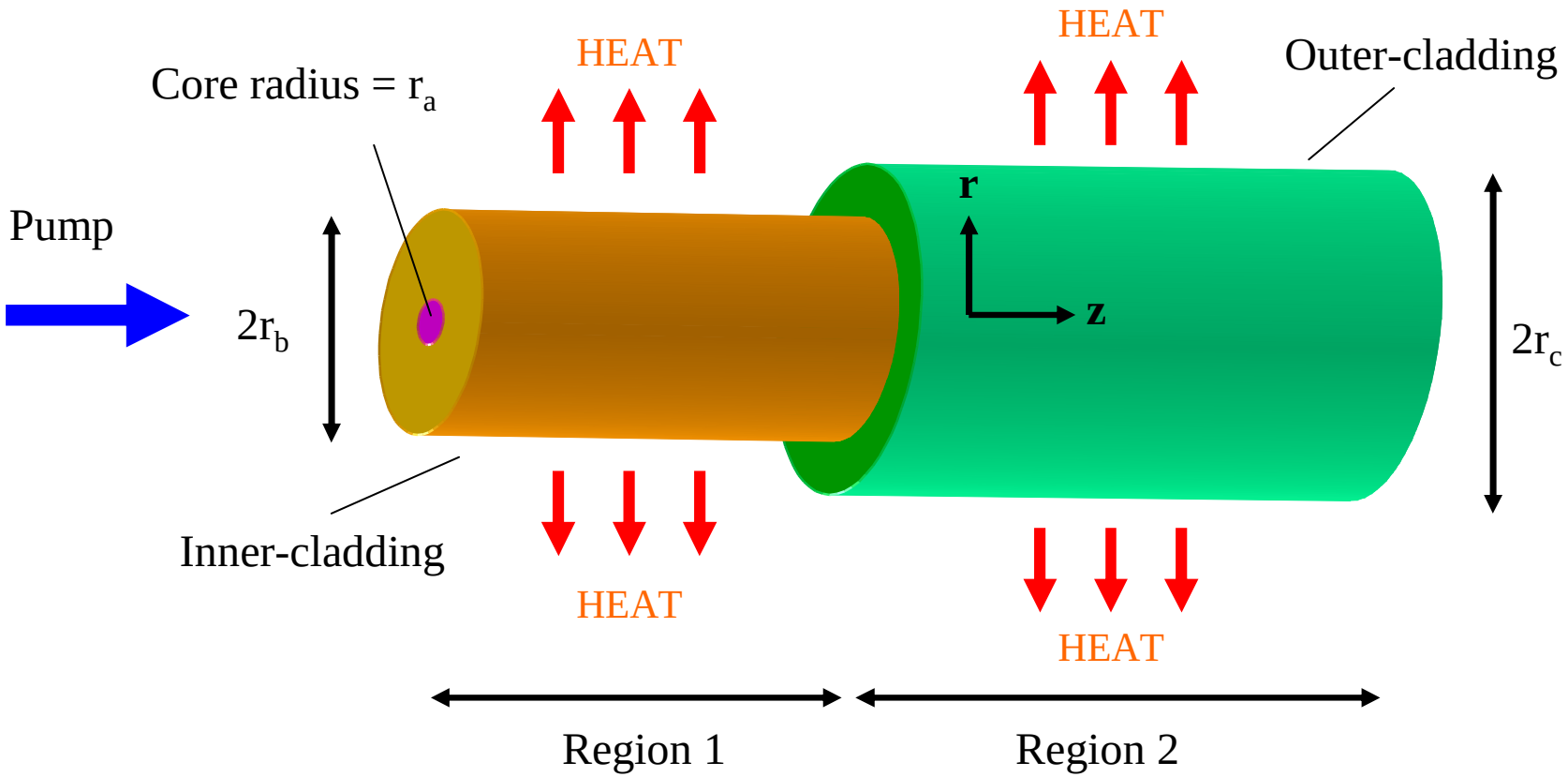

Under steady state conditions[6]: $\nabla . \mathbf{h}(r,z) = Q(r,z)$

$$\mathbf{h}(r,z) = -K_c \nabla T(r,z)$$

where h(r,z) is the heat flux, Q(r,z) is the heat deposition density, T(r,z) is the temperature and K_c is the thermal conductivity

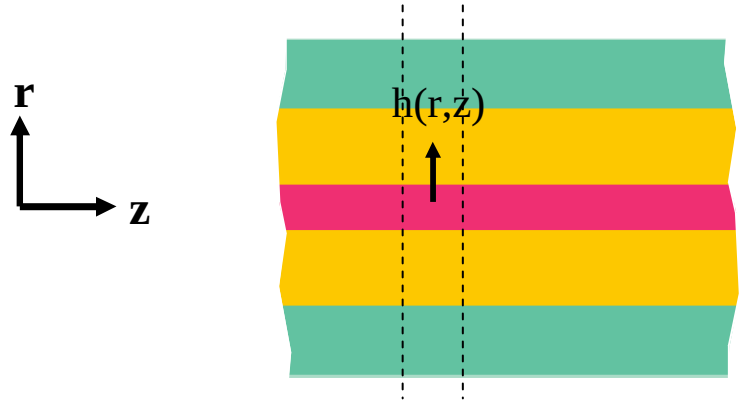

Assuming heat flow is purely radial, then total heat radial flow from volume bounded by z and z + Δz is equal to the net heat generated in this region

$$2\pi r\,\Delta z\,h(r,z) = \int_{z}^{z+\Delta z}\int_{0}^{r} 2\pi r' Q(r',z)\,dr'\,dz'$$

$$\longrightarrow \quad h(r,z) = \frac{P_p(z)\,\alpha_p\,\gamma_h\,r}{2\pi r_a^2} \qquad (r \le r_a)$$

$$\longrightarrow \quad h(r,z) = \frac{P_p(z)\,\alpha_p\,\gamma_h}{2\pi r} \qquad (r > r_a)$$

where $P_p(z) = P_p(0)\exp(\alpha_p z)$ is the pump power at position z and α_p is the absorption coefficient for pump light in the active ion doped core.

Boundary conditions: h(r,z) and T(r,z) are continuous at boundaries between layers

Thermal conductivity: $K_c=K_{ic}$ for $r \le r_b$ (i.e. core and inner-cladding have the same thermal conductivity)
$K_c=K_{oc}$ for $r > r_b$

Resulting temperature distribution can be obtained from:

$$\Delta T(r,z) = T(r,z) - T(0,z) = -\frac{1}{K_c}\int_0^r h(r',z)dr'$$

Region 1:

$$T(0,z) - T_s = \frac{P_h(z)}{4\pi}\left[\frac{1}{K_{ic}} + \frac{2}{K_{ic}}\log_e\left(\frac{r_b}{r_a}\right) + \frac{2}{r_b H_1}\right]$$

Region 2:

$$T(0,z) - T_s = \frac{P_h(z)}{4\pi}\left[\frac{1}{K_{ic}} + \frac{2}{K_{ic}}\log_e\left(\frac{r_b}{r_a}\right) + \frac{2}{K_{oc}}\log_e\left(\frac{r_c}{r_b}\right) + \frac{2}{r_c H_2}\right]$$

where $P_h(z) = P_p(z)\alpha_p\gamma_h$ is the heat generated per unit length, T_s is the ambient temperature of the surroundings, T(0,z) is the temperature at the core's centre and $H_{1,2}$ is the heat transfer coefficient for the inner/outer cladding in regions 1,2

Maximum heat deposition per unit length before onset of softening or melting:

Region 1:

$$P_{h\,max} = 4\pi(T_m - T_s)\left[\frac{1}{K_{ic}} + \frac{2}{K_{ic}}\log_e\left(\frac{r_b}{r_a}\right) + \frac{2}{r_b H_1}\right]^{-1}$$

For convective cooling, this term dominates and hence a larger diameter fiber with a larger surface area facilitates heat removal

Region 2:

$$P_{h\,max} = 4\pi(T_m - T_s)\left[\frac{1}{K_{ic}} + \frac{2}{K_{ic}}\log_e\left(\frac{r_b}{r_a}\right) + \frac{2}{K_{oc}}\log_e\left(\frac{r_c}{r_b}\right) + \frac{2}{r_c H_2}\right]^{-1}$$

For double-clad fibers with polymer outer-claddings $K_{oc} << K_{ic}$, so the outer-cladding should be as thin as possible to avoid a larger temperature rise.

where T_m is the softening/melting temperature of the core

Thermal loading limit for a typical double-clad silica fiber

Fibre design: Core diameter = 25μm
Inner-cladding diameter = 200, 300, 500μm
Outer-cladding diameter = 300, 400, 600μm
Pure silica inner-cladding: $K_c \approx 1$W/mK
Polymer outer-cladding: $K_c \approx 0.1$W/mK

For silica: $T_m \approx 2000$K and assuming $T_s = 293$K

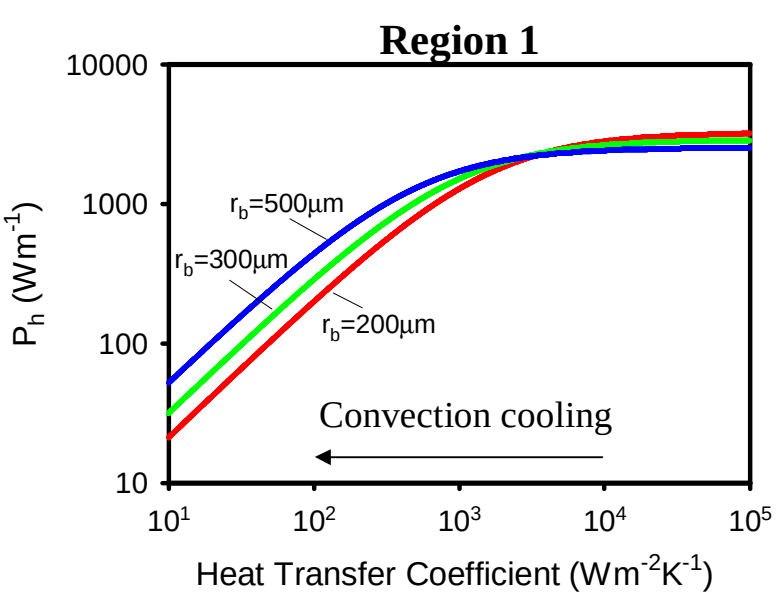

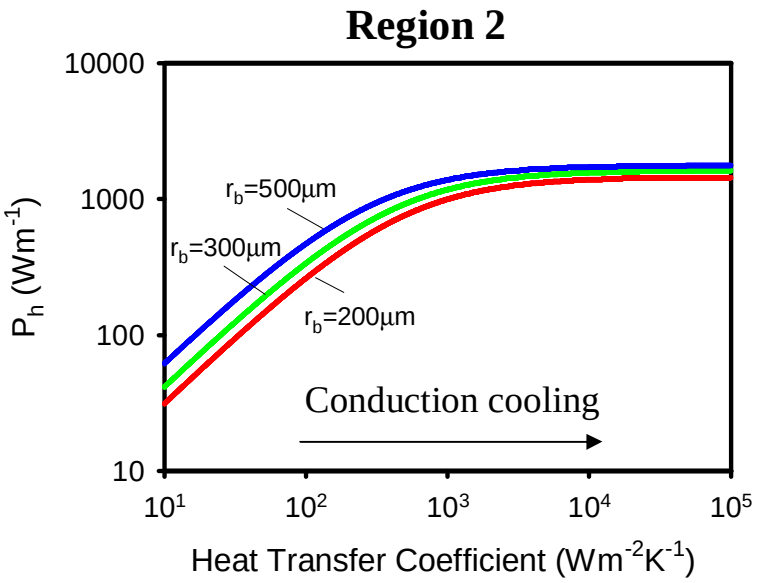

For convection cooling[1]: $H \sim 10$Wm^{-2}K^{-1}

Upper-limit on power that can be extracted from fiber: $P_{max} \approx P_h(1 - \gamma_h) / \gamma_h$

e.g. For an Yb fiber laser at 1080nm pumped at 980nm: $P_{max} \approx 10P_h$

For an Er,Yb fiber laser at 1550nm pumped at 980nm: $P_{max} \approx 1.7P_h$

Suggests that typical double-clad fibers can handle heat deposition densities in the range ~20 – 50W/m to >1kW/m depending on the cooling scheme before the onset of damage due to melting.

However, this is not the whole story since in Region 2 the threshold for damage to the outer-coating is reached first. For a typical polymer outer-coating the maximum temperature, T_d, that can be tolerated before the coating begins to degrade is ~150°C. This imposes the following upper-limit on the heat deposition density:

$$P_{h\,max} = 4\pi(T_d - T_s)\left[\frac{2}{K_{oc}}\log_e\left(\frac{r_c}{r_b}\right) + \frac{2}{r_c H_2}\right]^{-1}$$

→ Aggressive cooling needed for scaling to high power levels

→ Thinner coating + larger inner -cladding facilitates thermal management

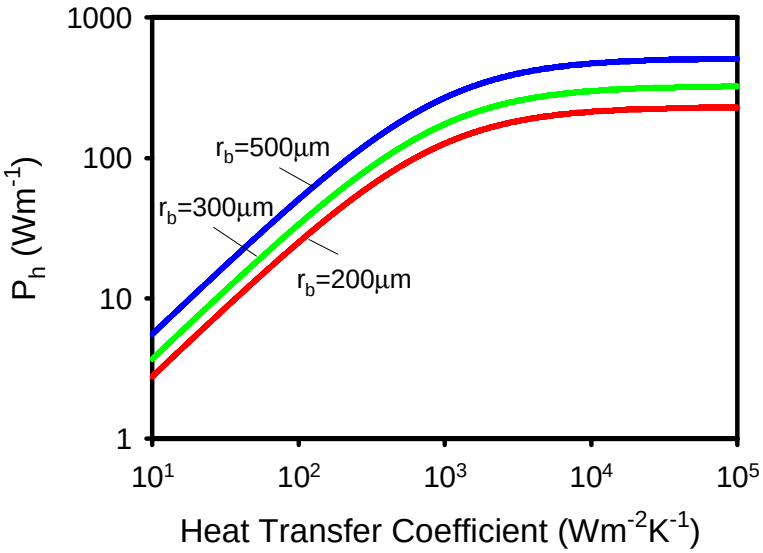

Temperature profile across fiber

P_h = 100W/m
Core diameter = 25μm
Inner-cladding diameter = 400μm
Outer-cladding diameter = 600μm

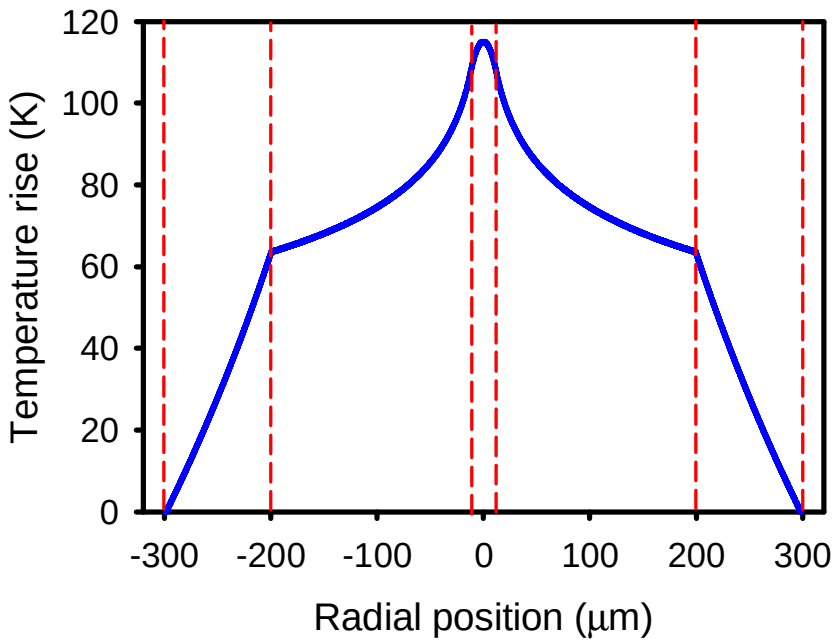

- Large temperature drop over outer-coating
  → Use thinner coating
- Temperature drop between outer-coating and heat-sink / surroundings depends on the heat-transfer coefficient and can be very large

Jacketed-Air-Clad Fibers

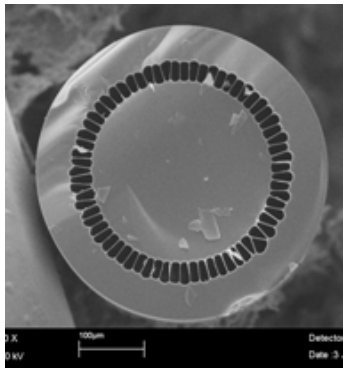

- Becoming increasingly popular for high power operation
- All glass structure with high NA for inner-cladding
- Pump light does not interact directly with outer-coating
- Outer-coating can be selected for thermal properties

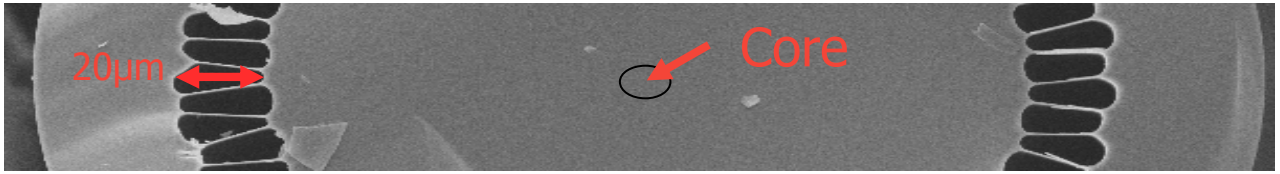

Temp rise across air cladding $\rightarrow$ $$\Delta T = \frac{P_h(z)}{4\pi}\left[\frac{2}{K_{eff}}\log_e\left(\frac{r_c}{r_b}\right)\right] \approx \frac{P_h(z)\,t}{2\pi K_{eff}\,r_b}$$

where K_{eff} is the effective thermal conductivity of the 'air' layer and t is the thickness of the air cladding. If the 'struts' that suspend the inner-cladding are very thin, then $K_{eff} \approx K_{air} \approx 0.025\text{-}0.025 Wm^{-1}K^{-1}$.

For a small temp rise we require: $t < K_{eff}\, r_b$

$\rightarrow$ $t \sim$ few µm

Thermal guiding

Two possibilities:

1. dn/dT > 0

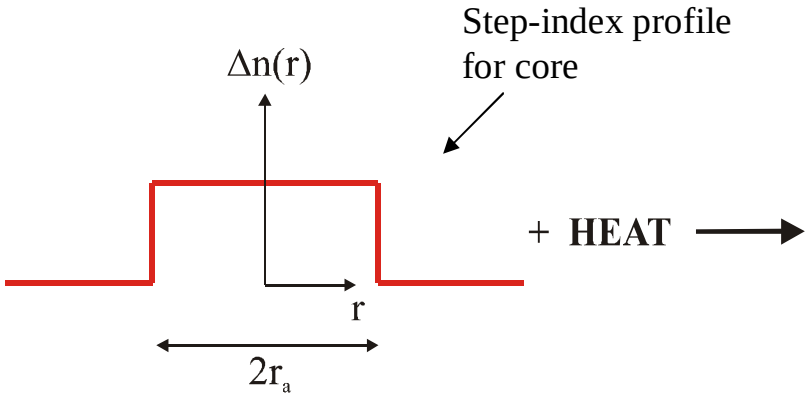

+ HEAT →

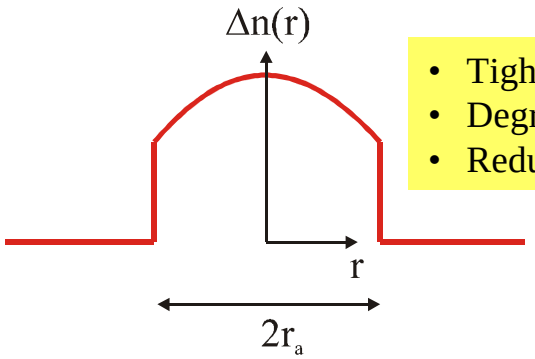

- Tighter mode confinement
- Degradation in beam quality
- Reduced efficiency

2. dn/dT < 0

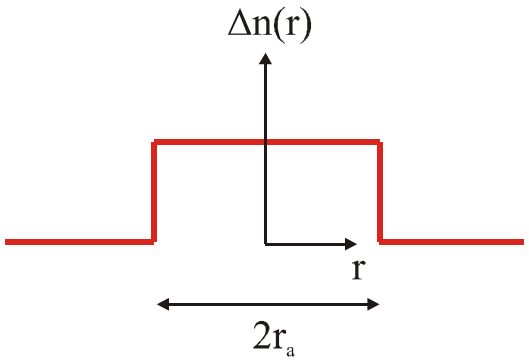

+ HEAT →

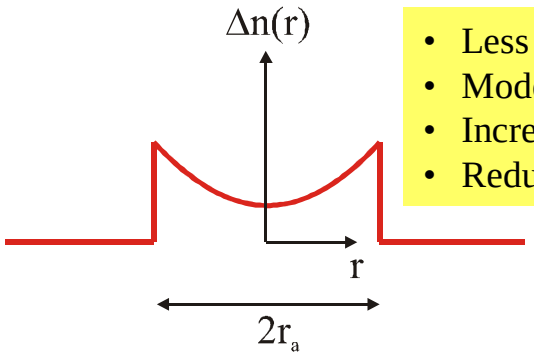

- Less mode confinement
- Mode distortion
- Increased propagation loss
- Reduced efficiency

For silica glass: dn/dT > 0 and for phosphate glass dn/dT < 0

Case 1:

Step-index waveguide has a fundamental mode radius w_o given by[7] $w_o \approx r_a / \sqrt{\log_e V}$
where $V \approx 4\pi\, n_o r_a \Delta n/\lambda$

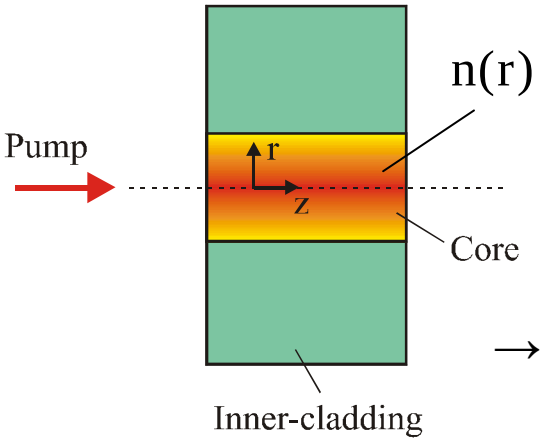

$n(r) = n_o - n_{th} r^2$ where $n_{th} \approx \dfrac{P_h\, dn/dT}{4\pi r_a^2 K_c}$

→ Thermal guiding with mode radius: $w_{th} \approx \left(\dfrac{2K_c \lambda^2 r_a^2}{\pi n_o P_h\, dn/dT} \right)^{1/4}$

Hence, thermal guiding starts to have a significant impact when $w_{th} \leq w_o$
i.e. when:

$$P_h \geq \frac{2K_c \lambda^2 (\log_e V)^2}{\pi r_a^2 n_o\, dn/dT}$$

→ Thermal guiding will have significant effect on guiding and hence performance in large-core fibers

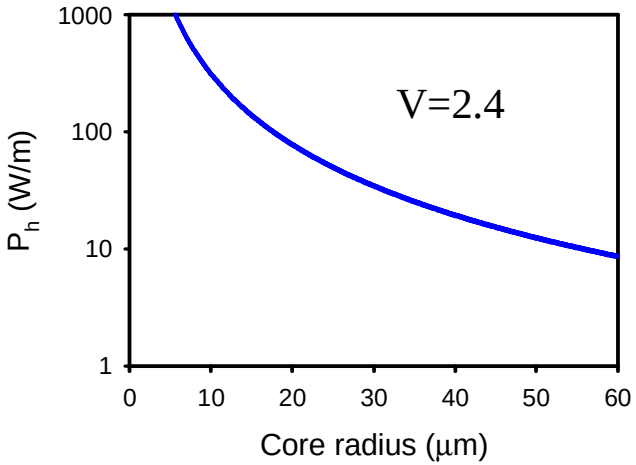

Summary

- Double-clad fibers have excellent thermal properties compared to conventional solid-state lasers, but are not immune from the effects of heat generation.

- Degradation and/or damage to the fiber outer-coating due to the high temperatures which result from heat generated in the core and poor thermal management is one of the main failure mechanisms at high power levels. Improved heat-sinking can remedy this allowing scaling to much higher power levels

- Thermal guiding is not a serious problem in conventional (small) core fiber designs, but will start to impact on performance in very large core / short length devices

- Thermal lensing in ‘free-space’ components (e.g. Faraday isolators) is an issue at high power levels and requires the use of very low absorption materials and careful design to eliminate and/or compensate for beam distortion

References

1. D. C. Brown and H. J. Hoffman, “Thermal, stress and thermo-optic effects in high average power double-clad silica fiber lasers,” IEEE J. Quantum Electron., vol.37, p.207-217 (2001).
2. L. Li, H. Li, T. Qiu, V. L. Temyanko, M. M. Morrell, A. Schulzgen, A. Mafi, J. V. Moloney and N. Peyghambarian, “3-Dimensional thermal analysis and active cooling of short-length high-power fiber lasers,” Opt. Express, vol.13, p.3420-3428 (2005).
3. N. A. Brilliant and K. Lagonik, “Thermal effects in a dual-clad ytterbium fiber laser,” Opt. Lett., vol.26, p.1669-1671 (2001).
4. D. C. Hanna, M. J. McCarthy, and P. J. Suni, “Thermal considerations in longitudinally pumped fibre and miniature bulk lasers,” in Fiber laser sources and amplifiers, M. J. F. Digonnet, eds., Proc. SPIE 1171, 160-166 (1989).
5. Y. Wang, “Thermal effects in kilowatt fiber lasers,” IEEE Photon. Tech. Lett. vol.16, p.63-65 (2004).
6. M. E. Innocenzi, H. T. Yura, C. L. Fincher and R. A. Fields, “Thermal modelling of continuous-wave end-pumped solid-state lasers,” Appl. Phys Lett., vol.56, p.1831-1833 (1990).
7. A. W. Snyder and J. D. Love, “Optical Waveguide Theory,” (Kluwer Academic Publishers, 2000).

5. Nonlinear processes

Introduction

The response of a dielectric medium to light becomes increasingly nonlinear as the intensity grows. In optical fibers, the combination of tight optical confinement of light in the core, a long interaction length and low loss leads to conditions where nonlinear processes can have a very dramatic impact on the fiber device performance[1]. Nonlinear effects in fibers can be beneficial or detrimental to performance depending on the particular nonlinear process and the desired mode of operation.

Light incident on a medium → Polarisation **P** induced by the electric field **E** according to the relation:

$$\mathbf{P} = \underbrace{\varepsilon_o \chi^{(1)} \mathbf{E}}_{\text{Linear response}} + \underbrace{\varepsilon_o \chi^{(2)} \mathbf{EE} + \varepsilon_o \chi^{(3)} \mathbf{EEE} + \ldots\ldots\ldots\ldots}_{\text{Nonlinear response}}$$

where ε_o is the permittivity of free space
$\chi^{(1)}$ the linear susceptibility → Main contribution to **P**
$\chi^{(2)}$ is the second-order susceptibility and is zero for materials (e.g. silica) with inversion symmetry
$\chi^{(3)}$ is the third-order susceptibility → third harmonic generation, four-wave mixing and nonlinear refraction

Nonlinear refraction is generally the most important $\chi^{(3)}$ process in fibers $n(\nu, I) = n_o(\nu) + n_2 I$
n_2 is the nonlinear refractive index coefficient and is related to $\chi^{(3)}$. In silica, $n_2 \approx 2.2 - 3.4 \times 10^{-20} m^2/W$

→ Self-phase modulation (SPM) and cross-phase modulation (XPM)
→ Spectral broadening of ultrashort pulses

Stimulated Inelastic Scattering

In addition, there are also nonlinear processes that result from stimulated inelastic scattering. Two important processes in optical fibers are stimulated Raman scattering and stimulated Brillouin scattering.

(a) Stimulated Raman scattering (SRS)

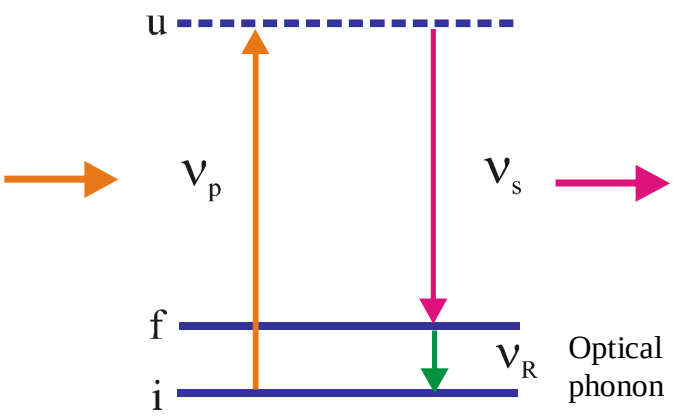

Spontaneous Raman scattering

Scattering of an incident (pump) photon (ν_p) to a lower frequency photon (ν_s) as the molecule makes a transition between two vibrational states

Energy difference $\Delta E = h\nu_R = h\nu_p - h\nu_s$ is absorbed in the medium as heat.

Frequency down-shifted wave (ν_s) is the Stokes wave and the frequency shift (ν_R) is known as the Raman shift

Phase-matching is not required for this process

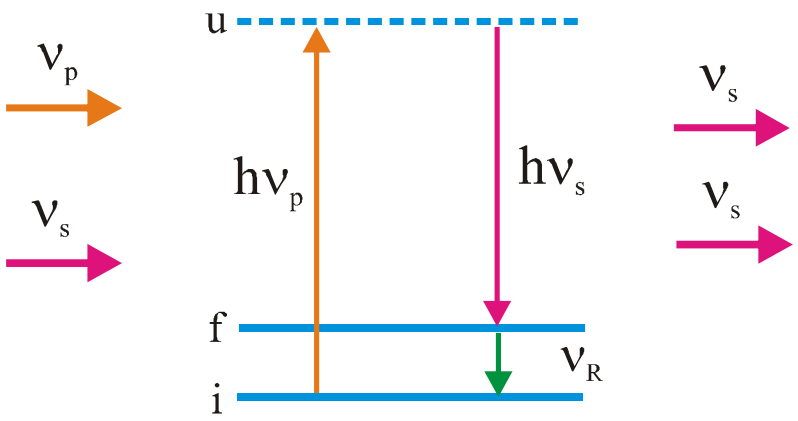

Stimulated Raman scattering

→ **Raman amplification**

$$\frac{dI_s}{dz} = g_R I_p I_s - \alpha_s I_s$$

$$\frac{dI_p}{dz} = -\frac{g_R I_p I_s \nu_p}{\nu_s} - \alpha_p I_p$$

α_p and α_s are the loss coefficients for the pump and Stokes wave, and g_R is the Raman gain coefficient

- The values for g_R and ν_R, and the frequency range over which Raman gain extends depend on the material.
- Amorphous materials have a very broad Raman gain spectrum. For silica, Raman gain can be achieved over a frequency range of up to ~ 40THz
- For silica the max value for $g_R \sim 1\times10^{-13}$m/W and corresponds to a Raman frequency shift of ~13THz
- g_R can vary significantly with the core composition (i.e. adding dopants can have a significant effect on the value for g_R and the value for the Raman frequency shift at which g_R is a maximum.

Stimulated Raman scattering has a number of important applications and there are a number of fiber-based devices which make use of SRS:

- Fiber Raman amplifiers[2] → Distributed + broadband amplification
- Fiber Raman lasers[3] → Extension to wavelength regimes that are not covered by RE-doped fiber lasers
- Broadband wavelength generation

However, SRS can also be detrimental to the performance of RE-doped fiber lasers and amplifiers since it act as a loss.

Threshold for SRS[1]:

$$P_{pth}^{SRS} \approx \frac{16A_{eff}}{g_R l_{eff}}$$

where $l_{eff} = \frac{1}{\alpha_p}\left[1-\exp(-\alpha_p l)\right]$ is the effective length and A_{eff} is the effective core area.

This assumes that the Raman gain spectrum has a Lorentzian lineshape and the polarisation of the pump and Stokes waves are maintained. Once the threshold for SRS is reached, the Stokes wave can grow very efficiently at the expense of pump power. The Stokes wave may then act as the pump for a second-order Stokes wave and so on. This is one of the limiting factors on the maximum power that can be obtained from a cladding pumped fiber laser or amplifier

Example: Typical cladding-pumped Yb-doped silica fiber laser with

Core diameter = 15μm $\rightarrow A_{eff} \approx 1.77\times10^{-10}m^2$
l_{eff} = 20m

$\rightarrow \quad P_{pth}^{SRS} \approx 1.4kW$

This is only a very rough guide, but it shows that SRS is potentially a problem in very high power cw fiber systems and quite modest peak power pulsed fiber sources.

Possible solutions include:

- Increasing the core area – Limited scope without degrading beam quality
- Shorten device length – More demanding on diode pump beam quality and thermal management
- Distributed loss filter to suppress Stokes generation

Raman Lasers

Attractions:
- Access to wavelength regimes not available in RE-doped lasers
- Low thermal loading if wavelength shift is small

Cascaded Raman Laser:

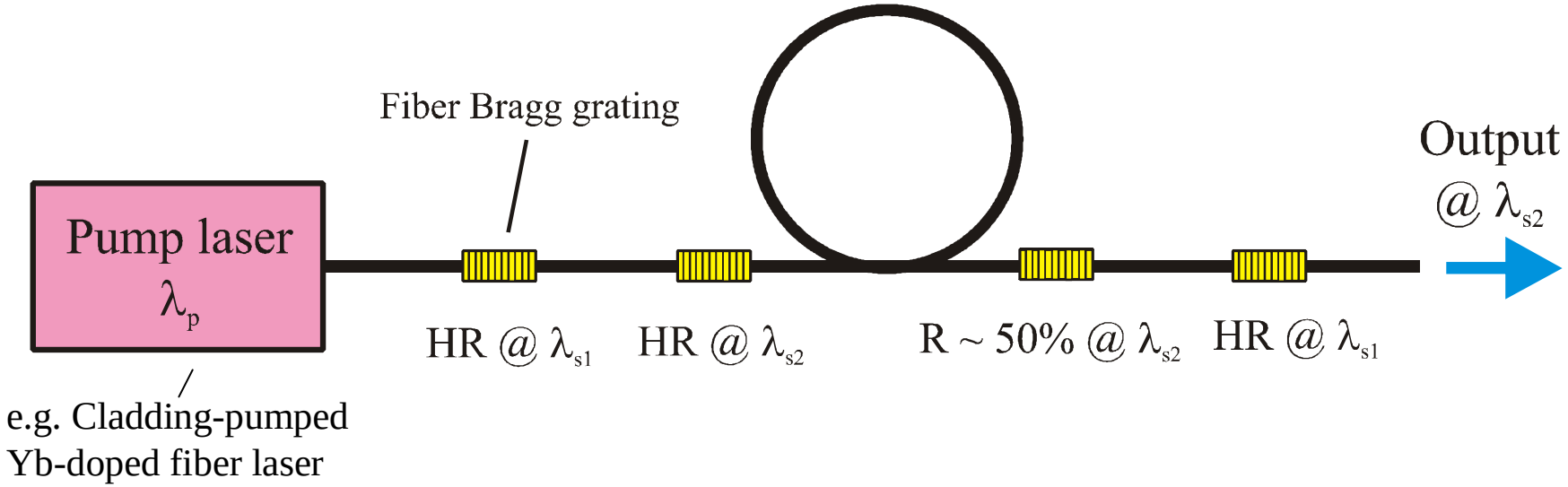

Example: Yb fiber pump laser at 1.06μm
Phosphosilicate Raman fiber: λ_{s1}=1.24μm and λ_{s2}=1.48μm
Requires very long lengths of fiber (~1km) for a low threshold

>1W power levels at 1.48μm have been generated[4,5,6] with efficiencies up to 48% wrt Yb fiber laser power.

Cladding-pumped Raman fiber laser

The cladding-pumping concept can also be applied to Raman fiber lasers as a means for enhancing brightness as well as extending wavelength coverage[7,8]. However, direct diode pumping with currently available high power diode sources is not practical due to their low brightness, so an intermediate 'brightness-enhancement' stage is needed.

Basic idea:

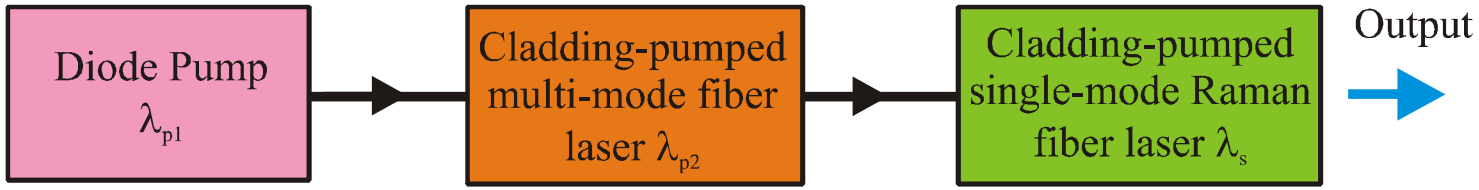

- Brightness enhancement in two stages
- Design constraints on RE-doped fiber laser are more relaxed
- Heat loading is distributed over two stages and can be very low in the Raman fiber laser
- Small cladding-to-core area ratio in Raman fiber laser
- Long fiber length needed for Raman laser, so core propagation loss must be very low

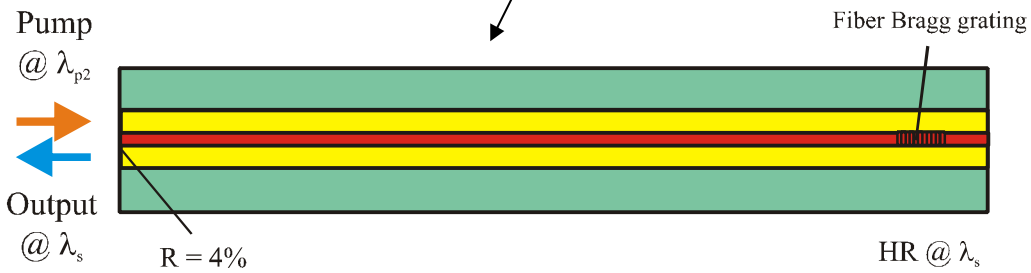

(b) Stimulated Brillouin scattering[1] (SBS)

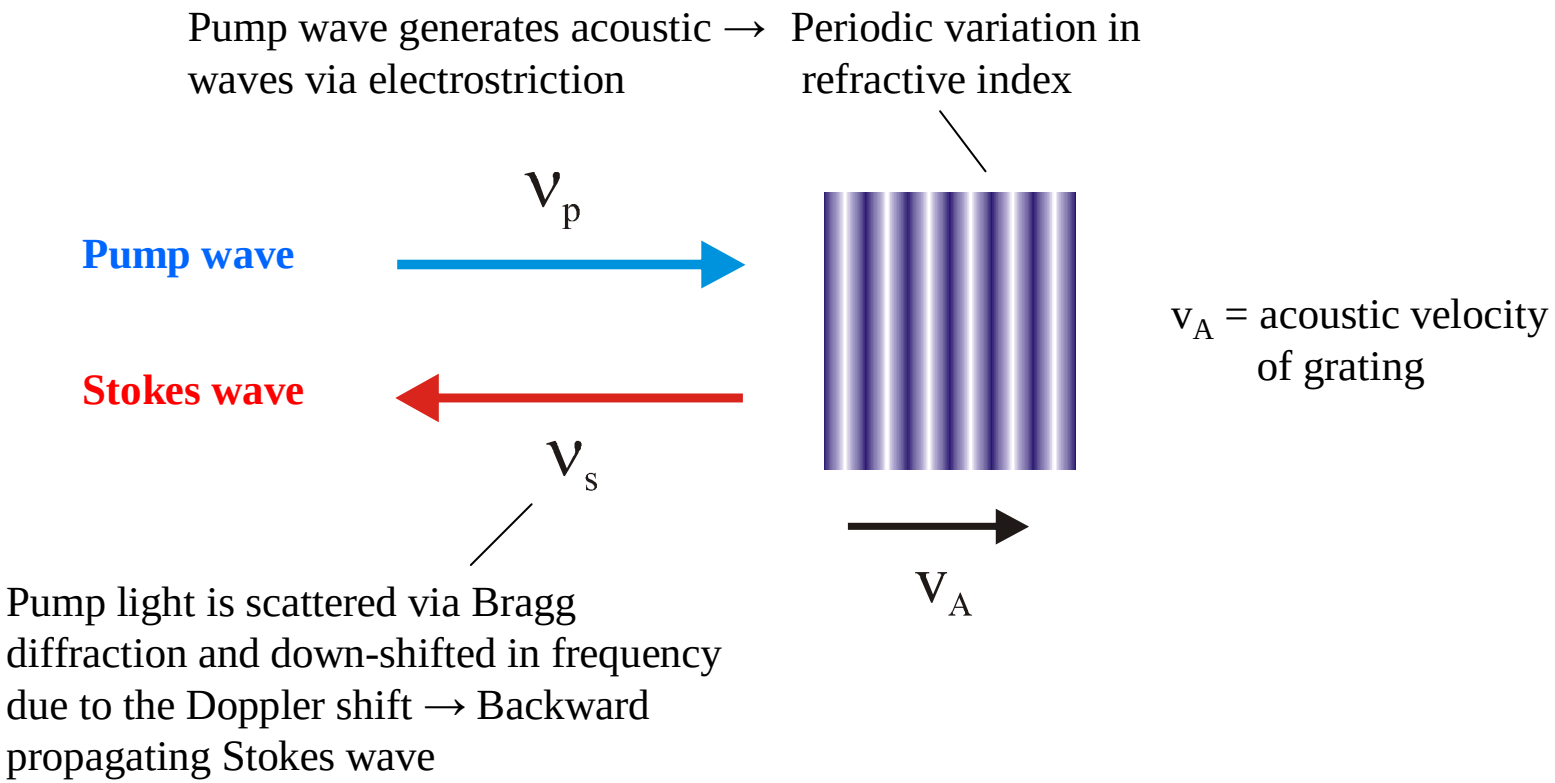

$$\rightarrow \quad \text{Frequency shift} \quad \nu_B = \nu_p - \nu_s = \frac{2nv_A}{\lambda_p}$$

- For silica, $v_A \approx$ 6km/s → $\nu_B \approx$ 17.5GHz at λ_p = 1μm. Hence frequency shifts for SBS are much smaller than for SRS.
- Scattering involves low energy acoustic phonon for SBS and higher energy optical phonons for SRS
- Stokes wave is backward propagating for SBS

Brillouin gain:

Due to the very small Brillouin frequency shift:

$$\frac{dI_s}{dz} = -g_B I_p I_s + \alpha I_s$$

$$\frac{dI_p}{dz} = -g_B I_p I_s - \alpha I_p$$

- Assuming $\nu_p \approx \nu_s$ and hence $\alpha_p \approx \alpha_s \approx \alpha$
- Note the 'minus' sign has been included to account for the propagation direction of the Stokes wave (c.f. SRS)

If the propagation loss (α) is negligible then $dI_s/dz = dI_p/dz$

g_B is the Brillouin gain coefficient. If the acoustic waves decay as $\exp(-t/\tau_B)$, where τ_B is the phonon lifetime, then

$$g_B(\nu) = \frac{\Delta\nu_B^2 \, g_B(\nu_B)}{4(\nu - \nu_B)^2 + \Delta\nu_B^2} \qquad \text{where} \qquad g_B(\nu_B) = \frac{2\pi n^7 p_{12}^2}{c\lambda_p^2 \rho \, v_A \Delta\nu_B}$$

$\Delta\nu_B = 1/\pi\tau_B$ =Brillouin gain bandwidth (FWHM)
p_{12} = longitudinal elasto-optic coefficient
ρ = density

For bulk silica, $\Delta\nu_B \sim 10$MHz and $g_B \sim 1\times10^{-10}$m/W. For silica-based fibers, the Brillouin gain may be reduced due to the presence of dopants (e.g. RE ions) and inhomogeneities, and hence the Brillouin linewidth is generally much broader in silica fibers

Brillouin gain vs pump bandwidth:

If the pump bandwidth $\Delta\nu_p$ is comparable or larger than $\Delta\nu_B$, then the maximum value for Brillouin gain coefficient will decrease significantly

$$g_{B\max} = \frac{\Delta\nu_B}{\Delta\nu_B + \Delta\nu_p} g_B(\nu_B)$$

→ SBS is mainly an issue in narrow-linewdth sources

Brillouin threshold:

The power in the Stokes wave increases exponentially in the backward (-z) direction according to:

$$I_s(0) = I_s(L)\exp(g_B I_p l_{eff} - \alpha l)$$

where $l_{eff} = \frac{1}{\alpha}\left[1 - \exp(-\alpha\, l)\right]$

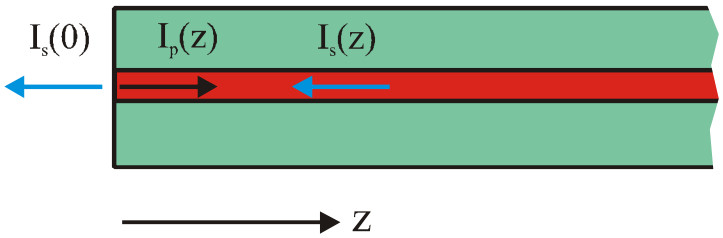

→ Threshold pump power for SBS: $P_{pth}^{SBS} \approx \frac{21A_{eff}}{g_B l_{eff}}$

Example: Typical cladding-pumped Yb-doped silica fiber amplifier with

Core diameter = 15μm $\rightarrow A_{eff} \approx 1.77\times10^{-10}m^2$
l_{eff} = 20m
Narrow-linewdth input signal ($\Delta\nu_p$ < 1MHz) at 1.06μm

$\rightarrow \quad P_{pth}^{SBS} < 2W$

This is only a very rough guide. In practice the SBS threshold would be somewhat higher due inhomogeneities in the fiber core. Nevertheless, this does show that SBS is a significant problem to overcome when scaling the output power from narrow-linewidth single-frequency cw fiber sources.

Possible solutions include:

- Increasing the core area – Limited scope without degrading beam quality
- Shorten device length – More demanding on diode pump beam quality and thermal management
- Deliberately modify the fiber properties along its length (e.g. using longitudinal variation in temperature[9,10])

References

1. G. P. Agrawal, “Nonlinear fiber optics,” Second Edition, (Academic Press 1995).
2. J. Stone, “CW Raman fiber amplifier,” Appl. Phys. Lett., vol. 26, p.163-165 (1975).
3. S. A. Skubchenko, A. Y. Vyatkin and D. V. Gapontsev, “High-power CW linearly polarized all-fiber Raman laser IEEE Photonics Tech. Lett., vol. 16 p.1014-1016 (2004).
4. D. Inniss, D. J. DiGiovanni, T. A. Strasser, A. Hale, C. Headley, A. J. Stenz, T. Pedrazzani, D. Tipton, S. G. Kosinaki, D. L. Brownlow, K. W. Quoi, K. S. Kranz, R. G. Huff, R. Espindola, J. D. Legrange and G. Jacobovitz-Veselka, “Ultra-high-power single-mode fiber lasers from 1.065-1.472μm using Yb-doped cladding-pumped and cascaded Raman Lasers,” CLEO 1997, Postdeadline paper CPD-31 (1997).
5. V. I. Karpov, E. M. Dianov, V. M. Paramonov, O. I. Medvedkov, M. M. Bubnov, S. L. Semyonov, S. A. Vasiliev, V. N. Protopopov, O. N. Egorova, V. F. Hopin, A. N. Guryanov, M. P. Bachynski and W. R. L. Clements, “Laser-diode-pumped phosphosilicate-fiber Raman laser with an output power of 1W at 1.48μm,” Opt. Lett., vol.24, p.887-889 (1999).
6. N. S. Kim, M. Prabhu, C. Li, J. Song and K. Ueda, “1239/1484nm cascaded phosphosilicate Raman fiber laser with CW output power of 1.36W at 1484nm pumped by a CW Yb-doped double-clad fiber laser at 1064nm and spectral continuum generation,” Opt. Comm., vol176, p.219-222 (2000).
7. J. Nilsson, J. K. Sahu, J. N. Jang, R. Selvas, D. C. Hanna and A. B. Grudinin, “Cladding-pumped Raman fiber amplifier,” Optical Amplifiers and their Applications (OAA 2002), post-deadline paper PD-2 (2002).
8. J. N. Jang, Y. Jeong, J. K. Sahu, M. Ibsen, C. A. Codemard, R. Selvas, D. C. Hanna and J. Nilsson, “Cladding-pumped continuous-wave Raman fiber laser,” OFC 2006, paper OThJ2.
9. V. I. Kovalev and R. G. Harrison, “Suppression of stimulated Brillouin scattering in high-power single-frequency fiber amplifiers,” Opt. Lett., vol.31, p161-163 (2006)
10. Y. Jeong, J. Nilsson, J. K. Sahu, D. B. S. Soh, C. Alegria, P. Dupriez, C. A. Codemard, D. N. Payne, R. Horley, L. M. B. Hickey, L. Wanzyck, C. E. Chryssou, J. A. Alverez-Chavez and P. W. Turner, “Single-frequency, single-mode, plane-polarised ytterbium-doped fiber master-oscillator power amplifier source with 264W of output power,” Opt. Lett., vol.30, p.459-461 (2005).

6. Scaling mode area

Scaling the core area and fundamental mode size whilst preserving single-spatial-mode operation and hence good beam quality is an important requirement for further power scaling, and hence is a topic which is currently attracting much interest. The main reasons for this are the following:

- Reduce the cladding-to-core area ratio to reduce fiber length
- Increase the threshold for unwanted nonlinear loss processes (e.g. SRS, SBS)

$$P_{pth}^{SBS,SRS} \propto \frac{A_{eff}}{l_{eff}}$$

- Raise the power/energy damage limit (especially for pulsed operation)
  Surface damage limit for bulk silica glass is ~2GW/cm^2 and is lower (~1GW/cm^2) for doped silica glass

- Increase the 'stored' energy for pulsed operation
- Decrease fiber propagation loss
- Flexibility in operating wavelength
- Reduce output beam divergence → Easier collimation of output with lower spec. lenses

Example: Double-clad Yb-doped fiber with a conventional step-index single-mode core design[1]

$$V = \frac{2\pi r_a}{\lambda}\sqrt{n_a^2 - n_b^2} = \frac{2\pi r_a}{\lambda} NA < 2.405$$

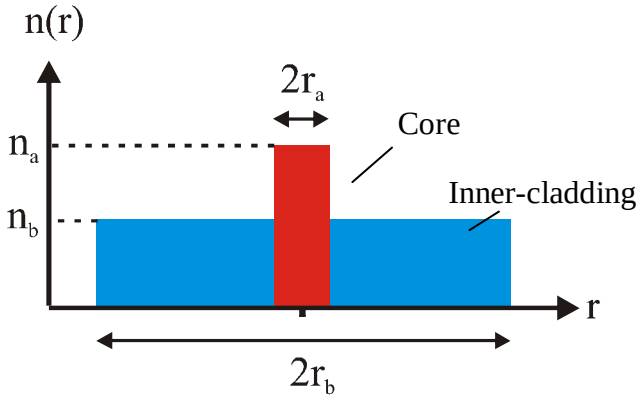

For λ = 1.06μm and NA = 0.15, then r_a = 2.6μm

If r_b = 200μm and [Yb^{3+}] = 7000ppm (i.e. for a typical double-clad fiber design) then:

→ Inner-cladding-to-core area ratio is 5900:1
→ Fiber length for efficient pump absorption (>10dB) at 975nm is ~ 120m
→ Threshold for SRS is ~ 28W
→ CW damage threshold is ~ 200W

Very rough guide to power limits (excluding thermal limits)

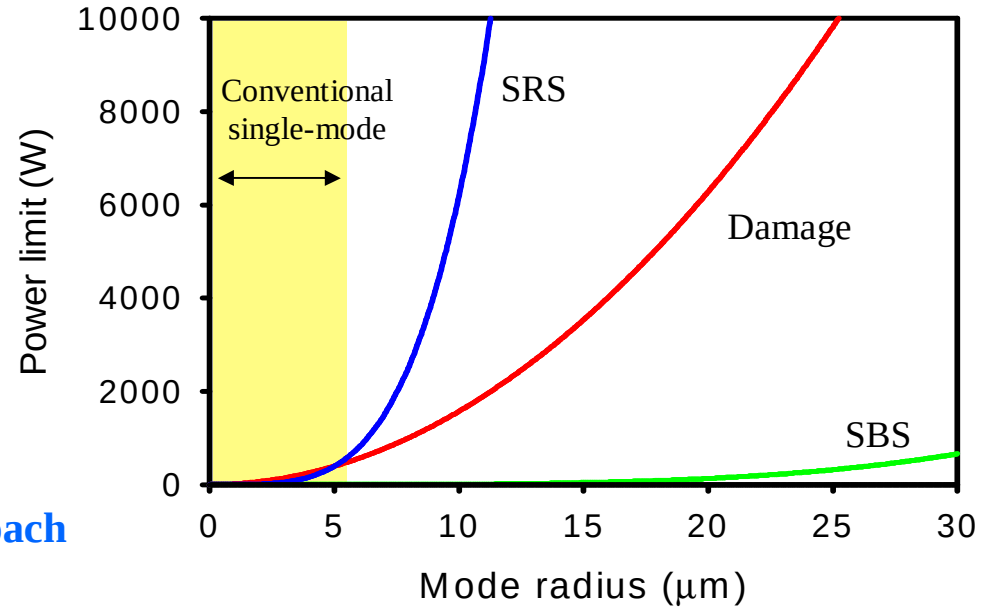

Difficult to fabricate conventional fibers with core NA's <0.04 - 0.05
→ Limited scope for power scaling

For higher power levels a different approach is needed

Novel core designs:

- **Large-mode-area core**
  - Complex refractive index profiles with ring structure to expand the fundamental mode area[2,3]
  - More difficult to fabricate

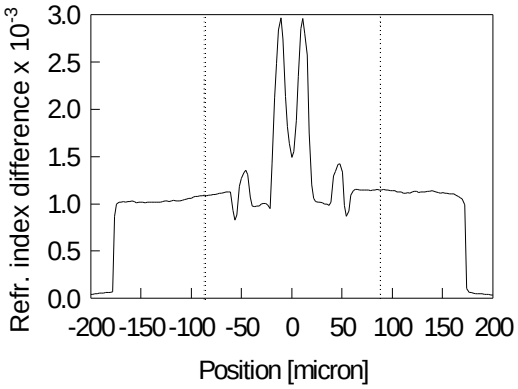

- **Microstructured (holey) fibers**

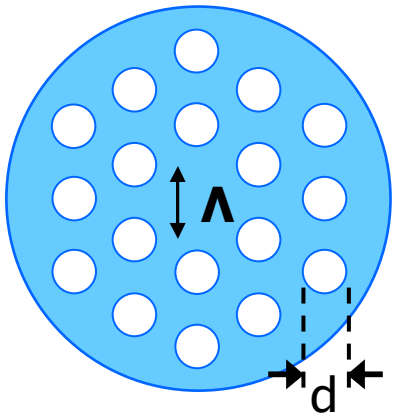

Λ = hole-to-hole spacing

d/Λ = relative hole size

$n_{core} > n_{clad}(\lambda,d,\Lambda)$

Light is guided by the effective refractive index difference between the core and cladding regions

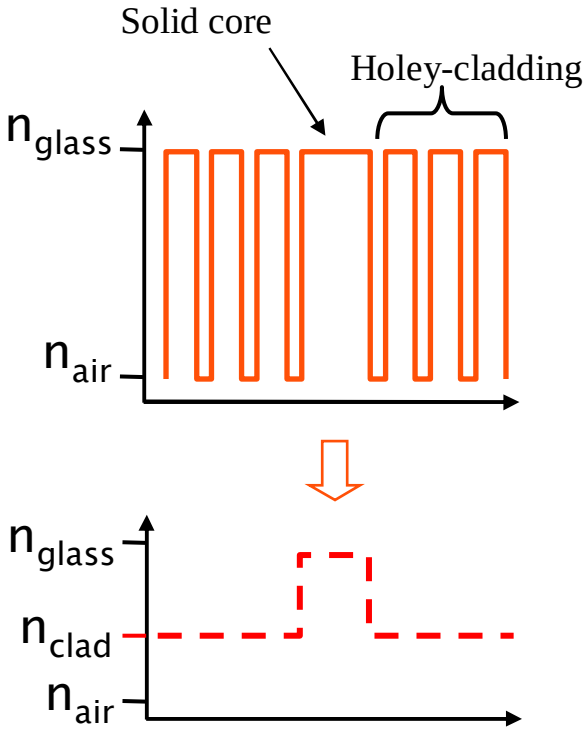

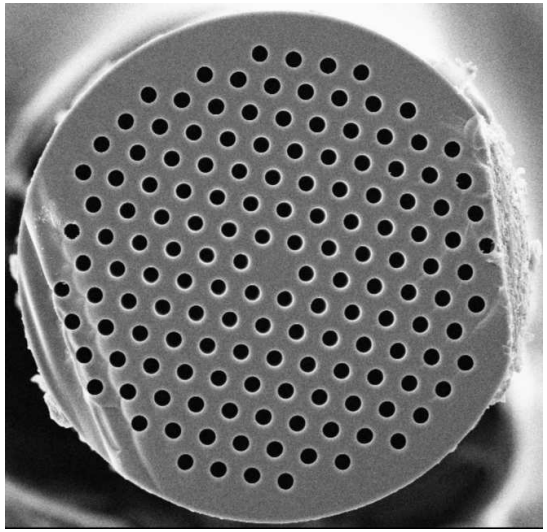

A_{eff} ~ 490μm at λ = 1μm
NA ~ 0.03 and can be reduced further by decreasing hole size.

Bend loss is the main limiting factor[4,5]

Mode selection in multimode cores

An alternative strategy for scaling mode area is to employ a multimode core design and restrict the number of modes, preferably to just the fundamental mode.

This is generally quite straightforward for cores that are only slightly multimode, but becomes increasingly difficult as the core size increases.

If we make the simplifying approximation that the fundamental LP_{01} mode has a Gaussian intensity profile: $I_{LP01}(r) = A\exp(-2r^2/w_o^2)$, then for relatively small V values ($V < 8$) the mode radius w_o is given by[6]

$$w_o = r_a\left(0.65 + \frac{1.619}{V^{3/2}} + \frac{2.879}{V^6}\right)$$

LP_{01} mode area increases with as core radius increases, but it occupies a smaller fraction of the core area as V increases

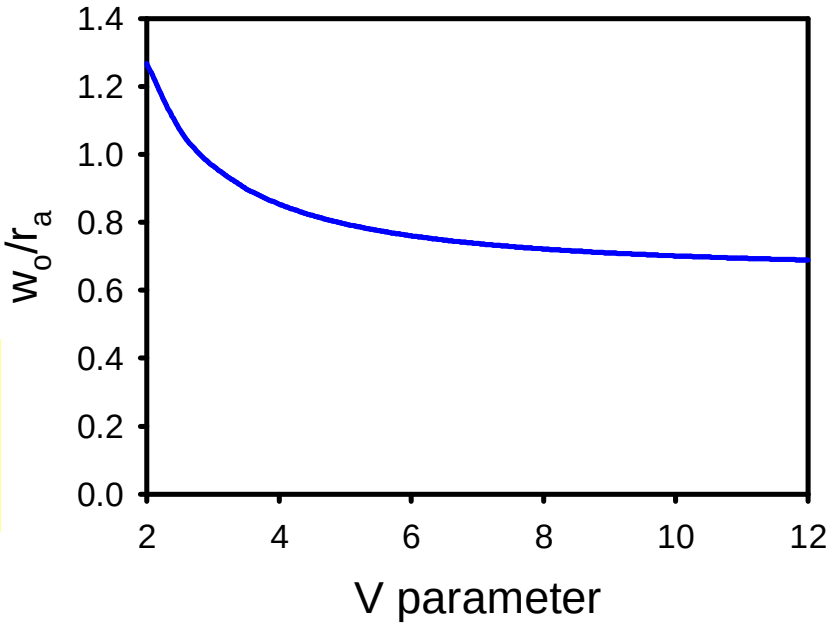

Main problems:

(a) Mode-coupling

In a 'perfect' multimode fiber there is no energy conversion from one guided mode to other guided modes[7]. However, in practice, multimode fibers have perturbations in refractive index due imperfections in the fiber, curved waveguide trajectory or bending which leads to coupling between modes. Thus, if a single-mode laser beam is launched into a multimode, then energy is coupled into higher order modes and the beam quality deteriorates as the light propagates along the fiber.

As a rough guide[8]:

$$M^2(z) \approx \left(1 + \frac{16\, r_a^2 D z}{\lambda^2}\right)^2$$

where D is the mode-coupling coefficient and $D \propto r_a^8 / (r_b^6 \lambda^4)$. D also depends on other details of the fiber (e.g. imperfections), which may be influenced by the fabrication procedure.

Multimode fibers with a core diameter of 45μm (NA = 0.13) and a low enough values for D for single-mode propagation over 20m at 1.55μm have been reported[5]. However, scaling to even larger core sizes and extending to shorter wavelengths around 1μm is difficult.

(b) Mode overlap

Single-mode core (V = 2.4)

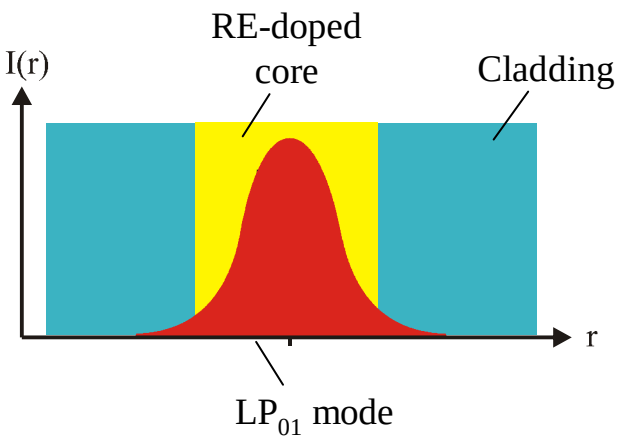

V increasing

Multimode core

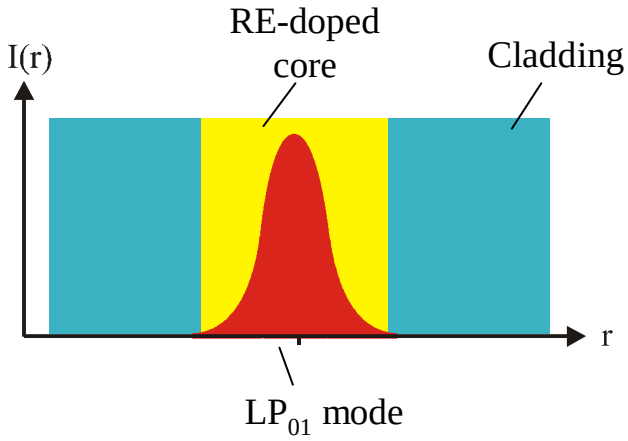

As the V parameter increases and the core becomes more multimode and the fundamental (LP_{01}) mode occupies a smaller fraction of the core area

→ Unused population inversion

→ Gain for higher order modes

→ Can promote multimode lasing in oscillators and is also a problem in amplifiers

One way to alleviate this problem is to use a core design with the RE dopant confined to the central region to improve the spatial overlap. However, this has the disadvantage of increasing the device length by virtue of increasing the effective absorption coefficient for cladding pumping.

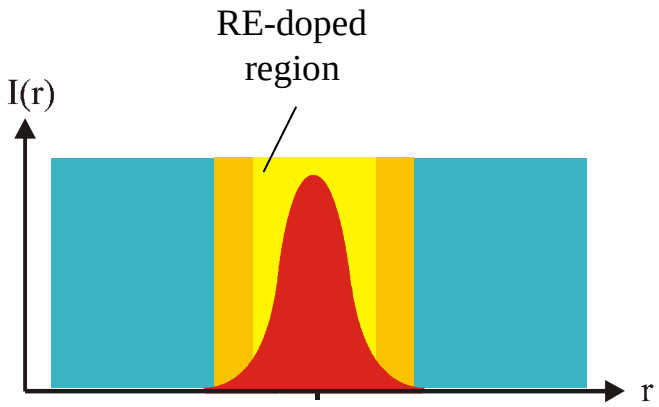

Mode selection using a taper

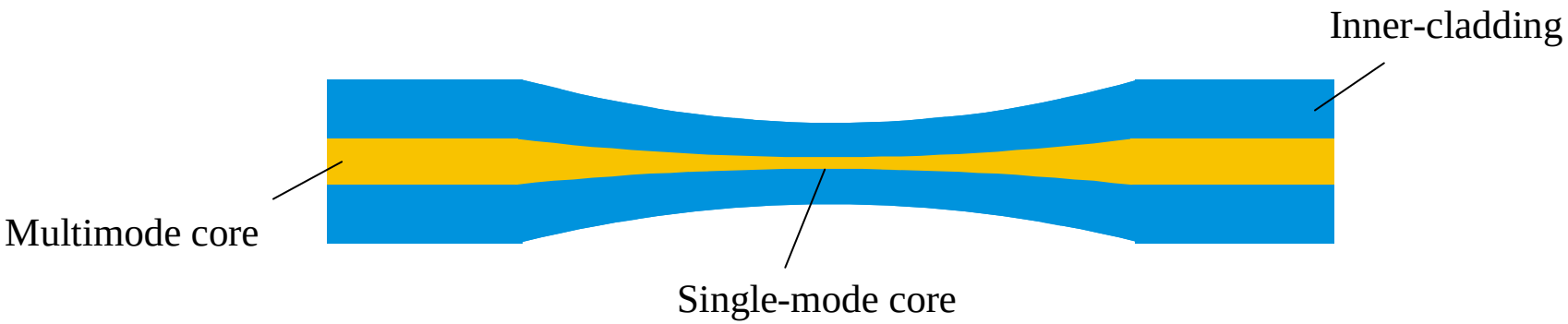

Basic idea: Taper fiber so that the multimode core is reduced in diameter so that only the fundamental mode can propagate in the core with low loss[9]

- Low loss for fundamental mode + high loss for higher order modes
- Requires low mode-coupling otherwise there is a significant decrease in efficiency
- Pump light in the cladding will experience a high loss in the tapered section, so pump light should be launched into the opposite end of the fiber
- Core damage may still be an issue due to the small core size in the tapered region

Distributed mode-filtering along the entire length of the fiber is generally a more effective technique (especially when mode-coupling is strong).

Mode selection by bending

Basic idea:

Bending a fiber results in increased propagation loss for all guided modes. However, the propagation loss for the fundamental mode (LP_{01}) is lower than for higher order modes, so bend-induced loss can be used as a very effective means for suppressing higher order modes in a multimode fiber[10].

The loss coefficient, γ, for the fundamental mode and higher-order modes in a bent fiber with a 'step-index' core can be estimated from[11]:

$$\gamma = \frac{1}{\rho}\left(\frac{\pi\rho}{R_b}\right)^{1/2} \cdot \frac{U^2}{e_\nu V^2 W^{3/2} K_{\nu-1}(W) K_{\nu+1}(W)} \cdot \exp\left(-\frac{2\beta R_b W^3}{3(knc l\rho)^3}\right)$$

where $e_\nu = 2$ if $\nu = 0$ (LP_{01}, fundamental mode) and $e_\nu = 1$ for higher order modes, U, V, and W are the waveguide modal parameters[1], K(W) is the modified Hankel function of W, β is the propagation constant of the mode in the fiber, k is the free space propagation constant, ρ is the fiber core radius and R_b is the bend radius of the fiber.

The fiber can be wound on a circular heat-sink → Distributed mode filter

Bend loss increases with:

- Decreasing bend radius
- Lower NA
- Longer wavelength
- Increasing core radius

Example: Bend loss versus bend radius for LP_{01} and LP_{11} modes at 1.06μm for a core with NA = 0.05

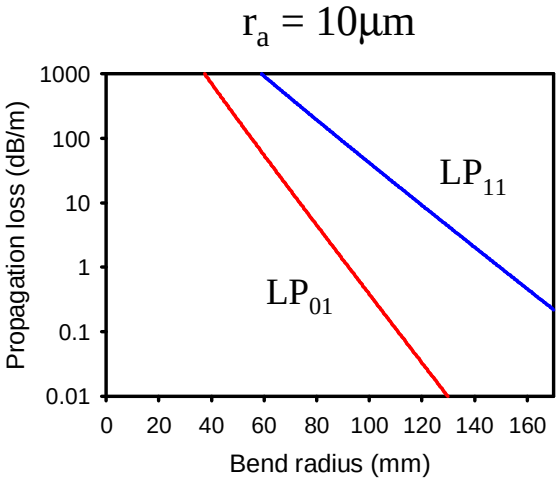

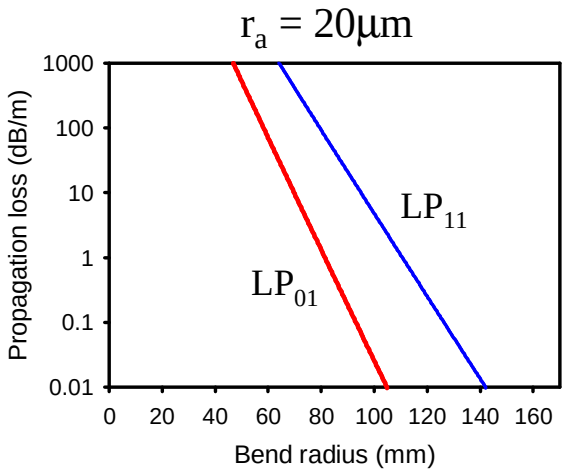

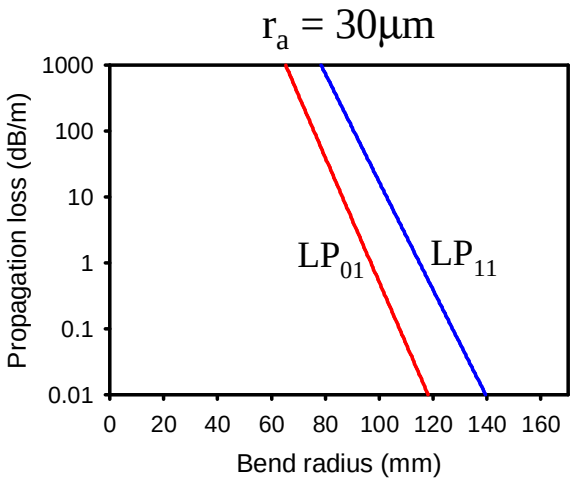

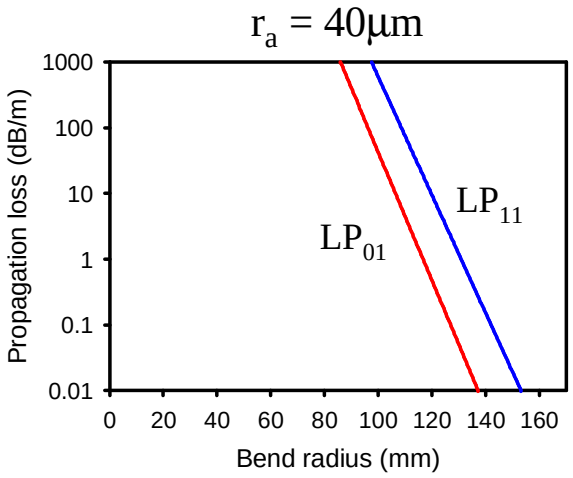

- Loss versus bend radius curves get steeper as the core radius is increased
  → Tighter tolerance on bend radius

Important points:

- Calculating the bend radius required for suppression of high-order modes is quite complicated as many factors need to be considered.
- Easier to estimate bend radius from bend loss calculation and then optimise design by experiment
- As the V value increases → Number of guide modes ~$V^2/2$. If all the modes are excited then $M^2 \rightarrow V/2$, but the fundamental mode still occupies a reasonable fraction of the core area → Spatial overlap between LP_{01} mode and higher order modes increases
  → Increasingly difficult to suppress higher order modes as the core size is increased

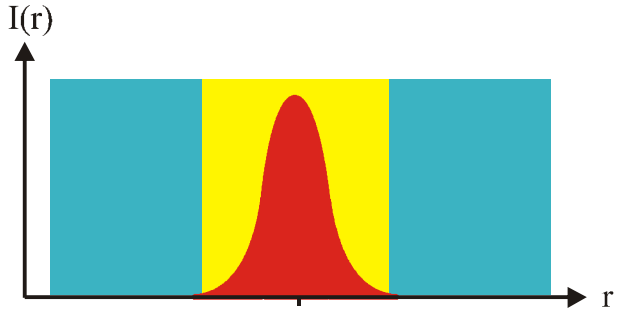

The lower limit on core NA in conventional fibers is ~ 0.04. This limit is currently determined by the fabrication procedure. Microstructured fibers offer the possibility of even lower NA's and hence larger core areas. However, bend loss for the LP_{01} mode becomes a serious problem as the NA is decreased further.

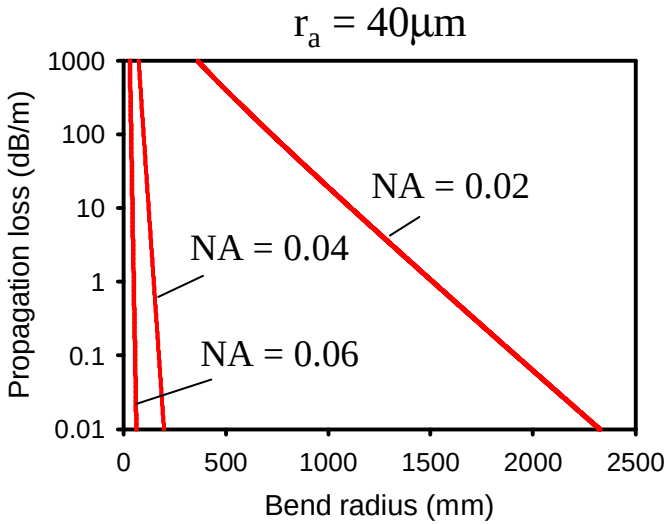

The use of bend loss as a means for suppressing higher order modes in large-core fibers has facilitated scaling of fiber cw powers to the ~kW regime[12] and pulse energies to the ~ mJ regime[13]

References

1. A. W. Snyder and J. D. Love, “Optical Waveguide Theory,” (Kluwer Academic Publishers, 2000).
2. N. G. R. Broderick, H. L. Offerhaus, D. J. Richardson, R. A. Sammut, J. Caplen and L. Dong, “Large mode area fibers for high power applications,” Opt. Fiber Tech., vol. 5, p.185-196 (1999).
3. H. L. Offerhaus, J. Alvarez-Chavez, J. Nilsson, W. A. Clarkson, P. W. Turner, D. J. Richardson and A. B. Grudinin, “Characteristics of Q-switched cladding-pumped ytterbium-doped fibre laser with different high energy fibre designs,” J. Quantum Electron., vol.37, p.199-206 (2001).
4. J. M. Fini, “Bend-resistant design of conventional and microstructure fibers with very large mode area,” Optics Express, vol. 14, p.69-81 (2006).
5. http://www.crystal-fibre.com
6. D. Marcuse, “Loss analysis of single-mode fiber splices,” Bell System Technical Journal, vol. 56. p.703-718 (1977).
7. D. Marcuse, “Theory of Dielectric Optical Waveguides,” (Academic Press, San Diego, 1974).
8. M. E. Fermann, “Single-mode excitation of multimode fibers with ultrashort pulses,” Opt. Lett., vol.23, p.52-54 (1998).
9. J. Alvarez-Chavez, A. B. Grudinin, J. Nilsson, P. W. Turner and W. A. Clarkson, “Mode selection in high power cladding pumped fibre lasers with tapered section,” Conference on Lasers and Electro-Optics 1999, Optical Society of America, Washington D.C., paper CWE7, p.247-248 (1999).
10. J. P. Koplow, D. A. V. Kliner, L. Goldberg “Single-mode operation of a coiled multimode fiber amplifier”,Opt. Lett., vol. 25, p. 442-444 (2000).
11. D. Marcuse, “Curvature loss formula for optical fibers”, J. Opt. Soc. Am., vol. 66, p.216-220 (1976).
12. A. Tunnermann, T. Schreiber, F. Roser, A. liem, S. Hofer, H. Zellmer, S. Nolte and J. Limpert, ”The renaissance and bright future of fiber lasers,” J. Phys. B: At. Mol. Opt. Phys., vol.38, p.681-693 (2005).
13. M. Y. Cheng, Y. C. Chang, A. Galvanauskas, P. Mamidipudi, R. Changkakoti and P. Gatchell, “High-energy and high-peal-power nanosecond pulse generation with beam quality control in 200-μm core highly multimode Yb-doped fiber amplifiers,” Opt. Lett., vol.30, p.358-360 (2005).

7. Wavelength selection and tuning

One of the attractions of fiber-based sources is the flexibility in operating wavelength owing to the broad transition linewidths for a glass host. The range of operating wavelengths depends on a number of factors, including:

- Spectroscopy of the laser transition (i.e. emission and absorption cross-sections, upper-state lifetime, linewidth, loss processes)
- Wavelength selection scheme
- Fiber configuration (RE ion doping level, pumping scheme, pump wavelength, device length)

Yb-doped silica:

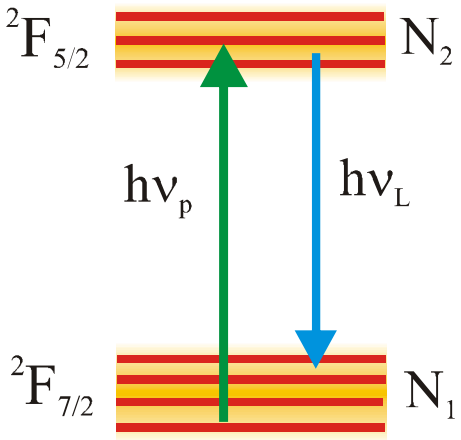

N_1 and N_2 are the total population densities of the lower and upper manifolds respectively and $N = N_1 + N_2$ is the doping concentration.

For transparency we require: $N_1\sigma_a(\lambda_L) = N_2\sigma_e(\lambda_L)$

$$\rightarrow \quad N_2 = \frac{N\sigma_a(\lambda_L)}{\sigma_a(\lambda_L)+\sigma_e(\lambda_L)}$$

where $\sigma_e(\lambda_L)$ and $\sigma_a(\lambda_L)$ are the emission and absorption cross-sections at lasing wavelength λ_L respectively. As $\sigma_a(\lambda_L)/\sigma_e(\lambda_L)$ increases, the transition has a stronger three-level character and hence the threshold increases → Short wavelength limit

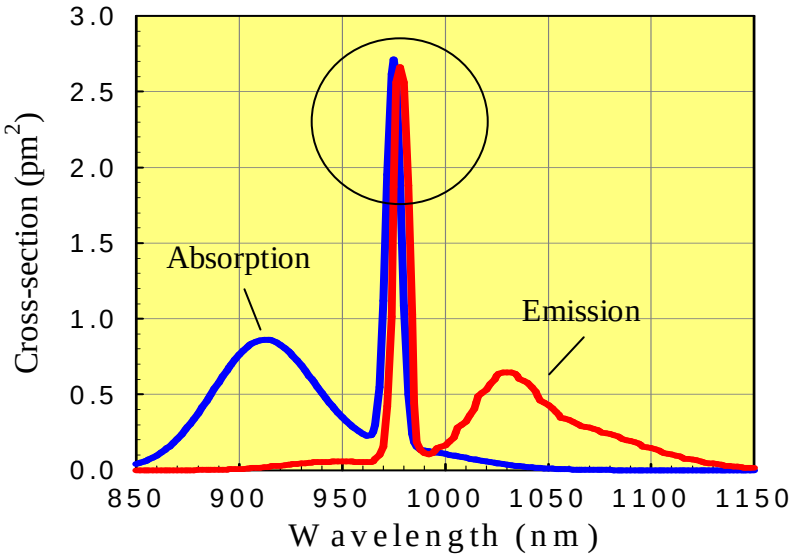

Pump power required for transparency is given by[1]

$$P_{trans} = \frac{A_c h\nu_p}{\eta_p \tau_f \left(\frac{\sigma_e(\lambda_L)\sigma_a(\lambda_p)}{\sigma_a(\lambda_L)} - \sigma_e(\lambda_p) \right)}$$

where A_c is the core area, τ_f is the lifetime of the upper level and η_p is the overlap factor for pump light with the doped core

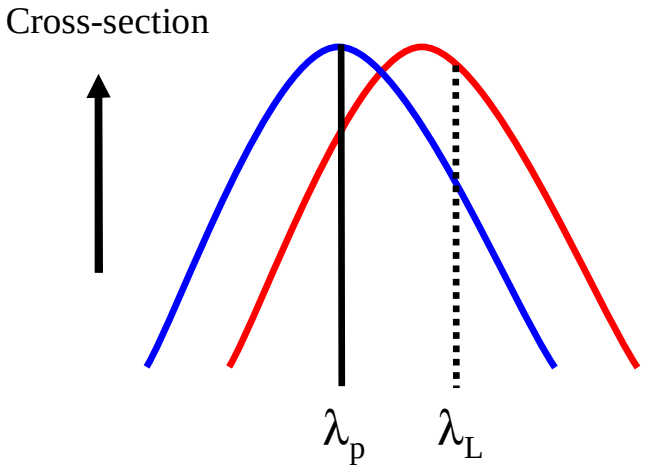

$$\frac{\sigma_e(\lambda_L)}{\sigma_a(\lambda_L)} > \frac{\sigma_e(\lambda_p)}{\sigma_a(\lambda_p)}$$

→ Threshold increases dramatically as the lasing wavelength approaches the emission peak at ~980nm

→ Very short wavelength operation requires pumping at shorter wavelengths (e.g. ~915nm) and a high value for η_p

Cladding pumping → Long device lengths and high reabsorption loss at short wavelengths
Moves the effective gain peak towards the longer wavelength end of the emission spectrum
Flexibility in operating wavelength is reduced compared to core pumping

Wavelength selection and tuning schemes

(a) External cavity with diffraction grating[2]

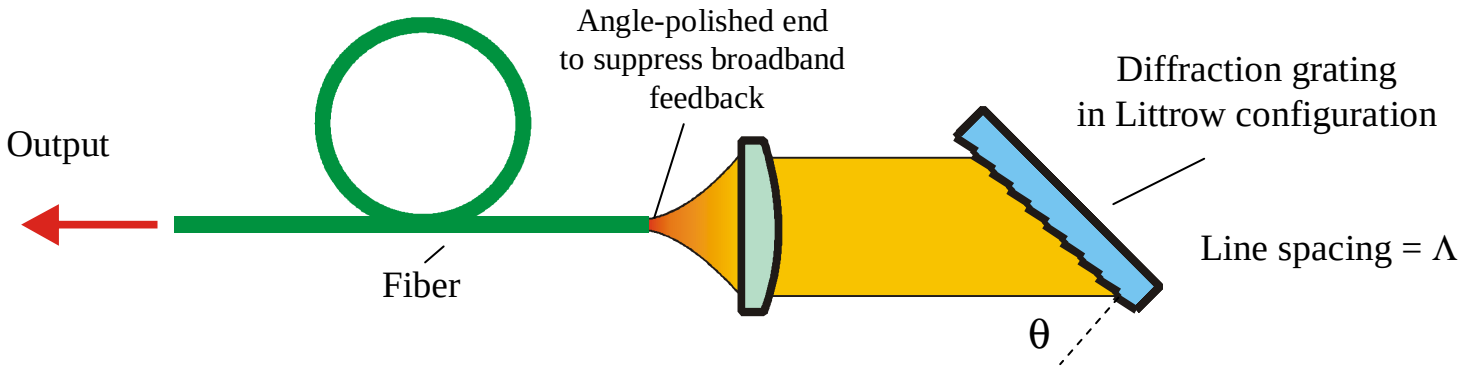

- Lasing wavelength can be selected by adjusted grating angle: $\lambda_L = 2\Lambda \sin\theta$
- Wavelength tuning range depends on many factors (see previous slides)
- Bandwidth of emission depends on the grating, the feedback cavity design and the fiber

Spectral selectivity of feedback cavity: $\Delta\lambda_L \propto \dfrac{\lambda_L M^2 \Lambda \cos\theta}{f \sin^{-1}(NA)}$

→ Linewidths < 0.1nm are easy to achieve

Note: Damage due to self-pulsing can occur if the grating angle is adjusted to select a wavelength beyond the tuning range.

Example:

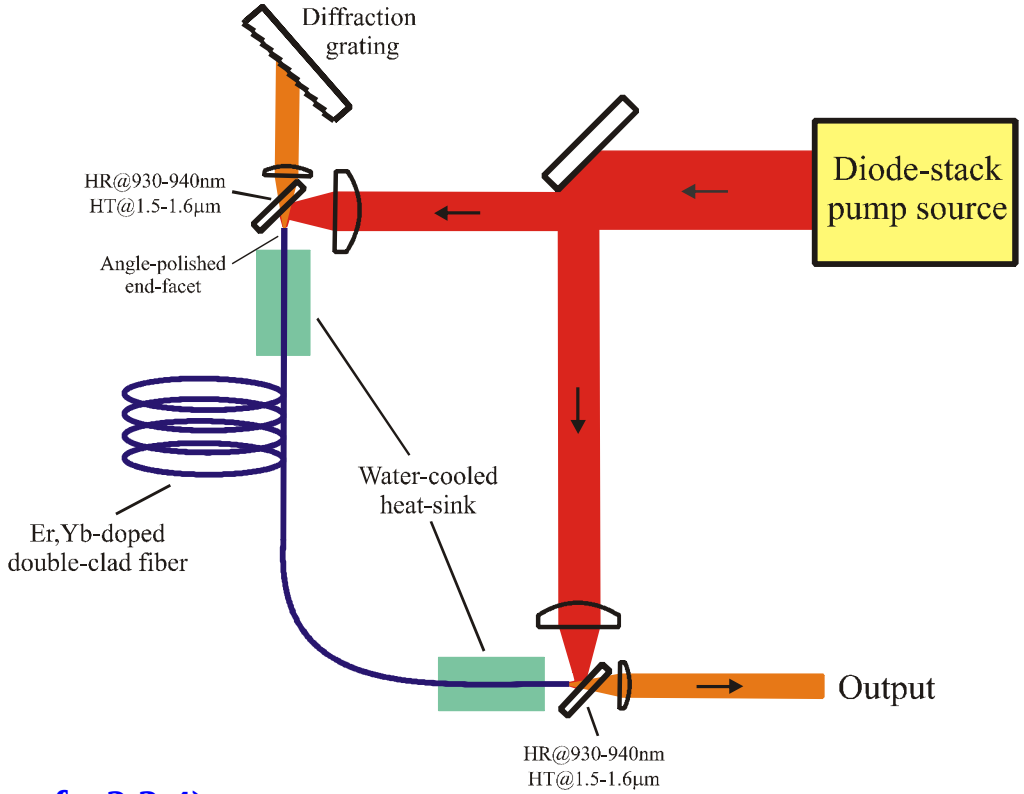

Typical tuning curves (see refs. 2,3,4):

Yb-doped alumino-silicate fiber

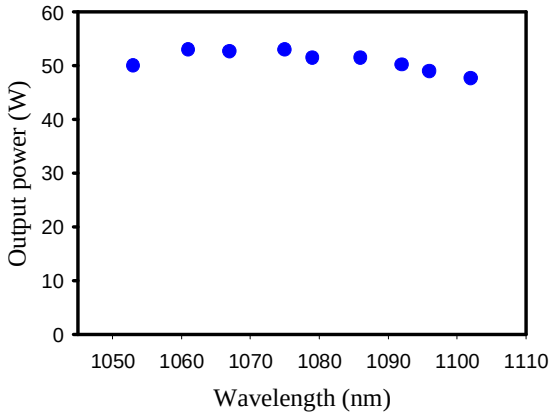

Er,Yb-doped phospho-silicate fiber

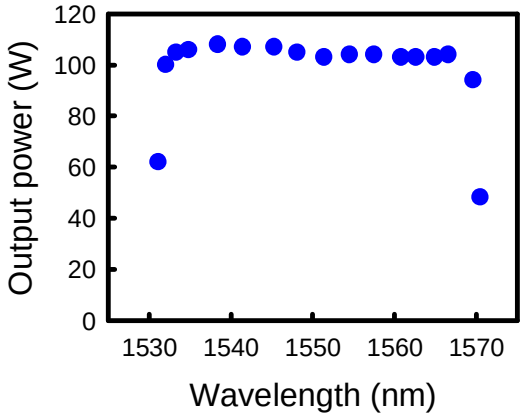

Tm-doped alumino-silicate fiber

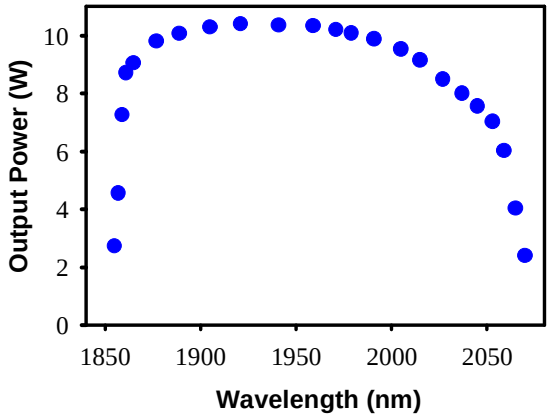

(b) In-fiber Bragg grating[5,6,]

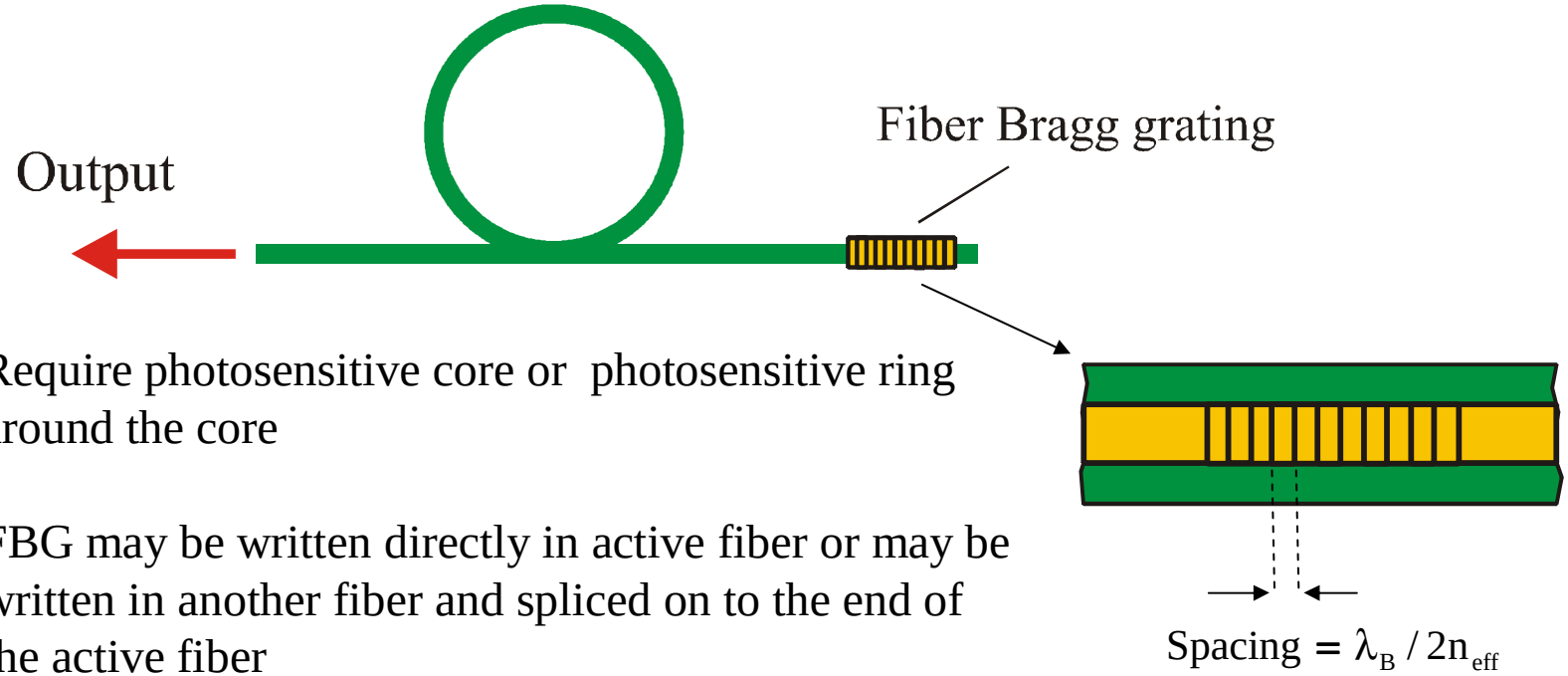

- Require photosensitive core or photosensitive ring around the core
- FBG may be written directly in active fiber or may be written in another fiber and spliced on to the end of the active fiber
- Reflectivity at central wavelength[5]: $R = \tanh^2\left(\frac{\pi \delta n l_G g \eta_G}{\lambda}\right)$

where δn is the refractive index change, l_G is the length of the grating, g is the average value of the envelope weighting function and η_G is the modal overlap factor

→ FBG reflectivity >99% can be achieved

→ Wavelength tuning over a few % of λ_B can be achieved by compressing/stretching the grating[6]

→ Narrow linewidth (<0.01nm) achievable, but is generally much broader in multimode devices

Power handling issues at high power levels may be avoided using a MOPA configuration

Single-frequency fiber sources

There are a number of different approaches for achieving single-frequency operation[7]. One of the most popular is to use a distributed feedback (DFB) architecture[8]

DFB fiber laser:

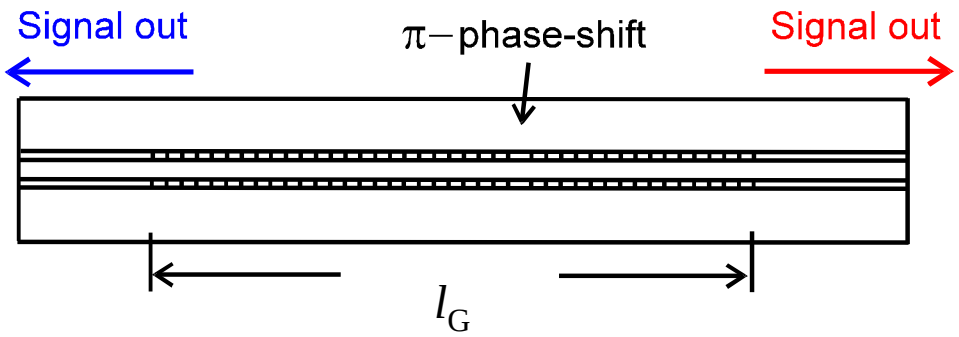

Typical operating characteristics:

- Low temperature sensitivity (<0.01nm/K or ~1GHz/K)
- Ultra high Signal-to-Noise-Ratio, SNR (>70dB)
- Narrow line-width (~1-100kHz)
- Tuneable over >20nm
- High polarisation purity (>30dB)
- Typical output power (10 – 100mW)
- Simple + low cost +monolithic construction

Power scaling of DFB fiber lasers is difficult since a high power single-mode pump source is needed and the pump light must be absorbed within a length of ~10cm or less.

→ Use a MOPA to scale to higher power levels

High-power single-frequency fiber sources

Typical arrangement:

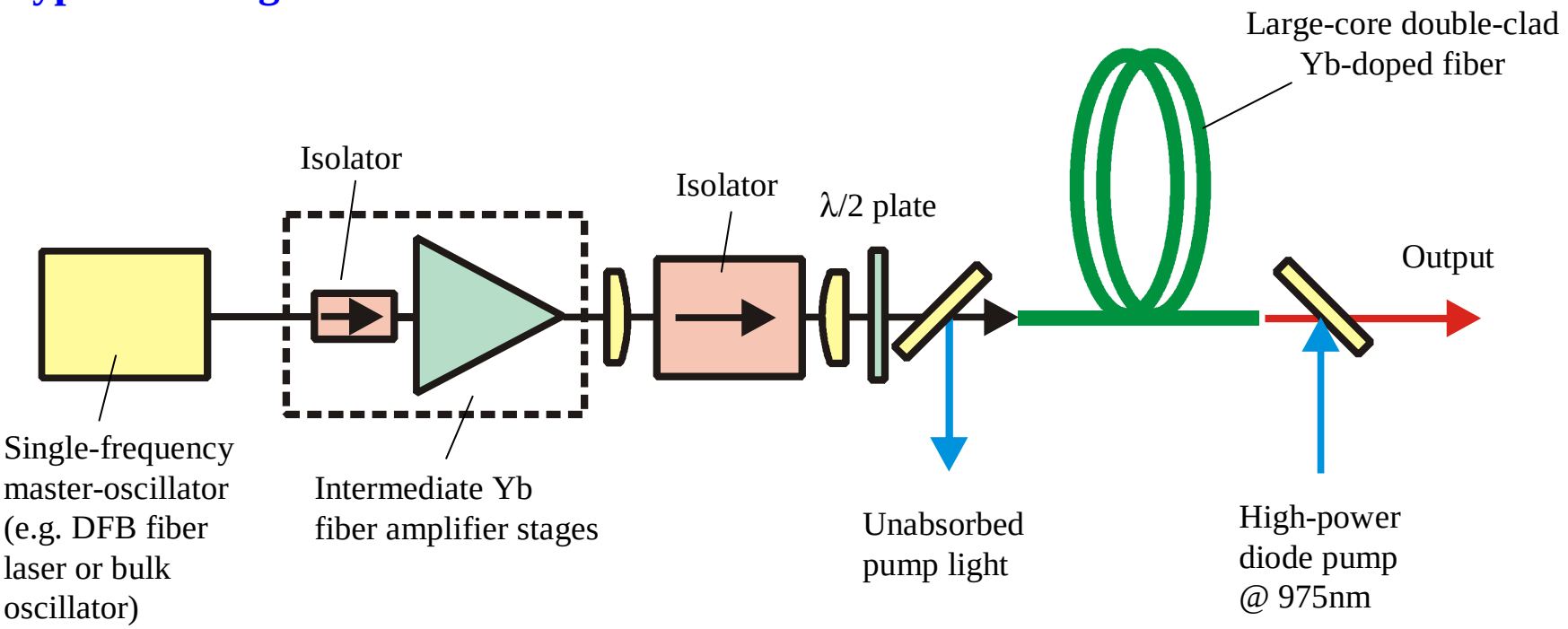

- Number of intermediate amplifiers depends on master-oscillator power
- Large core fiber needed for final power amplifier stage to increase the threshold for SBS
- Polarisation maintaining fiber is required for a single-polarisation output

Using this generic approach single-frequency powers of over 100W have been demonstrated[9,10]

References

1. R. Paschotta, J. Nilsson, A. C. Tropper and D. C. Hanna, “Ytterbium-doped fiber amplifiers,” IEEE J. Quantum Electron., vol.33, p.1049-1056 (1997).
2. J. Nilsson, W. A. Clarkson, R. Selvas, J. K. Sahu, P. W. Turner, S-U. Alam and A. B. Grudinin, “High-power wavelength-tunable cladding-pumped rare-earth-doped silica fiber lasers,” Optical Fiber Technology, vol.10, p.5-30 (2004).
3. W. A. Clarkson, N. P. Barnes, P. W. Turner, J. Nilsson and D. C. Hanna, “High-power cladding-pumped Tm-doped silica fiber laser with wavelength tuning from 1860 to 2090nm,” Opt. Lett., vol.27, p.1989-1991 (2002).
4. D. Y. Shen, J. K. Sahu and W. A. Clarkson, “Highly efficient Er,Yb-doped fiber laser with 188W free-running and >100W tunable output power,” Opt. Express, vol.13, p.4916-4921 (2005).
5. K. O. Hill and G. Meltz, “Fiber Bragg grating technology fundamentals and overview,” IEEE J. Lightwave Technology, vol.15, p.1263-1275 (1997).
6. Y. Jeong, C. Alegria, J. K. Sahu, L. Fu, M. Ibsen, C. A. Codemard, M. R. Mokhtar and J. Nilsson, “A 43-W C-band tunable narrow-linewidth erbium-ytterbium co-doped large-core fiber laser,” IEEE Photon. Tech. Letters, vol.16, p.756-758 (2004).
7. N. Langford, “Narrow-linewidth fiber sources,” in *Rare-Earth-Doped Fiber Lasers and Amplifiers*, edited by M. J. F. Digonnet, 2nd Edition, (Marcel Dekker, Inc., NewYork, 2001).
8. W. H. Loh and R. I. Laming, “1.55μm phase-shifted distributed feedback fibre laser,” Electron. Lett., vol.31, p.1440-1442 (1995).
9. A. Liem, J. Limpert, H. Zellmer and A. Tunnermann, “100W single-frequency master-oscillator fiber power amplifier,” Opt. Lett., vol.28, p.1537-1539 (2003).
10. Y. Jeong, J. Nilsson, J. K. Sahu, D.B. S.Soh, C. Alegria, P. Dupriez, C. A. Codemard, D. N. Payne, R. Horley, L. M. B. Hickey, L. Wanzcyk, C. E. Chryssou, J. A. Alvarez-Chavez and P. W. Turner, “Single-frequency, single-mode, plane-polarised ytterbium-doped fiber master-oscillator power amplifier source with 264W of output power,” Opt. Lett., vol.30, p.459-461 (2005).

8. High-power CW and pulsed fiber sources

Example: Cladding-pumped Yb-doped fiber laser with 1.4kW output power[1]

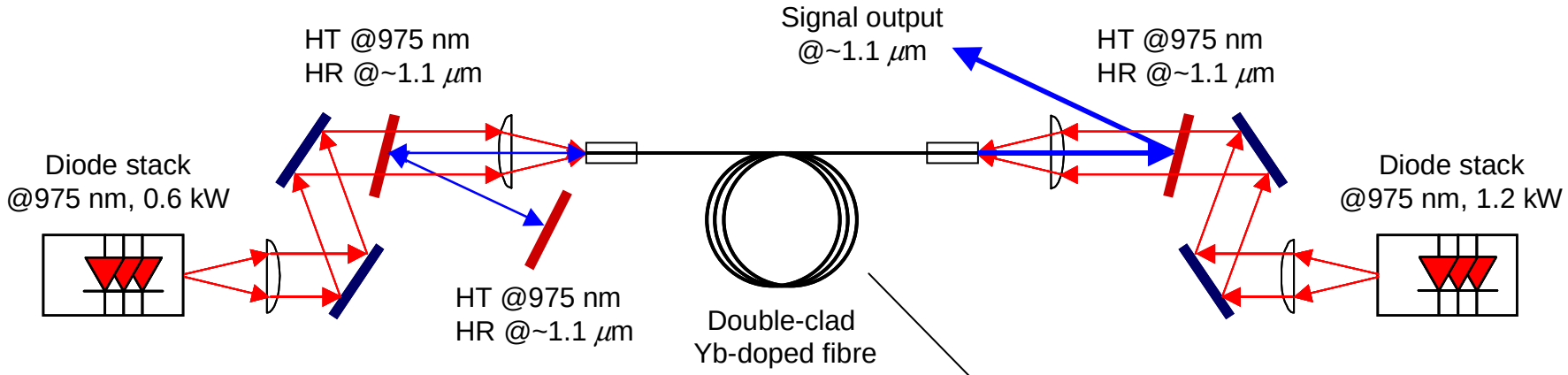

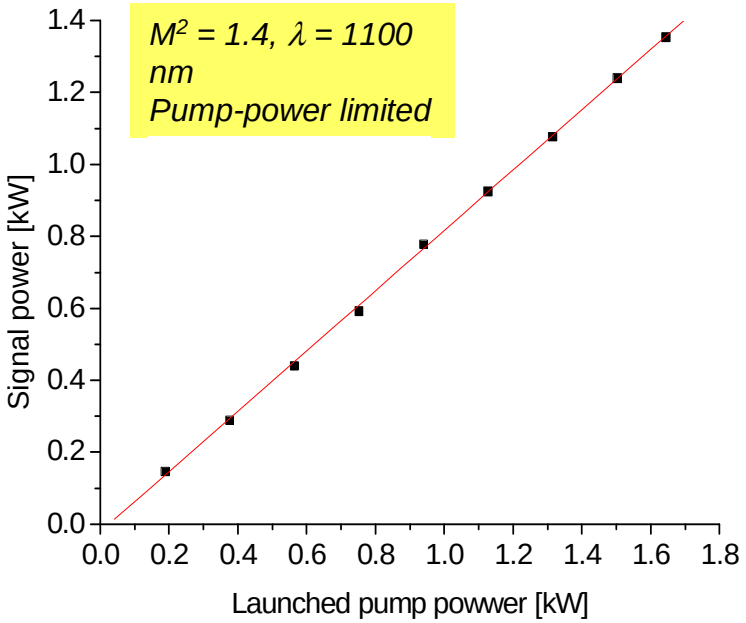

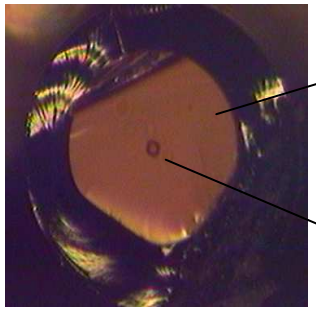

Pure silica D-shaped inner-cladding (Diameter = 650μm, NA = 0.4-0.5)

Core diameter = 40μm, NA <0.5

Using polarisation-maintaining fiber (inner-cladding diameter = 380μm and core diameter = 25μm) and a modified external cavity design with a polariser + half-wave plate → 633W of linearly-polarised output for ~1kW of launched pump power[2]

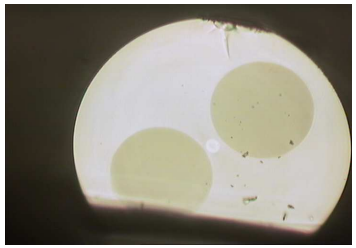

For further examples of high-power cw fiber lasers see refs. 3, 4 and 5

Owing to the:

- Wide range of operating wavelengths
- Broad emission linewidth
- Long upper-state lifetime
- High-power handling capability
- Good beam quality

→ Cladding-pumped fiber sources are also very attractive for generating high average output power and high peak power in pulsed mode

Two main approaches:

- **Laser oscillator** (Q-switched or mode-locked)
  - Single gain element + external cavity required → Simple + low cost
  - Limited flexibility
  - Limited peak power

- **Master-oscillator power-amplifier (MOPA)**
  - Low power oscillator + multiple gain stages
  - Flexibility in pulse duration, pulse shape, repetition rate, etc
  - Power scalable, but can be quite complicated

High-power Q-switched Yb-doped fiber lasers

Extractable energy[6]:

$$E_{ext} = h\nu_L A_{co}\left[\int_0^l N_2(z)dz - \frac{N l \sigma_a(\lambda_L)}{\sigma_e(\lambda_L)+\sigma_a(\lambda_L)}\right]$$

As a very rough guide, the extractable energy stored in a fiber is limited by ASE to around ten times the saturation energy $E_{sat} \approx h\nu_L A_{co}/[\sigma_a(\lambda_L)+\sigma_e(\lambda_L)]\eta_L$. In other words, the upper-limit on pulse energy is determined mainly by the core area. E_{ext} is ~2 - 5mJ for typical Yb-doped fiber with a 20μm diameter core. In practice, the maximum pulse energy also depends on other factors as well (e.g. cavity design, fiber length, nonlinear loss processes (SRS, SBS) and fiber damage).

Example[7]:

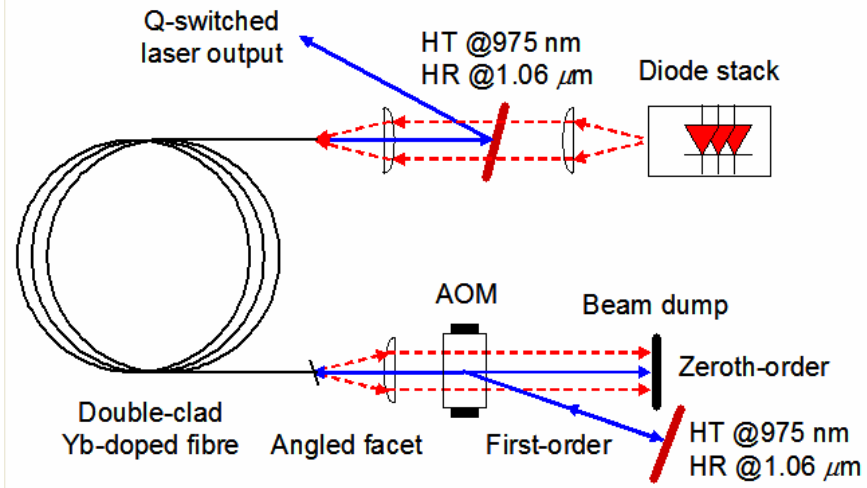

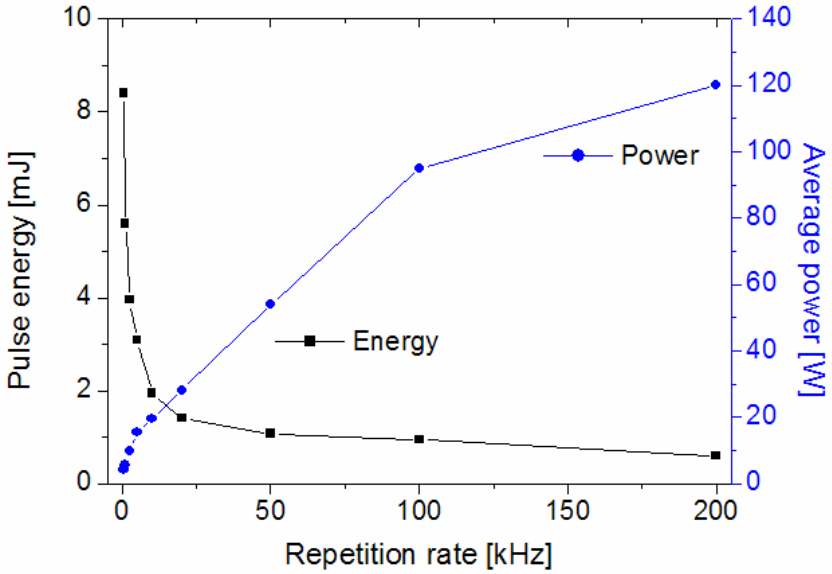

8.4 mJ @ 0.5 kHz, pulse duration = 460ns
0.6 mJ @ 200 kHz (120 W)
Beam quality $M^2 \sim 4$

Shorter pulse durations can be achieved using a shorter fiber[8]

Fiber Facet damage

Damage example

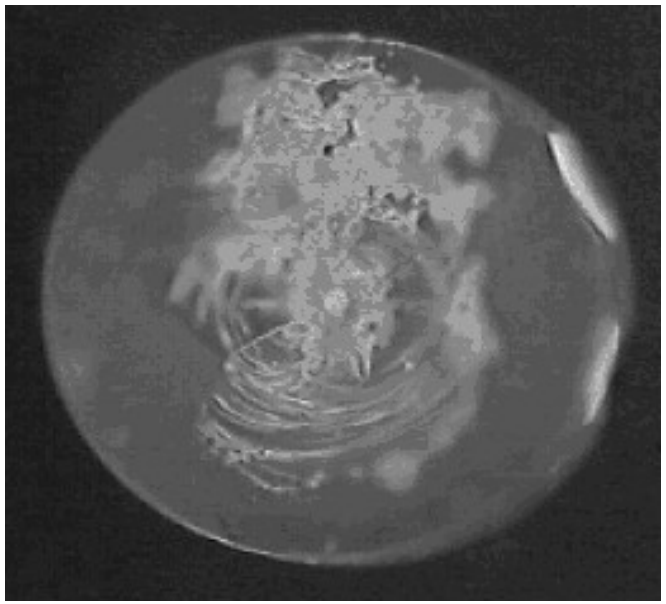

- Damage threshold of pure silica:
  ~2 GW/cm^2 (20 W/μm^2)
  ~50J/cm^2 (~ 10ns pulse)
- Dependent on surface quality, dopants, impurities, inhomogeneities, especially at facets → Large core + end caps needed
- Suppression of self-pulsing

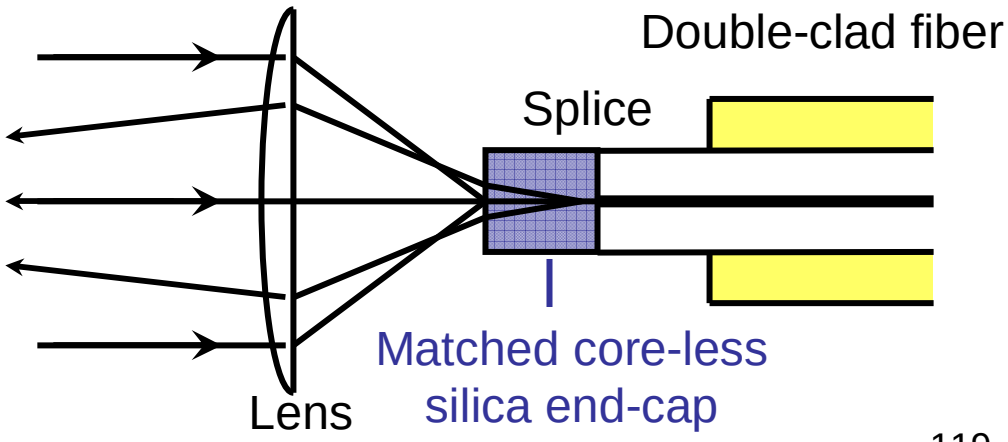

MOPA configurations

Master-oscillator (diode, fiber or bulk)
- low power cw oscillator
- Pulsed (Q-switched)
- Short pulse

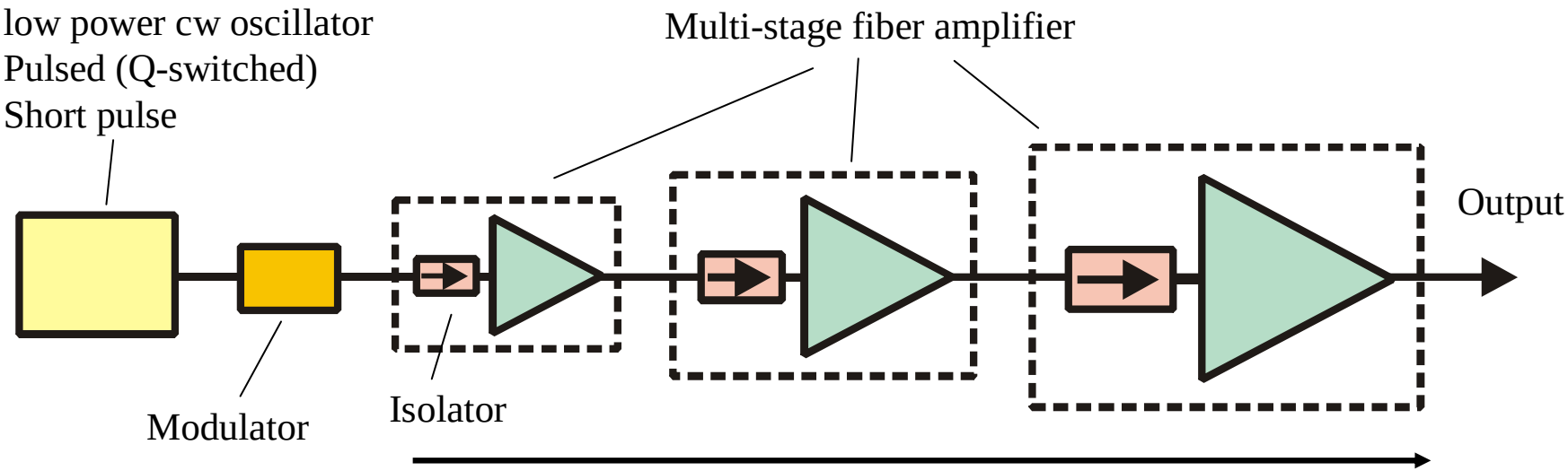

May also require band-pass filters between amplifier stages to suppress ASE

For long pulse operation: High gain + low saturation energy → Strong pulse re-shaping

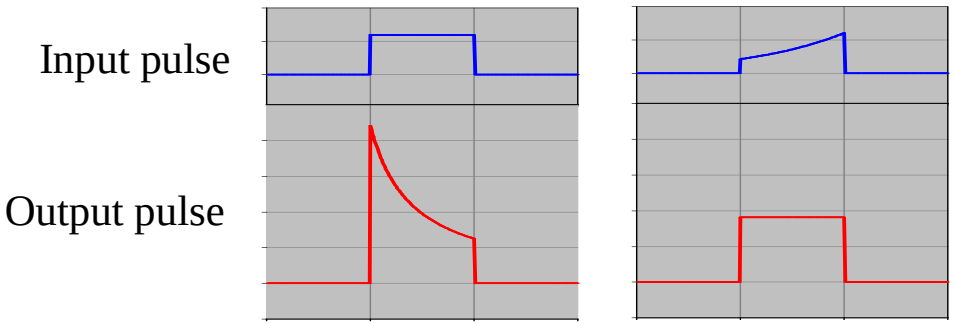

Output pulse shape can be controlled by modifying the input pulse shape

Example: High energy Yb fiber MOPA[9]

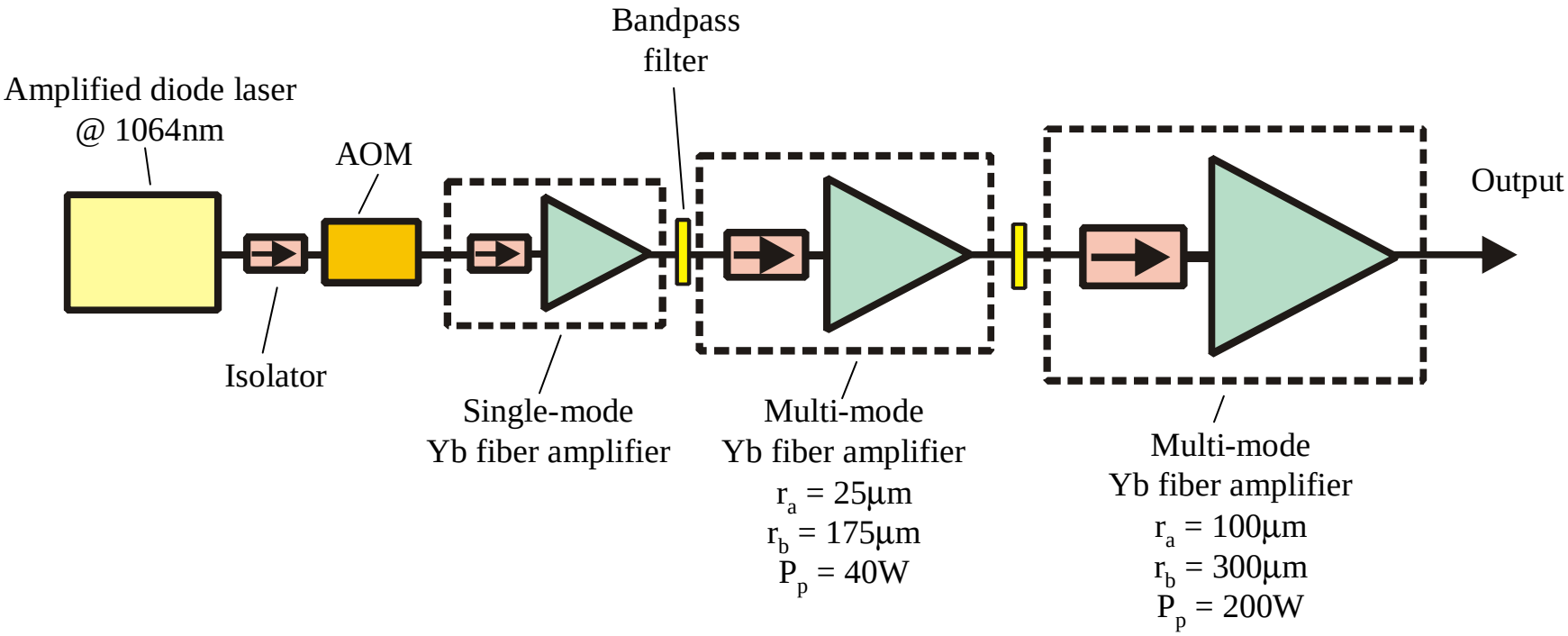

Pulse energies ~ 82mJ for 500ns pulses were reported, and coiling the fiber in the final amplifier with a radius of ~12cm produced strong enough mode-filtering to reduce the M^2 parameter to 6.5 (see ref. 9)

Cladding-pumped fiber amplifier schemes employing chirped pulse amplification have also been used amplify ultrashort pulse oscillators to average power levels >100W (see ref. 10).

References

1. Y. Jeong, J. K. Sahu, D. N. Payne and J. Nilsson, "Ytterbium-doped large-core fiber laser with 1.36kW continuous-wave output power," Opt. Express, vol.12, p. 6088-6092 (2004).
2. Y. Jeong, J. Nilsson, J. K. Sahu, D. B. S. Soh, P. Dupriez, C. A. Codemard, S. Baek, D. N. Payne, R. Horley, J. A. Alvarez-Chavez and P. W. Turner, "Single-mode plane polarised ytterbium-doped large-core fiber laser with 633-W continuous-wave output power," Opt. Lett., vol.30, p.955-957 (2005).
3. A. Tunnermann, T. Schreiber, F. Roser, A. liem, S. Hofer, H. Zellmer, S. Nolte and J. Limpert, "The renaissance and bright future of fiber lasers," J. Phys. B: At. Mol. Opt. Phys., vol.38, p.681-693 (2005).
4. C-H. Liu, B. Ehlers, F. Doerfel, S. Heinemann, A. Carter, K. Tankala, J. Farroni, and A. Galvanauskas, "810 W continuous-wave and single-transverse-mode fibre laser using 20 /spl mu/m core Yb-doped double-clad fibre," Electron. Lett., vol.40, p.1471-1472 (2004).
5. http://www.ipgphotonics.com/ and http://www.spioptics.com/
6. C. C. Renaud, H. L. Offerhaus, J. A. Alvarez-Chavez, J. Nilsson, W. A. Clarkson, P. W. Turner, D. J. Richardson, A. B. Grudinin, "Characteristics of Q-switched cladding-pumped ytterbium-doped fiber lasers with different high-energy fiber designs," IEEE Journal of Quantum Electronics, vol.37(2) p.199-206 (2001).
7. Y. Jeong, J. K. Sahu, M. Laroche, W. A. Clarkson, K. Furusawa, D. J. Richardson and J. Nilsson, "120W Q-switched cladding-pumped Yb-doped fibre laser", CLEO/Europe-EQEC 2003, paper CL5-4 (2003).
8. J. Limpert, N. Deguil-Robin, S. Petit, I. Manek-Hönninger, F. Salin, P. Rigail, C. Hönninger and E. Mottay, "High power Q-switched Yb-doped photonic crystal fiber laser producing sub-10 ns pulses," Appl. Phys. B., vol.81, p.19-21 (2005).
9. M. Y. Cheng, Y. C. Chang, A. Galvanauskas, P. Mamidipudi, R. Changkakoti and P. Gatchell, "High-energy and high-peak-power nanosecond pulse generation with beam quality control in 200µm core highly multimode Yb-doped fiber amplifiers," Opt. Lett., vol.30 (4), p.358-360 (2005)
10. F. Röser, J. Rothhard, B. Ortac, A. Liem, O. Schmidt, T. Schreiber, J. Limpert, and A. Tünnermann, "131W 220 fs fiber laser system," Opt. Lett., vol. 30, p.2754-2756 (2005).

9. Power and brightness scaling via beam combination

Introduction

Scaling the output power and radiance beyond the upper limit for a single fiber core can be achieved via the use of multiple fiber sources or a multi-core fiber source and beam combining[1]. Beam combining schemes fall into one of two categories:

(a) Incoherent beam combining:

Spatial beam combining

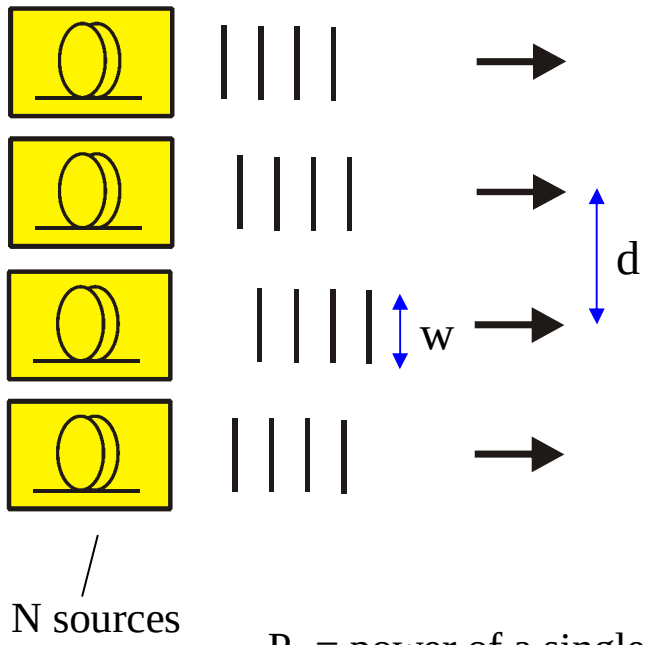

Far-field beam divergence of array = θ_A
Far-field beam divergence of single element = θ_S

No phase relationship between elements $\rightarrow$ $\theta_A = \theta_S$

$$M_S^2 \approx \frac{\pi w \theta_S}{2\lambda} \quad \text{and} \quad M_A^2 \approx \frac{\pi N d \theta_S}{2\lambda}$$

$$\longrightarrow \quad P_A = N P_S$$

$$\longrightarrow \quad \frac{B_A}{B_S} \approx \frac{w}{d} = \eta_{fill}$$

P_S = power of a single element, P_A = power of array, B_S = brightness of a single element, B_A = brightness of array and η_{fill} is the fill-factor

→ Simple and robust way to scale output power, but brightness cannot exceed the brightness of a single element

Examples:

(a) Multi-fiber sources

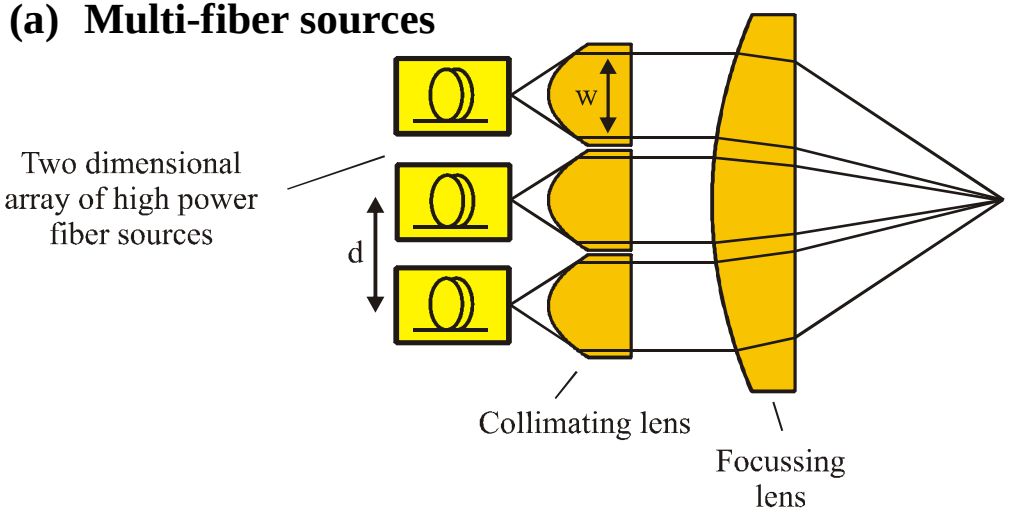

→ Multi-kilowatt power levels are achievable[2]

(b) Multi-core fiber sources

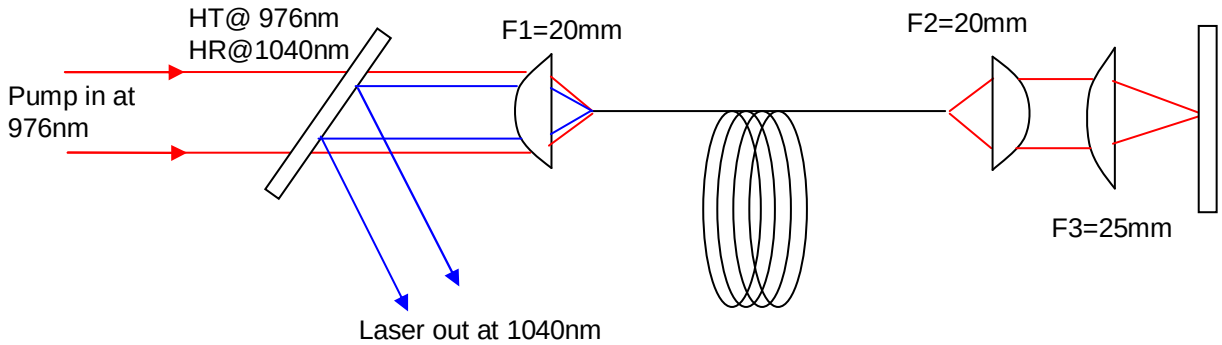

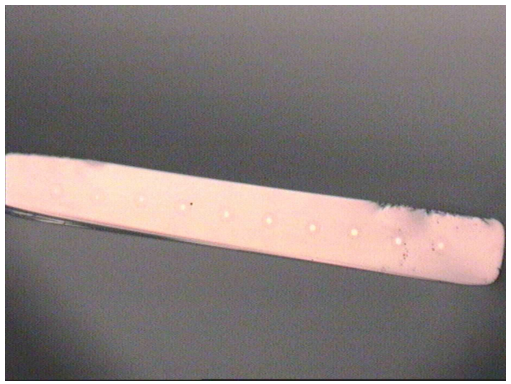

Yb-doped multi-core ribbon fiber[3]

→ Output power > 320W demonstrated (limited by pump power)[3]

Polarization beam combining

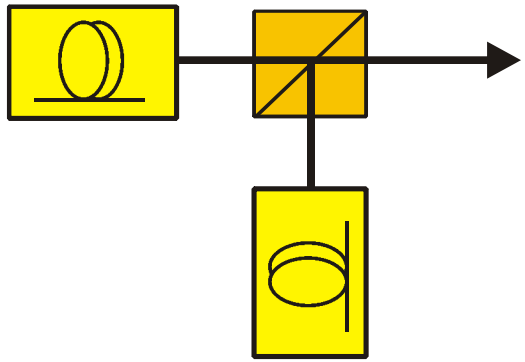

$$B_A = 2\eta_c B_S$$

where η_c is the combining efficiency, which takes into account loss and misalignment

Wavelength beam combining

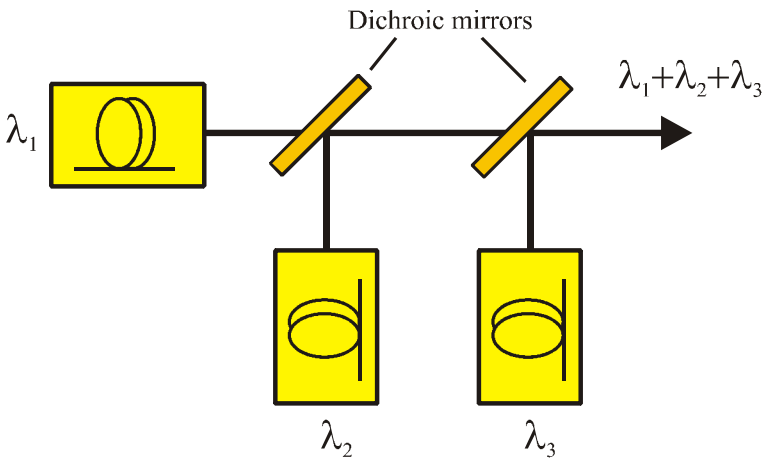

or

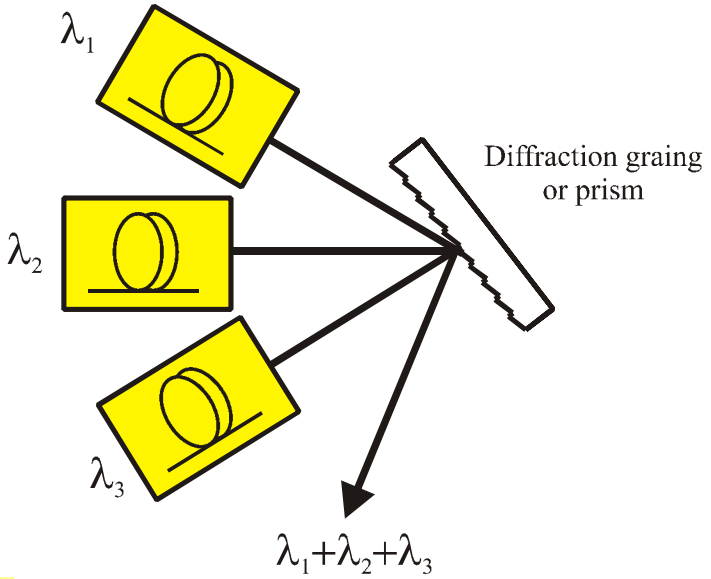

$$B_A = N\eta_c B_S$$

Example:

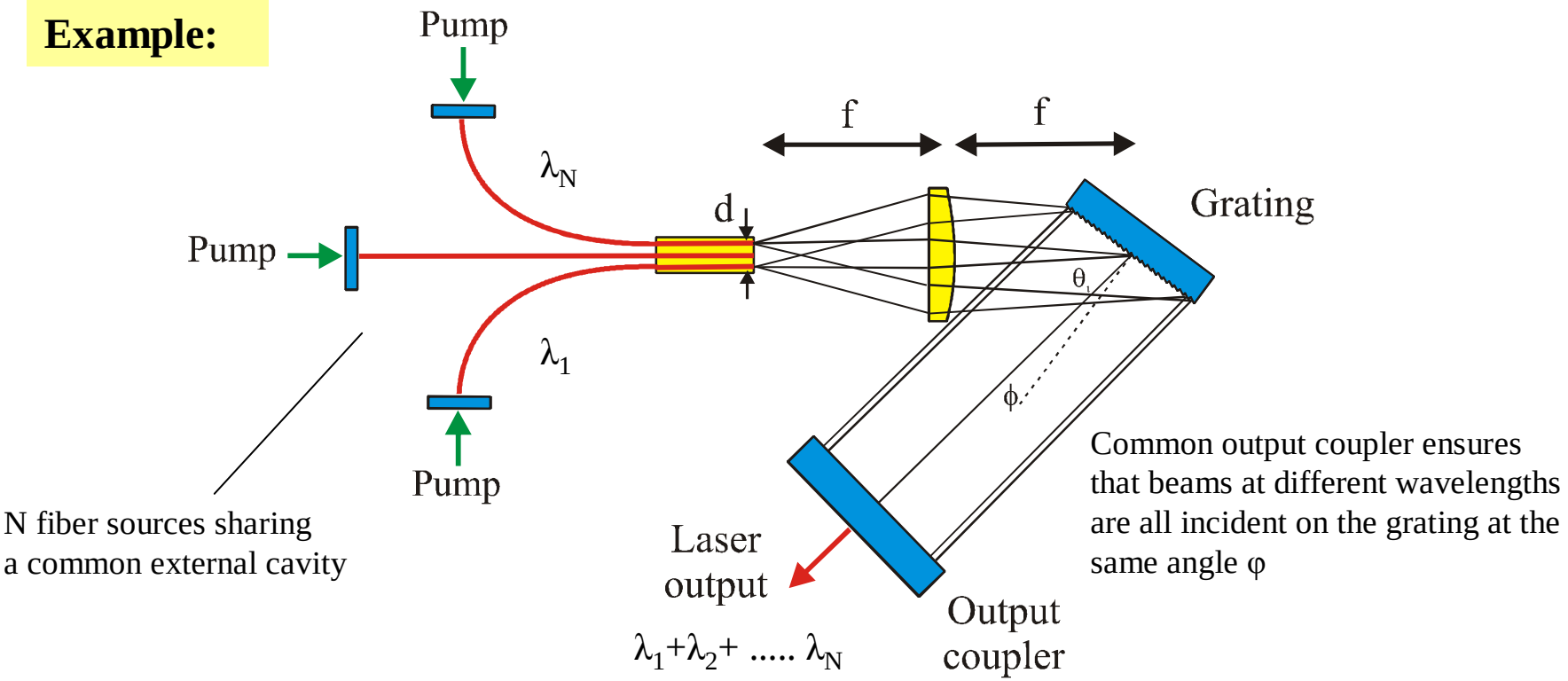

Spacing between 1st and Nth fiber cores = d, grating period = Λ, spacing of adjacent cores = s

Wavelength for i^{th} fiber laser: $\lambda_i = \Lambda(\sin\theta_i + \sin\phi)$ and dispersion of grating: $d\theta/d\lambda = 1/(\Lambda\cos\theta)$

→ Wavelength spread for fiber laser array: $\Delta\lambda_A = \Lambda d[(\cos\theta)/f] \leq \Delta\lambda_L$
→ Wavelength spacing between adjacent fibers is $\Delta\lambda_s = \Lambda s[(\cos\theta)/f]$

where $\Delta\lambda_L$ is the gain bandwidth for the transition and can be quite large (>100nm) in a glass host

→ **Power scaling limit ≈ $P_s \Delta\lambda_L / \Delta\lambda_s$**

where P_s is the power of a single element

This approach has been used to combine diode[4] and fiber laser arrays[5,6]. For the latter, power levels of >100W have been realised for an array of three cladding-pumped Yb-doped fibers using a fused silica transmission grating as the dispersive element[6].

Main challenges for power and brightness scaling[7]:

- Accurate positioning of fiber cores in a linear array to avoid degradation in beam quality
- Lens design – Minimising degradation in beam quality due to aberrations
- Dispersive element design – Good wavelength discrimination, high efficiency, thermal handling
- Tight alignment tolerances

(b) Coherent beam combining:

Filled-aperture beam combining

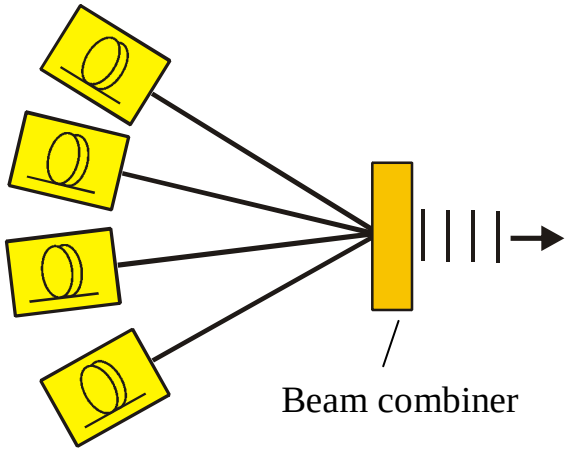

All elements have the same wavelength and are in phase or there is a defined phase relationship between adjacent elements

$$\text{Strehl ratio} = S = \frac{I_o}{I_o'}$$

where I_o is the actual on-axis intensity and I_o' is the on-axis intensity for a perfect 'top-hat' beam with the same overall aperture size

$$S_{\text{phased array}} = NS_{\text{incoherent array}}$$

Tiled-aperture beam combining

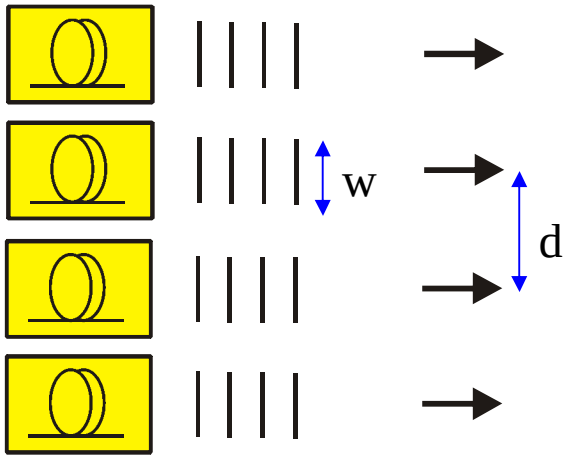

Can be viewed as trying to synthesize a plane wave

→ Fill-factor must be as large as possible to minimise proportion of light in side-lobes

Phase error must be $<<2\pi$ to avoid a reduction in on-axis intensity

Example: 1D array of single-frequency fiber lasers with the same wavelength and in phase (N = 5, d = 500μm)

$$I(\theta) \propto \frac{\eta_{fill}}{N^2}\left(\frac{\sin\beta}{\beta}\right)^2\left(\frac{\sin N\alpha}{\sin\alpha}\right)^2 \quad \text{where } \beta = \frac{\pi w}{\lambda}\sin\theta \quad \text{and} \quad \alpha = \frac{\pi d}{\lambda}\sin\theta$$

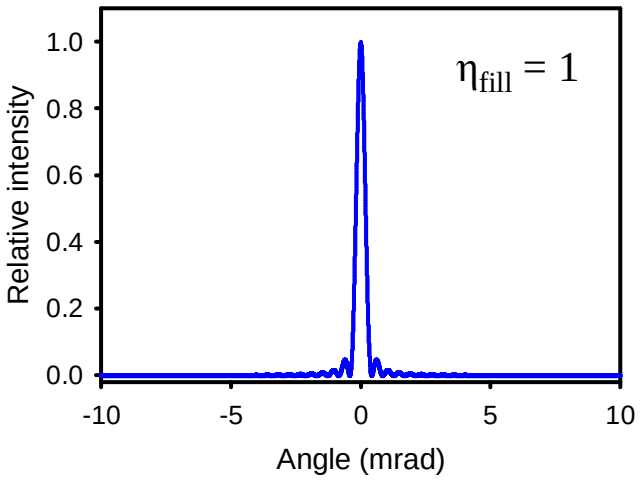

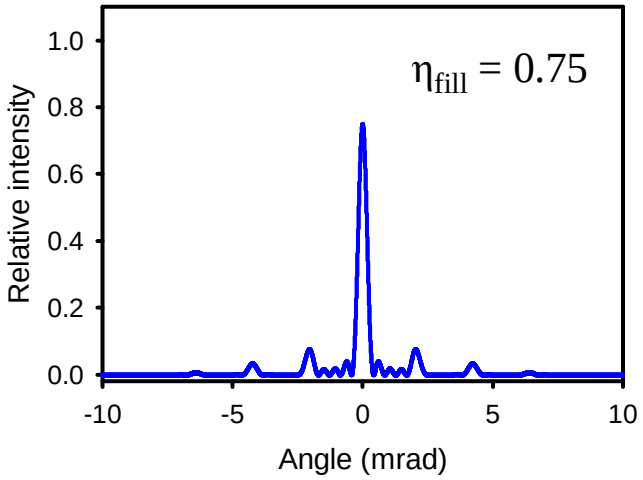

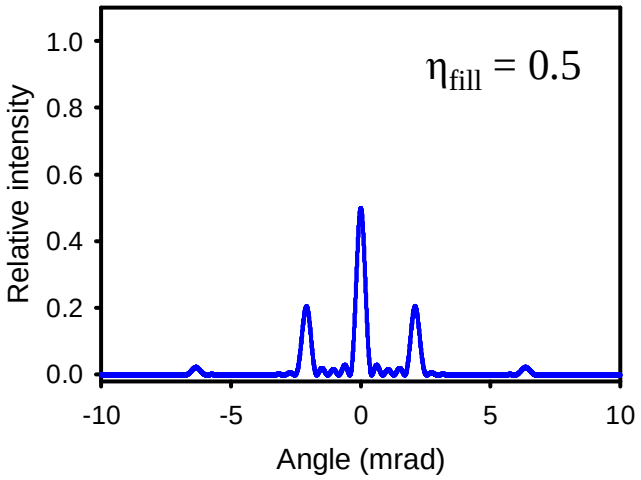

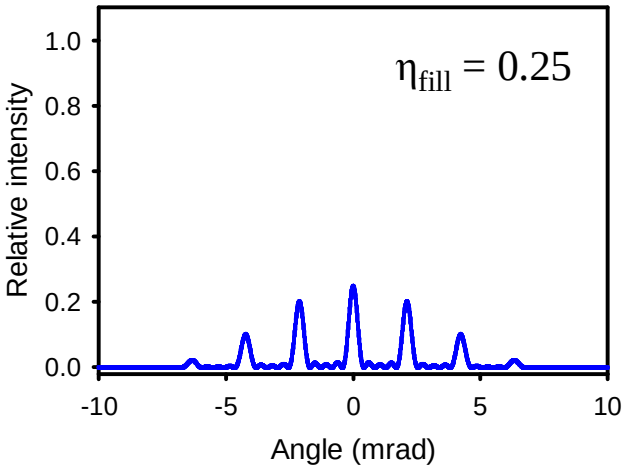

There are a number of possible implementation schemes. Most employ a MOPA architecture with one or more amplification stages (e.g. see refs. 8 and 9)

Example:

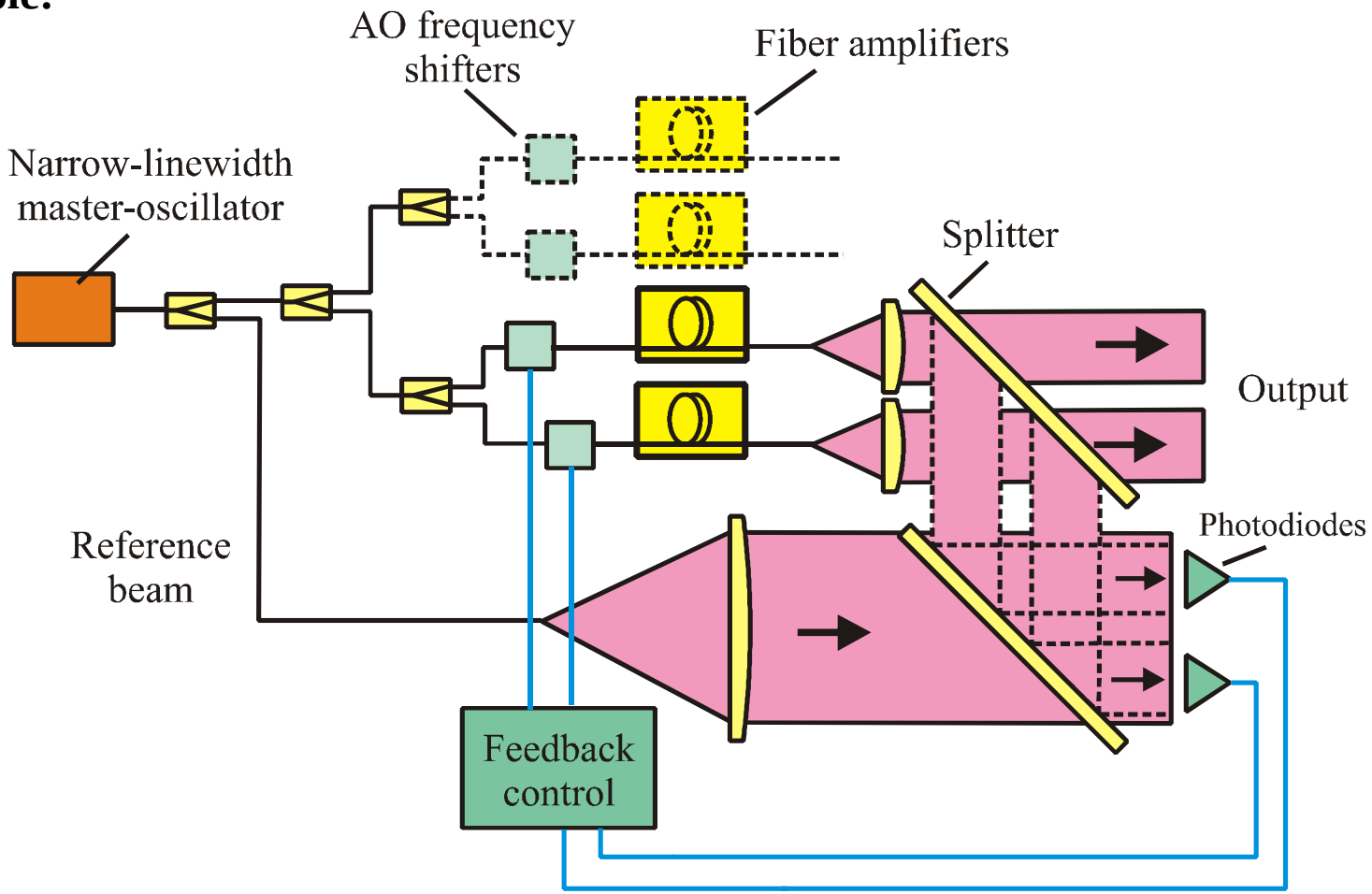

Optical path differences between array elements are detected and actively controlled using acousto-optic frequency shifters (or some alternative means) to compensate variations in OPD due to differences in fiber length, temperature variations, etc

Coherent beam combining offers a route to very high power and very high brightness from a fiber-based source. Power levels up to 470W have been demonstrated for a 4-element array[9].

Some practical issues and challenges:

- Many narrow-linewidth, polarized fiber sources (each comprising a multi-stage fiber amplifier) are required.
- Maximum power for a single-frequency polarised fiber source is currently ~400W (limited by pump power)[10].
- SBS is likely to be an issue for further power scaling.
- As the number of array elements increases, the alignment tolerance of output beams from individual elements in the near-field and far-field (i.e. to avoid pointing errors) will be much more difficult to meet.
- Very high fill-factor + 'top-hat' beam profile are needed to ensure that there is very little power in the side-lobes.
- Power per element needs to be carefully controlled to avoid non-uniformity across the array.
- Accurate monitoring and robust control of the relative phase between elements is needed.

References

1. T. Y. Fan, “Laser beam combining for high-power high-radiance sources,” IEEE J. Selected Topics in Quantum Electronics, vol.11, p.567-577 (2005).
2. http://www.ipgphotonics.com
3. L. J. Cooper, P. Wang , R. B. Williams, J. K. Sahu, W. A. Clarkson, A. M. Scott and D. Jones, Opt. Lett., vol.30, p2906-2908 (2005).
4. C. Hamilton, S. Tidwell, D. Meekhof, J. Seamans, N. Gitking and D. Lowenthal,” High power laser source with spectrally beam combined diode laser bars,” Proc. SPIE, vol.5336 (2004).
5. S. J. Augst, A. K. Goyal, R. L. Aggarwal, T. Y. Fan and A. Sanchez, “Wavelength beam combining of ytterbium fiber lasers,” Opt. Lett., vol.28, p331-333 (2003).
6. F. Röser, S. Klingebiel, A. Liem, T. Schreiber, S. Höfer, J. Limpert, T. Peschel, R. Eberhardt, A. Tünnermann, “Spectral combining of fiber lasers”, Proc. SPIE Vol. 6102, p. 196-201, Fiber Lasers III: Technology, Systems, and Applications; Andrew J. Brown, Johan Nilsson, Donald J. Harter, Andreas Tünnermann; Eds. (2006).
7. E. J. Bochove, “Theory of spectral beam combining of fiber lasers,” IEEE J. Quantum Electron., vol.38, p.432-445.
8. S. J. Augst, T. Y. Fan, A. Sanchez, “Coherent beam combining and phase noise measurements of ytterbium fiber amplifiers,” Opt. Lett., vol.29, p.474-476.
9. J. Anderegg, S. Brosnan, E. Cheung, P. Epp, D. Hammons, H. Komine, M. Weber, M. Wickham, “Coherently coupled high-power fiber arrays,” Proc. SPIE Vol. 6102, p. 202-206, Fiber Lasers III: Technology, Systems, and Applications; Andrew J. Brown, Johan Nilsson, Donald J. Harter, Andreas Tünnermann; Eds. (2006).
10. D. N. Payne, Y. Jeong, J. Nilsson, J. K. Sahu, D. B. S. Soh, C. Alegria, P. Dupriez, C. A. Codemard, V. N. Philippov, V. Hernandez, R. Horley, L. M. B. Hickey, L. Wanzcyk, C. E. Chryssou, J. A. Alvarez-Chavez, and P. W. Turner, “Kilowatt-class single-frequency fiber sources”, in Fiber lasers II: technology, systems, and applications, L. N. Durvasula, A. J. W. Brown, and J. Nilsson, Eds., Proc. SPIE vol. 5709, p. 133 -141 (2005).